AlbaNova and Nordita Colloquium, Oskar Klein Auditorium (FR4) November 12, 2009

Theory and Applications to Energy, Water, Catalysis, Materials Science, and Pharma

William A. Goddard III
Charles and Mary Ferkel Professor of
Chemistry, Materials Science, and Applied Physics
Director, Materials and Process Simulation Center (MSC)
California Institute of Technology
email:wag@wag.caltech.edu

Fall 2009

World Class University Professor
EEWS-KAIST, Daejeon Korea
Email:wag@kaist.ac.kr

We must increase the pace of achieving Energy, Environmental Water Sustainability (EEWS)

In recent decades huge investments have been made in fuel cell, solar energy, hydrogen energy, and water technologies

Progress has been made but it is not adequate to address the demands for energy and water by our rapidly increasing populations

How can we change this?

We must increase the pace of achieving Energy, Environmental Water Sustainability (EEWS)

In recent decades huge investments have been made in fuel cell, solar energy, hydrogen energy, and water technologies

Progress has been made but it is not adequate to address the demands for energy and water by our rapidly increasing populations

How can we change this?

Answer: By developing and using first-principles based theory and simulation to drive the design of new paradigm-changing materials.

By a huge margin most research and development in the new materials required for solving the EEWS problems has been experimental. Such empirical developments have led to steady but slow progress. Faster solutions require innovation with new strategies. Theory and Computation will be an essential element of meeting these problems

But a great deal of funding already goes into theory and simulation, what is new?

Enormous investments have been made in supercomputer facilities and in using current methods to STUDY fuel cell, solar energy, hydrogen energy, and water technologies

But relatively little has gone into DEVELOPING NEW METHODS that are SUFFICIENTLY ACCURATE AND RELIABLE THAT THE THEORY AND SIMULATION CAN LEAD EXPERIMENT.

All too much of the theory and simulation has been focused on understanding and confirming the experiments.

We need improved theories that are used to PREDICT THE OPTIMUM MATERIALS BEFORE THE EXPERIMENTS. Then the experiments can focus on the best 1% or best 5% of the predicted materials, saving huge experimental costs and allowing big leaps in materials (not just incremental changes)

Challenge in Design of Materials
Connect to 1st Principles for Realistic Systems

Need 1st Principles simulations of macroscale systems so can predict NEW materials never before synthesized and optimize them prior to experiment

1st Principles→ connect Macro to QM. Strategy use an overlapping hierarchy of methods (paradigms) (fine scale to coarse)

Allows Design of new materials and drugs (predict hard to measure properties)

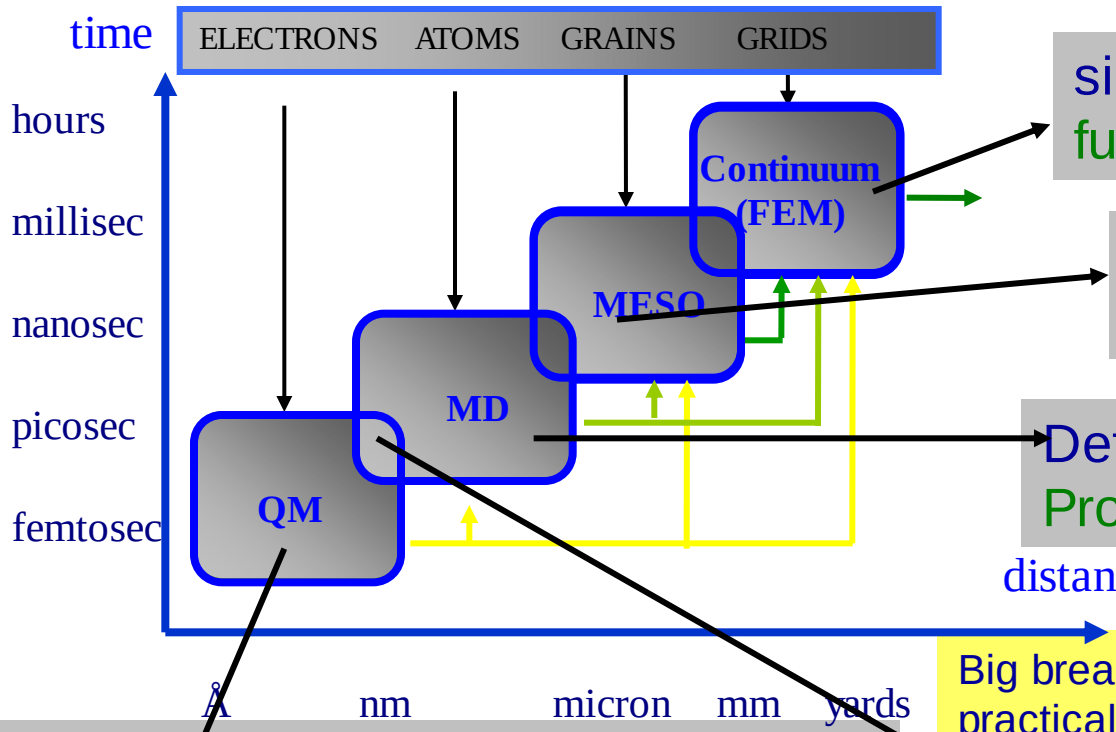

simulations real devices and full cell (systems biology)

Micromechanical modeling
Protein clusters

Deformation and Failure
Protein Structure and Function

Accurate calculations for bulk phases and molecules (EOS, bond dissociation)
Chemical Reactions (P-450 oxidation)

Big breakthrough making FC simulations practical:
reactive force fields based on QM
Describes: chemistry,charge transfer, etc. For metals, oxides, organics.

Materials Design Requires Improvements in Methods for Maximum Accuracy. The Goddard Focus:

1: Quantum Mechanics

Challenge: increased accuracy

- New Functionals DFT (dispersion)
- Quantum Monte Carlo methods
- Tunneling thru molecules (I/V)

2: Force Fields

Challenge: chemical reactions

- **ReaxFF- Describe Chemical Reaction processes,** Phase Transitions, for Mixed Metal, Ceramic, Polymer systems
- **Electron Force Field** (eFF) describe plasma processing

4: Biological Predictions

1st principles structures GPCRs

1st principles Ligand Binding

5: MesoScale Dynamics

Coarse Grained FF

Hybrid MD and Meso Dynamics

3: Molecular Dynamics

Challenge: Extract properties essential to materials design

- Non-Equilibrium Dynamics
  - Viscosity, rheology
  - Thermal Conductivity
- Solvation Forces (continuum Solv)
  - surface tension, contact angles
- Hybrid QM/MD
- Plasticity, Dislocations, Crack
- Interfacial Energies
- Reaction Kinetics
- Entropies, Free energies

6: Integration: Computational Materials Design Facility (CMDF)

•Seamless across the hierarchies of simulations using Python-based scripts

Major problem: little funding for methods

Goal: develop methods and software simultaneously with Applications to the most challenging problems.Goddard Focus

FUEL CELL CATALYST: Oxygen Reduction Reaction (Pt alloy, nonPGM)

ENVIRONMENT and WATER: Captymers for Selective Encapsulation

BATTERIES: Li and F ion systems for primary and secondary applications

CATALYSTS for METHANE TO LIQUID : Ir, Os, Rh, Ru organometallic (220C)

HYDROGEN STORAGE: MOFs, COFs, metal alloys, nanoclusters, graphenes

CATALYSTS for ALKANE SELECTIVE OXIDATION, AMMOXIDATION : Mixe metal oxides (Mo, V, Ta, Te, Bi)

POLYMERS: Higher Temperature Fuel Cell PEM (Replace Nafion)

CERAMICS: Fuel Cell electrodes and membranes, Ferroelectrics, Superconductors

NANOSYSTEMS: Nanoelectronics, molecular switches, CNT Interconnects

SEMICONDUCTORS: damage free etching for 32 nm generation

THERMOELECTRICS: (high ZT)

BIOTECHNOLGY: GPCR Membrane Proteins, Pharma, Novel Amino Acids

ENERGETIC MATERIALS: PETN, RDX, HMX, TATB, TATP, propellants

MultiParadigm Strategy enables application of 1st principles to complex systems

Our Stimulation: industrially supported projects

Always Impossible, forces new theory developments

Chevron Corporation: catalysis CH_4 to CH_3OH, ionic liquids for catalysis
Dow Solar: CIGS-CdS solar cells
Dow Corning: Catalysts for Production of Silanes for Silicones
Ford Motor Company: Fuel Cells: degradation of Nafion, Cathode catalyst
Intel Corp: Carbon Nanotube Interconnects, nanoscale patterning
AquaNano-Nestle: water treatment
Pfizer Corp: Structures and Function of GPCRs
PharmSelex: Design new pharma for GPCRs

Now active

Allozyne: non natural AA, Structure GLP-1R and binding to GLP-1
Asahi Glass: Fluorinated Polymers and Ceramics
Asahi Kasei: Ammoxidation Catalysis, polymer properties
Avery-Dennison: Nanocomposites for computer screens Adhesives, Catalysis
Berlex Biopharma: Structures and Function of chemokine GPCRs
Boehringer-Ingelheim: Structures and Function of GPCRs
BP: Heterogeneous Catalysis (alkanes to chemicals, EO)
Dow Chemical: Microstructure copolymers, Catalysis polymerize polar olefins
Dupont: degradation of Nafion PEM
Exxon Corporation: Catalysis (Reforming to obtain High cetane diesel fuel)
General Motors - Wear inhibition in Aluminum engines
GM advanced propulsion: Fuel Cells (H2 storage, membranes, cathode)
Hughes Satellites/Raytheon: Carbon Based MEMS
Hughes Research Labs: Hg Compounds for HgCdTe from MOMBE
Kellogg: Carbohydrates/sugars (corn flakes) Structures, water content
3M: Surface Tension and structure of polymers
Nippon Steel: CO + H2 to CH3OH over metal catalysts
Nissan: tribology of diamond like carbon (DLC) films
Owens-Corning: Fiberglas (coupling of matrix to fiber)
Saudi Aramco: Up-Stream additives (Demulsifiers, Asphaltenes)
Seiko-Epson: Dielectric Breakdown, Transient Enhanced Diffusion Implanted B

Completed successfully

Spin-Offs:
Accelrys (public) - software
Schrödinger - software
Eidogen-Sertanty – protein structures
Allozyne – therapeutics new AA
PharmSelex (new) –pharma GPCRs
Systine (new) – Etching 32 nm
AquaNano (new)- water treatment

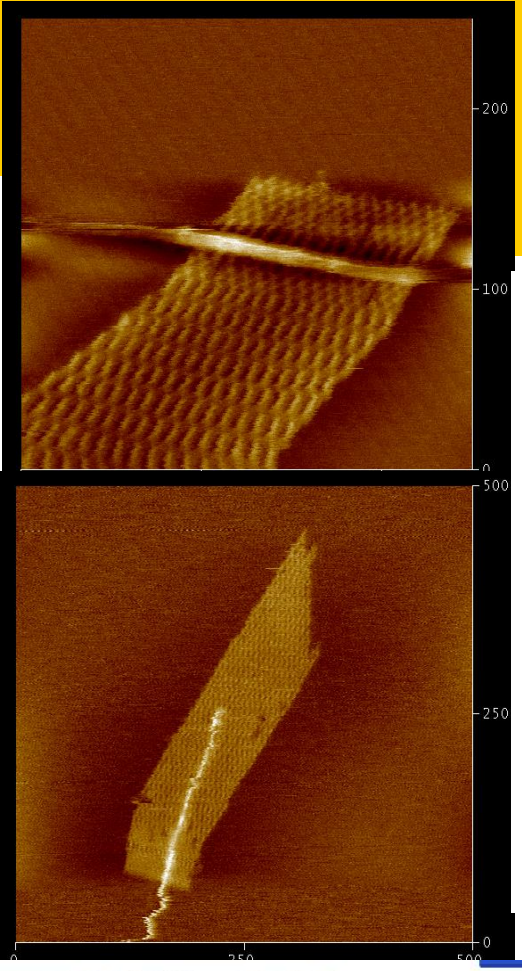

DNA Nanoscaffold Directed Self-Assembly of Carbon Nanotube Devices (nature nanotech, Nov. 8, 2009)

- Carbon Nanotubes have remarkable properties
- For commercial application must have scalable technology to self-assemble these nanoscale SWNT devices by the millions
- Our approach uses DNA origami as template for active self assembly
- We have demonstrated this technology by successful self assembly of Field Effect Transistors (FET)

Funding **NSF NIRT, MARCO-FENA**

What do we need from a template?

Basic Idea

- Must enable Self-assembly
- Must allow Arbitrary geometric patterns
- Must provide Nanoscale feature resolution
- Must enable Chemically distinguishable features

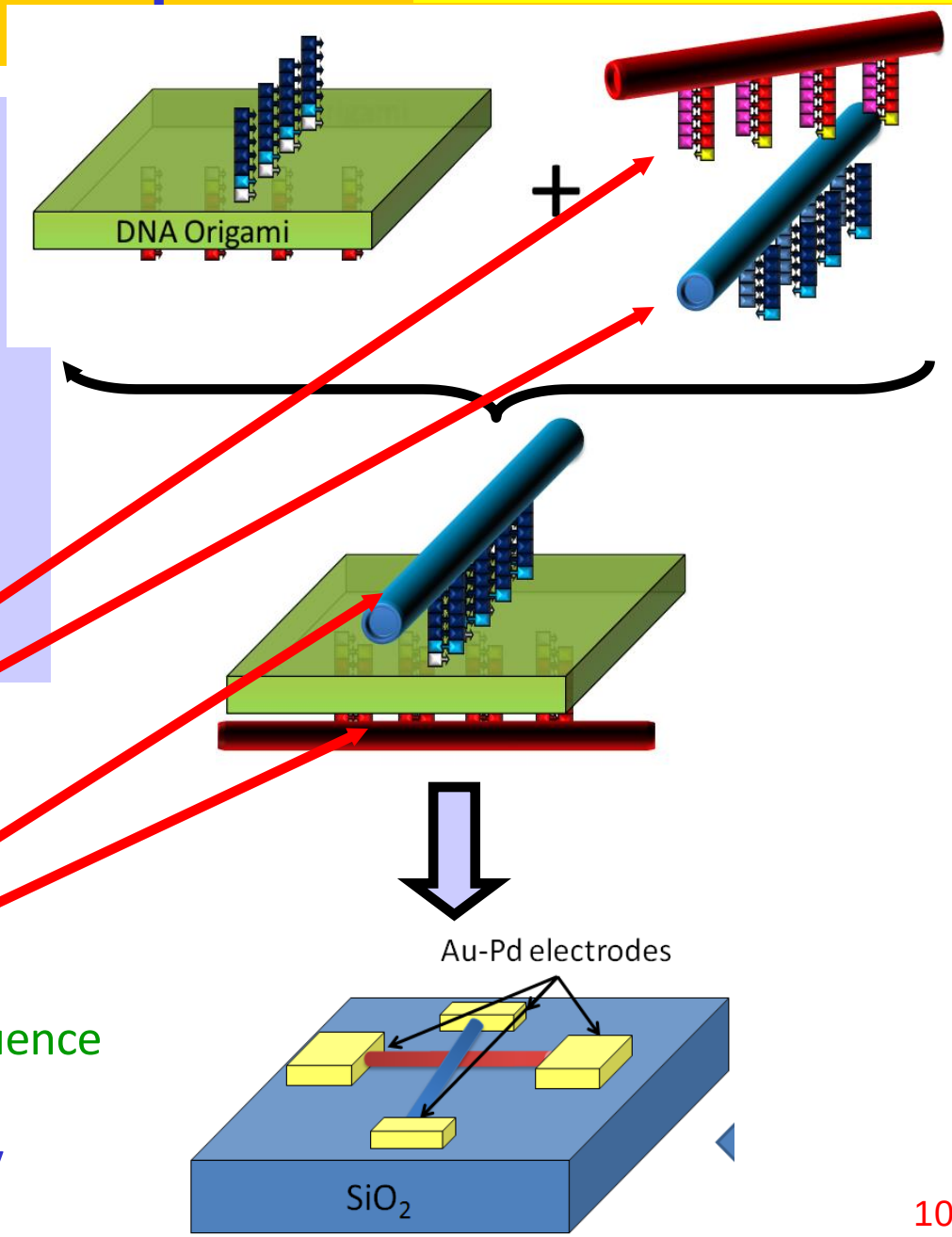

DNA labels and differentiates different SWCNTs

Rows of DNA hooks with the same sequence defines a pathway

Different pathways are distinguished by different hook sequences

DNA-Origami can serve as nanoscale scaffold

DNA self assembly uses DNA as a structural material that self-assembles into prespecified forms based on the sequences of custom synthesized DNA oligos

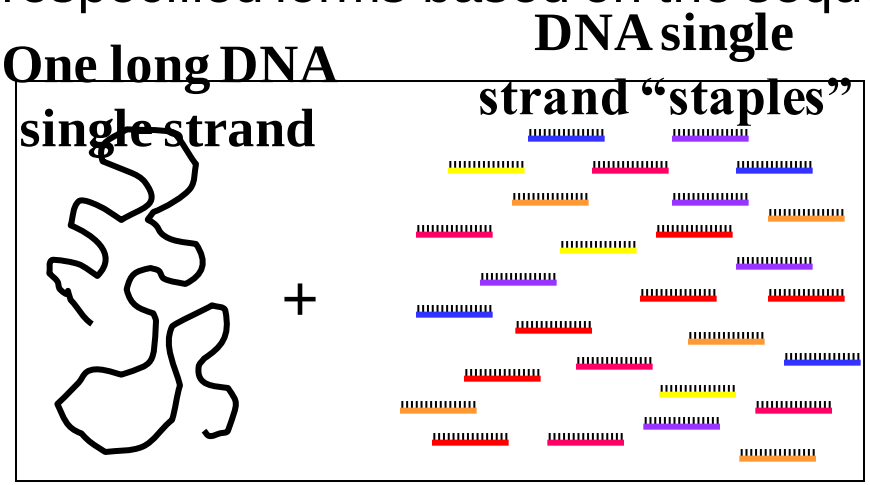

Scaffolded DNA origami

90º C -> 20º C
12.5 mM Mg++
TAE buffer

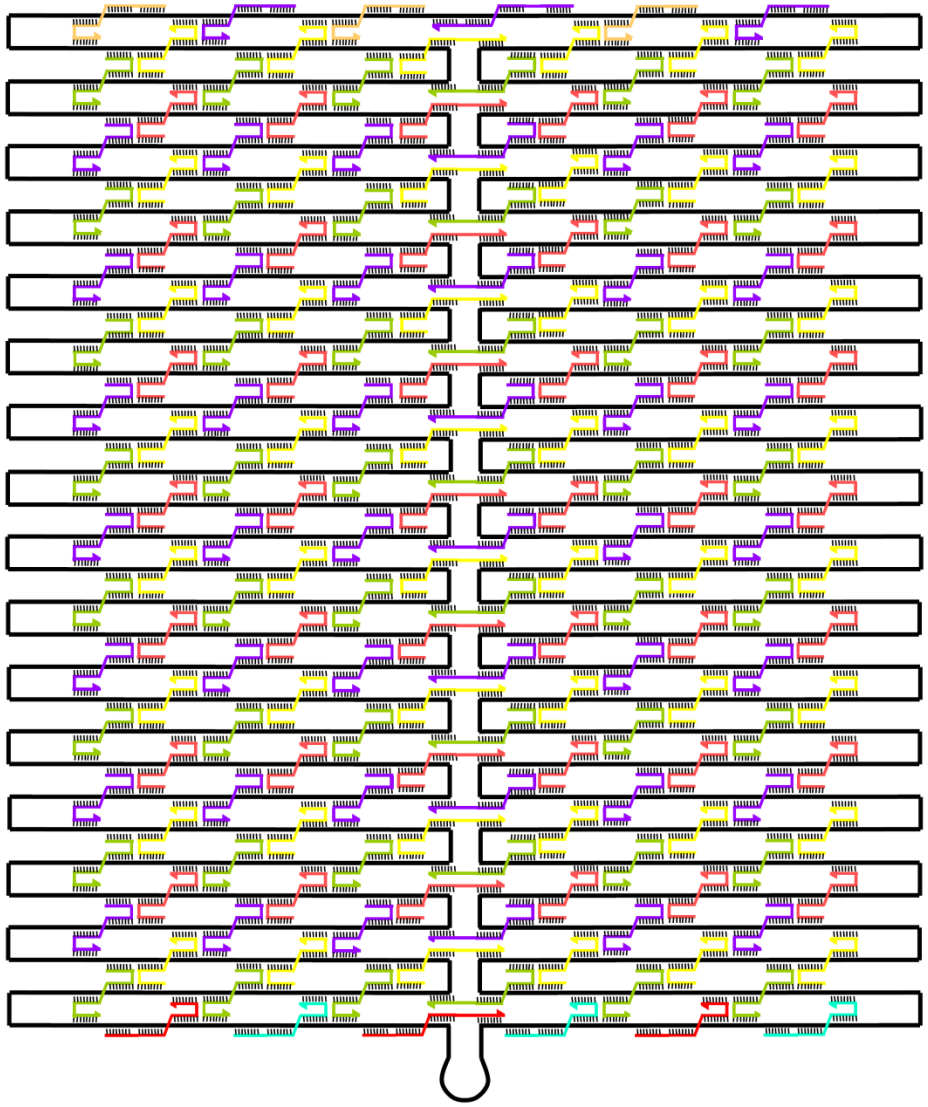

Staple strands guide the virus scaffold to fold into a geometrical shape

200 staple strands offer ***6nm*** resolution

1 nm assembled concentration = ***10^{11} structures per 1 mL solution***

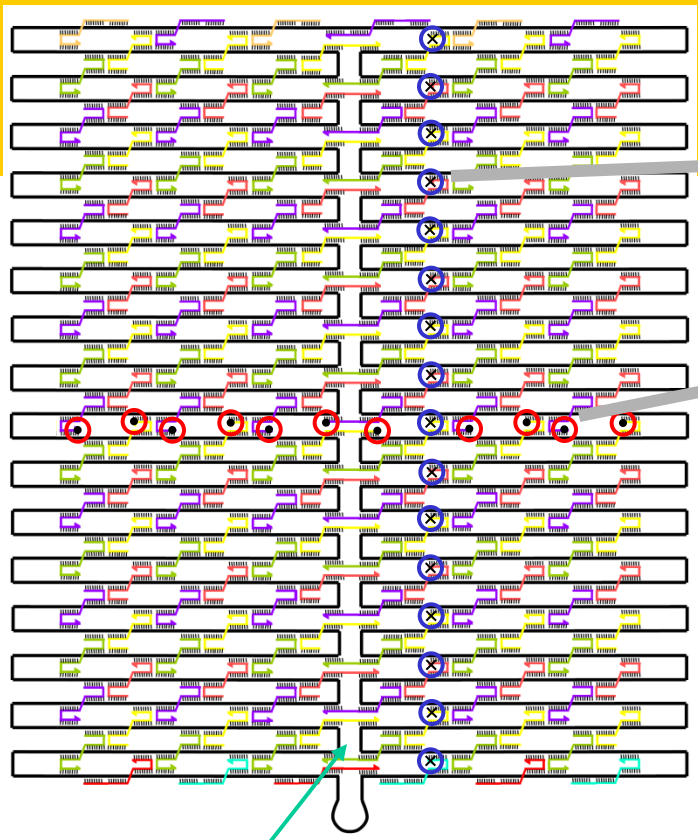

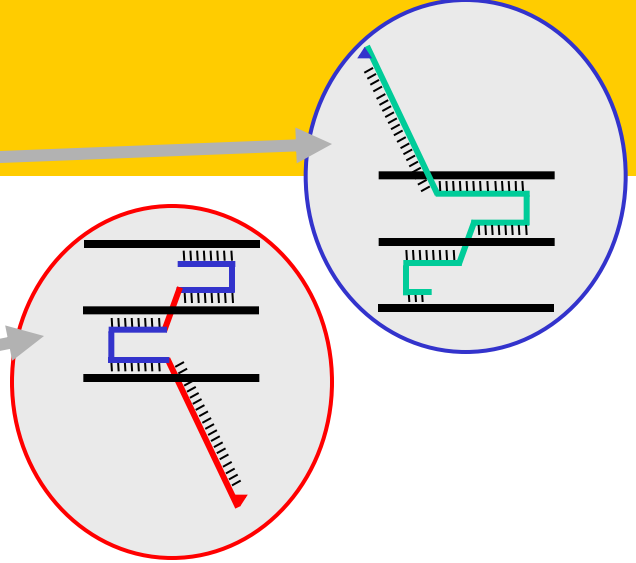

Can extend Staple strands to project ssDNA Hooks

Origami seam

Sequence specific "red" hooks

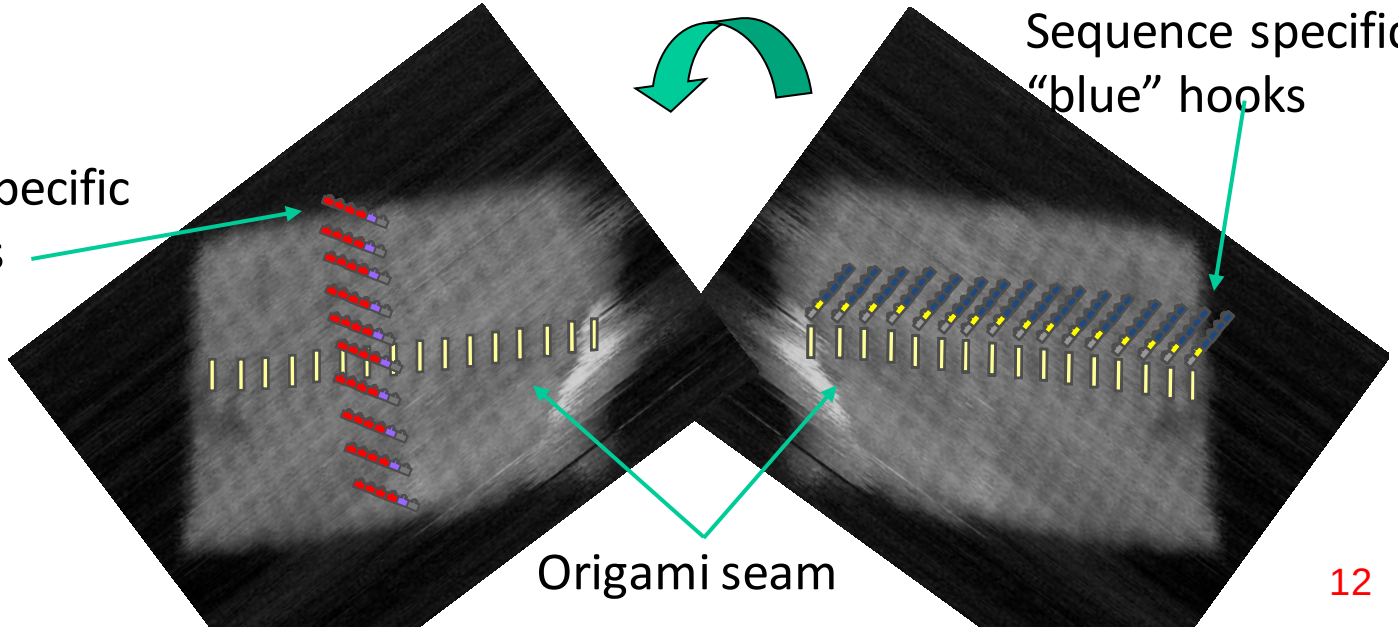

We can project hooks from either

Appropriate ssDNA adsorbs non-covalently on carbon nanotubes

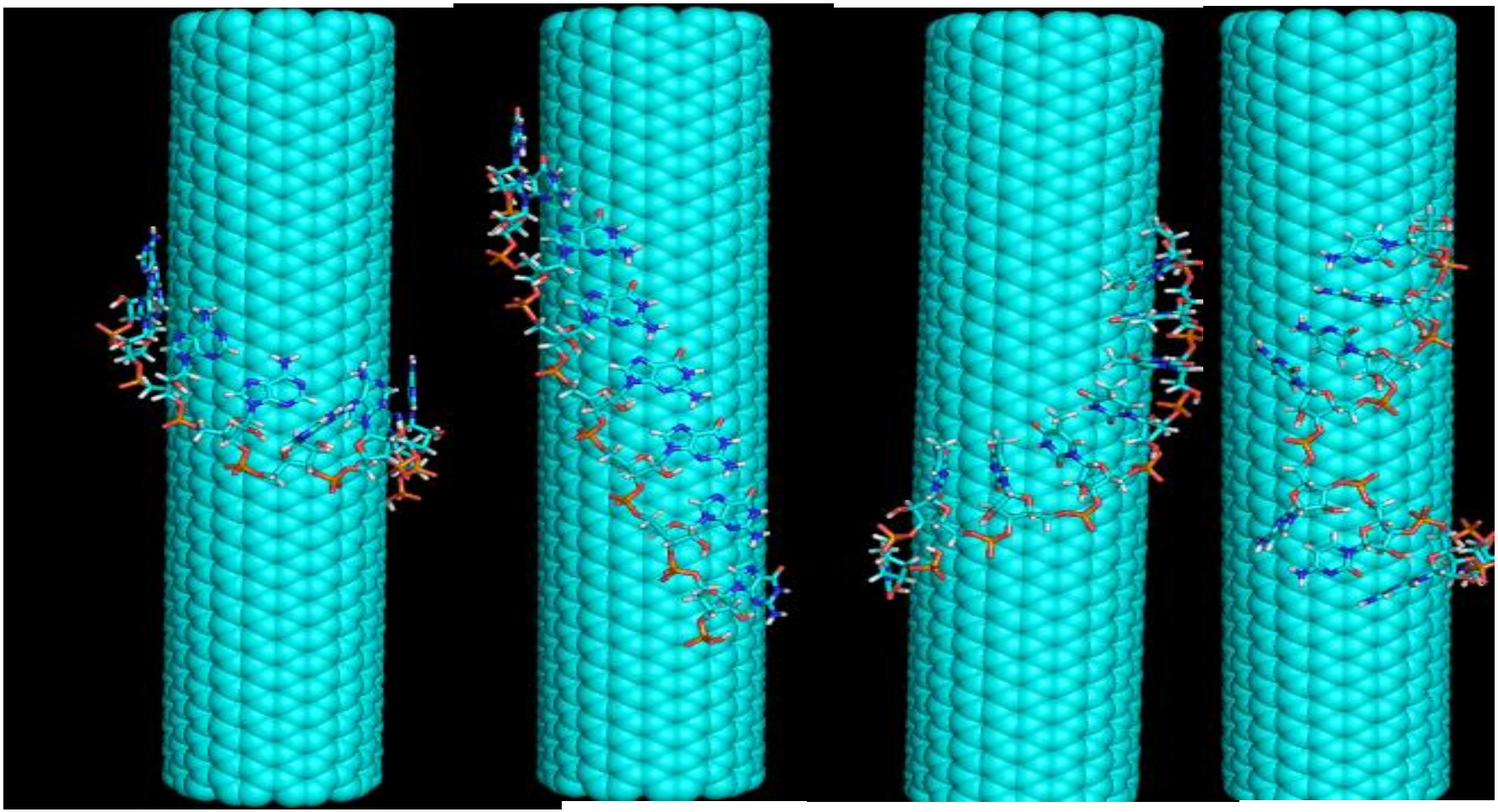

Non-covalent ➔ ***retain favorable CNT electronic characteristics***

Must ***ensure that adsorption does not interfere with DNA base pairing***

Details of the DNA hook and linker

First attempt: Used equal concentration of dispersal complexes without protection strand in same salt conditions

Did not work. No assembly after extensive filtration (equal level of DNA in effluent)

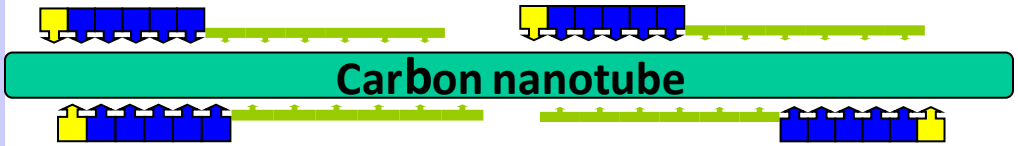

Did not work!

Added Protections Strand Worked!

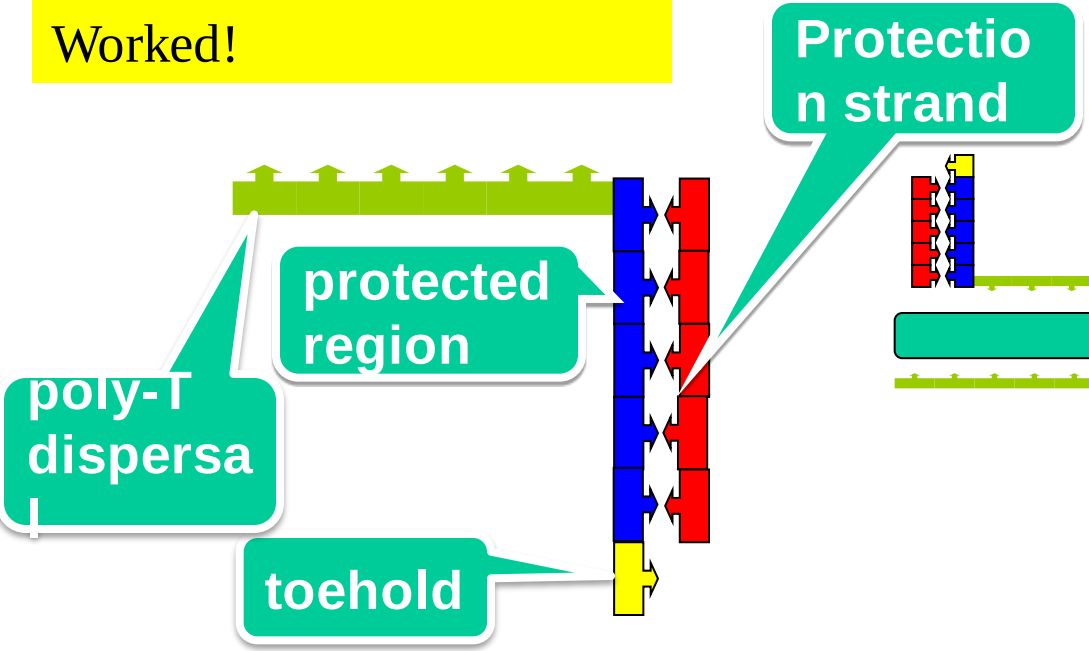

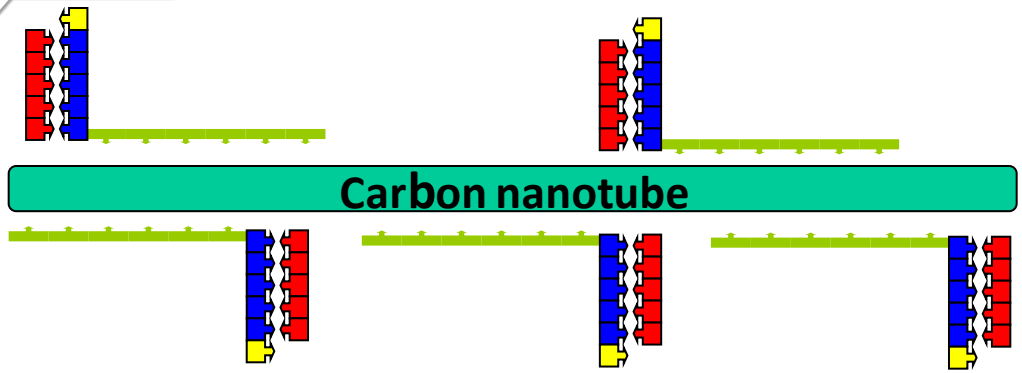

Worked!

Self assembly on a DNA template

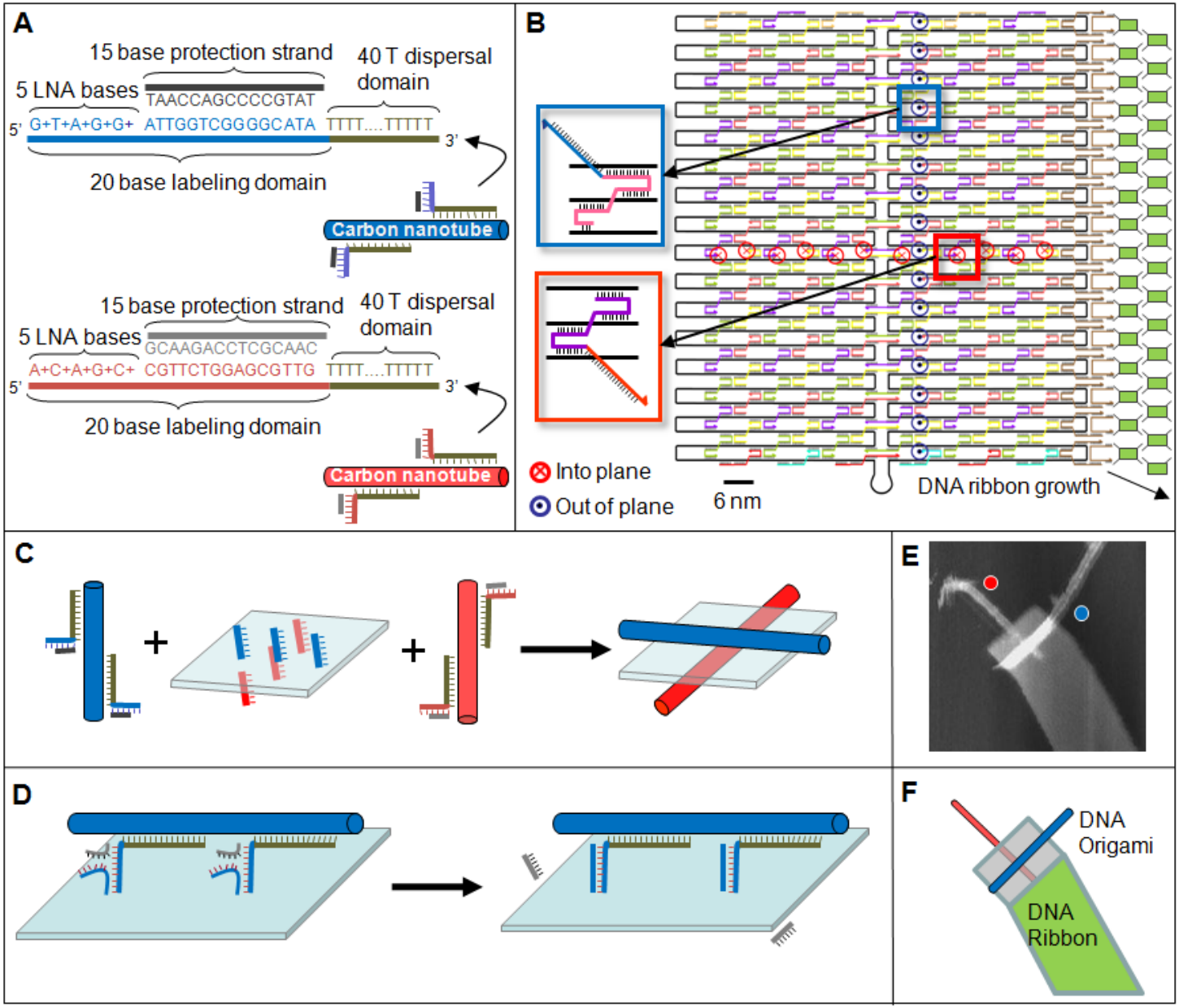

15

The assembled structures

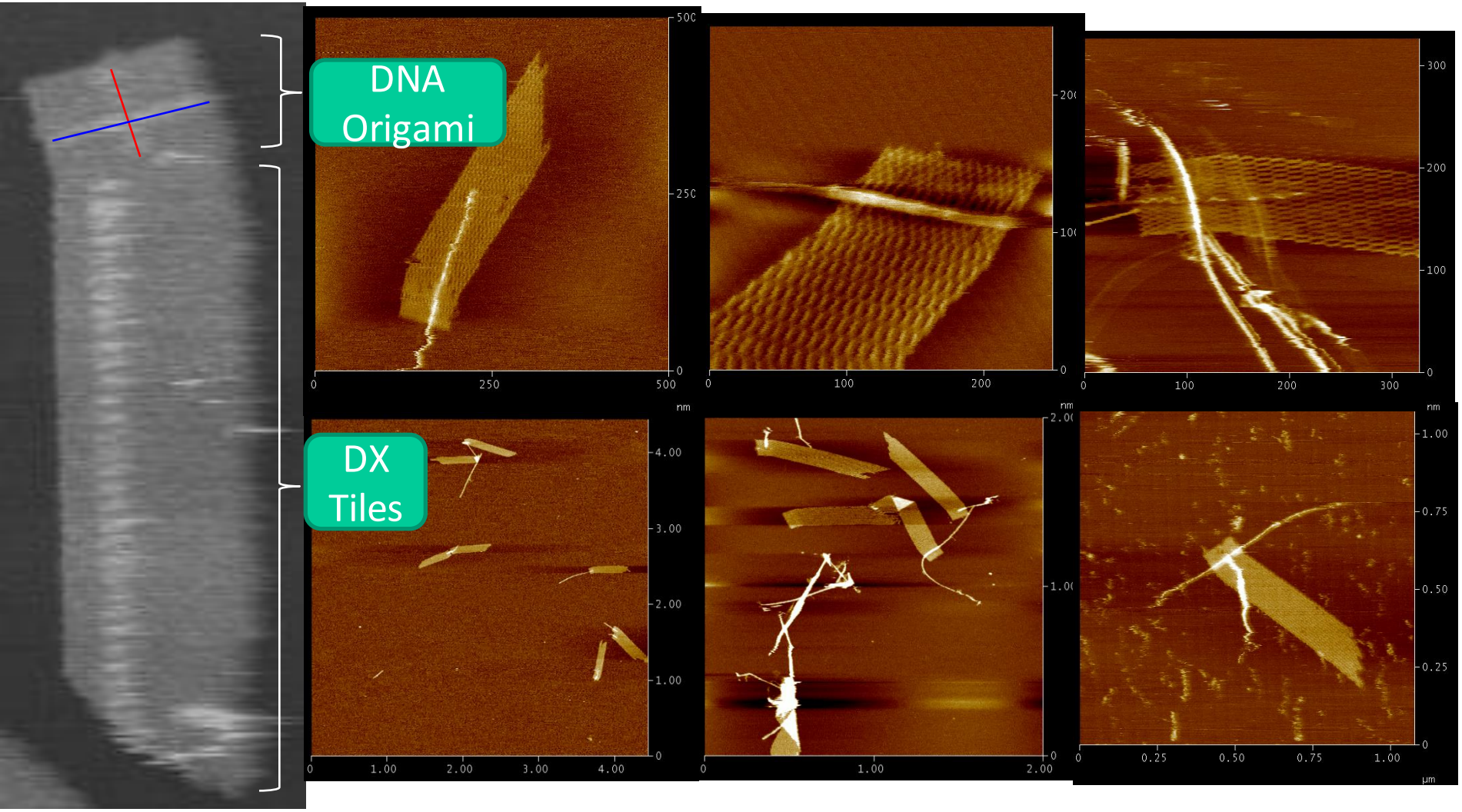

Position of hooks

Red assembly

Blue assembly

Crossbar

Self-Assembled SWCNT FET

Attempted: 23
Measured: 6
FETs: 1 stable (2 unstable)
Resistance comparable to before treatment for our HIPCO batch

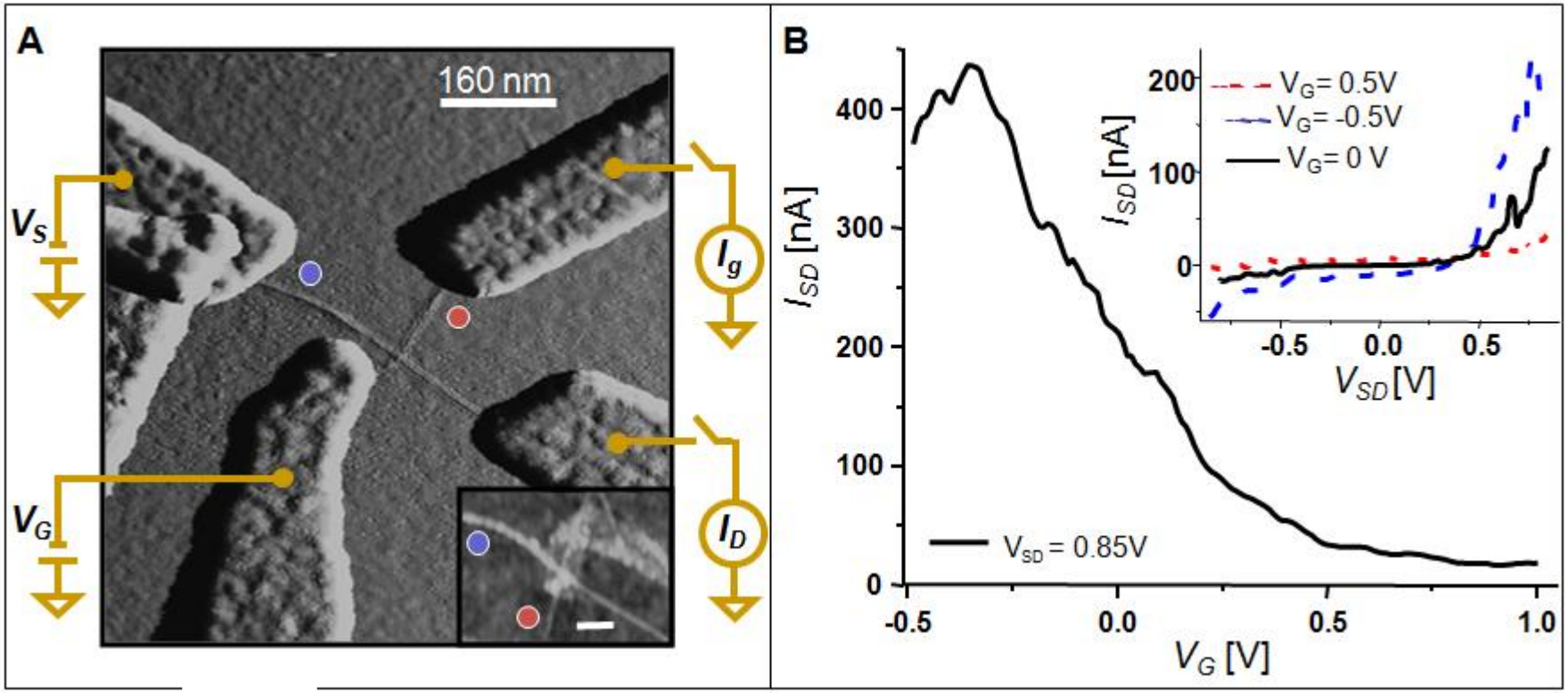

P-type conducting channel

Conclusion

- We have achieved *placement and orientation* of DNA labeled SWCNTs on *sequence specific* patterned templates.
- We make devices at 0.1 nm concentration
- We have not destroyed the electronic characteristics of the system

Future work:

- Push towards control over nanotube placement in the axial direction
- Utilize electronic property sorting and modification
- Hierarchical assembly
- Better contact and processing to create "clean" electronic functionality
- Multi-component circuits
- Incorporation of other nanoscale components (nanoparticles, QD, proteins)

(nature nanotech, Nov. 8, 2009)

Formation of SWNT dimers

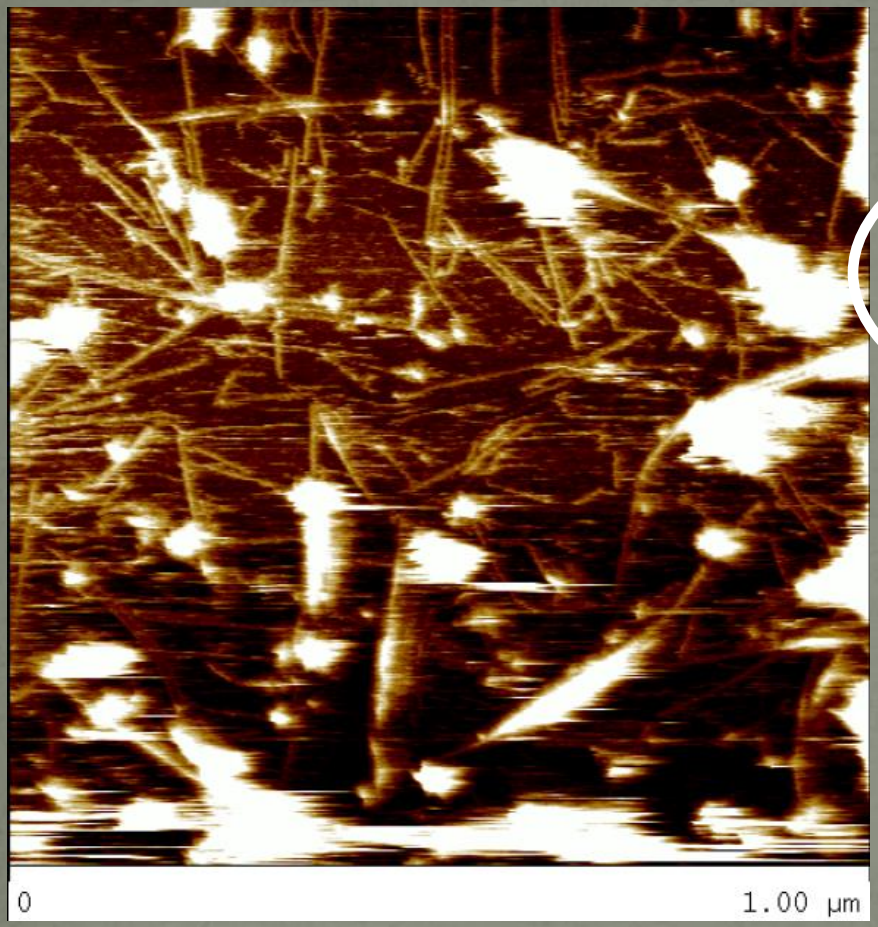

- Center to center distance ~ 1 duplex
- A large proportion of dimers

Linker complex v0.1

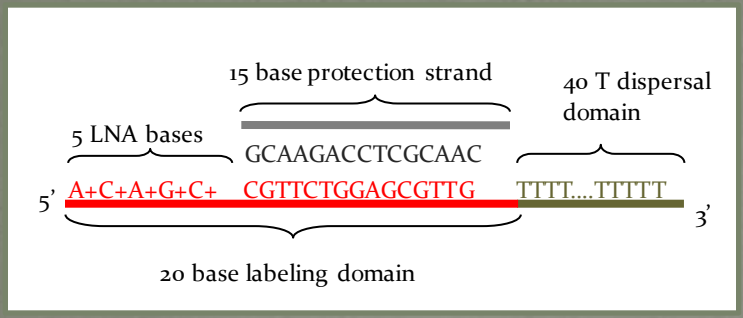

Final linker complex

Linker 0.1 intended for use in labeling the CNT with streptavidin

A 7 base and a 10 base toehold were tried

HipCo SWNTs dispersed in tris-acetate EDTA, 12.5 mM Mg^{2+}

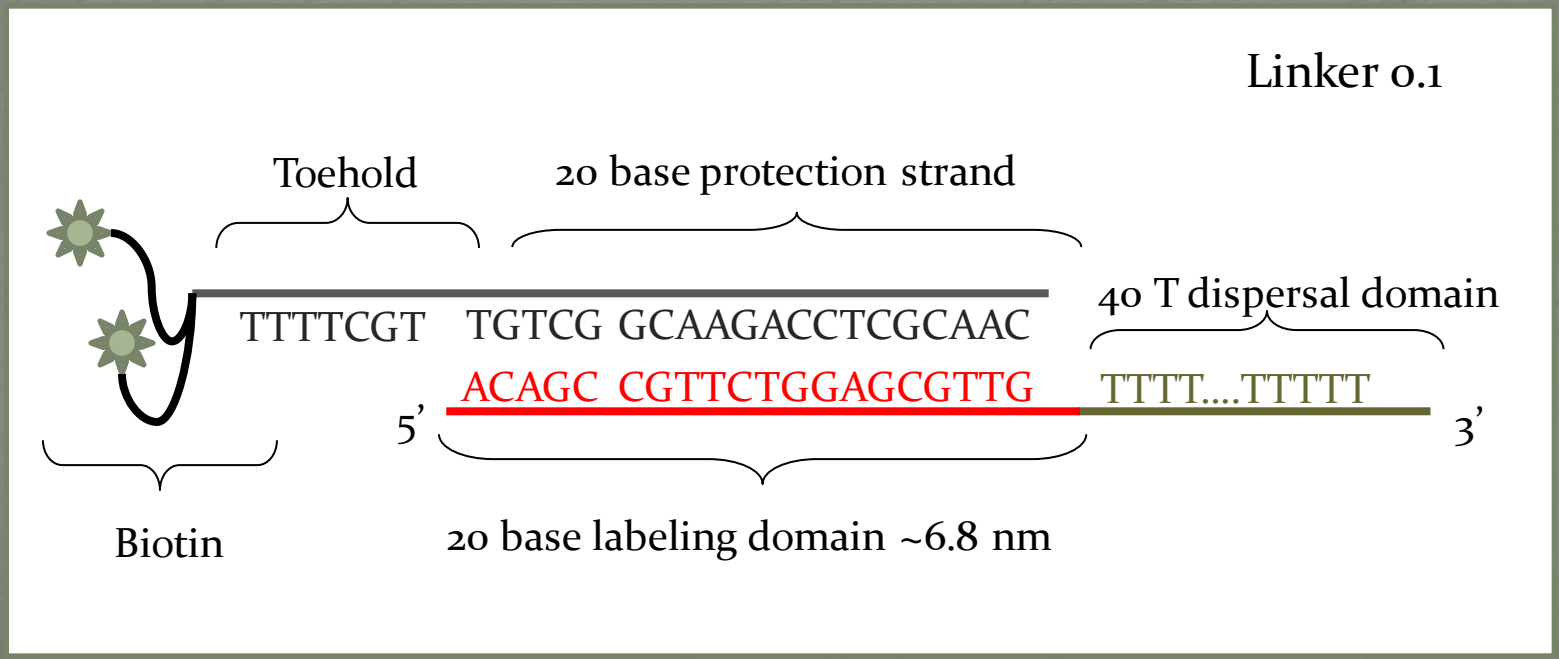

Explanation

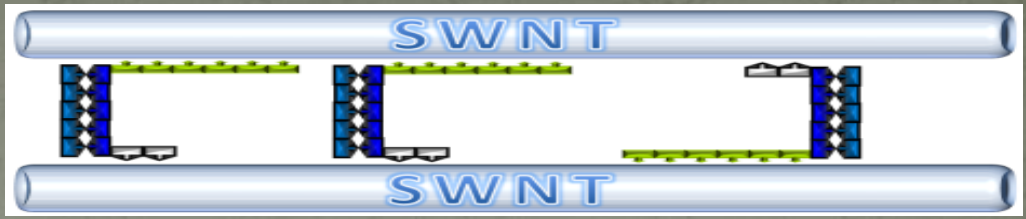

- Observations
  - All ssDNA will adsorb on SWNT surfaces
  - Adsorption energy is length and sequence dependent
  - When SWNTs are dispersed, a large amount of linker complexes are left in solution -> SWNT surface is saturated for linker complexes
  - Longer 10 base toehold leads to disordered aggregation (data not shown)
- Hypothesis:
  - A SWNT surface saturated for 40-T adsorption domain still has room for smaller toeholds
  - Dimers form when multiple linker toeholds adsorb to neighboring CNT
  - Duplex acts as a spacer
  - Short toehold length requires multiple complexes adsorb cooperatively => ordered dimers
  - Long toeholds allow binding via a single toehold => disorder

Attempt to replicate

- Linker 0.1 (polyT1)
- 0.1 M NaCl, pH 7.0
- Laser ablation SWNT
- Only 1 dimer observed
- Na+ vs Mg++ could be critical
  - With final linker, SWNTs precipitate in 1xTAE Mg++
  - CNT-CNT interaction and DNA conformation could be affected
- Different CNTs could contribute
  - Average diameter differences

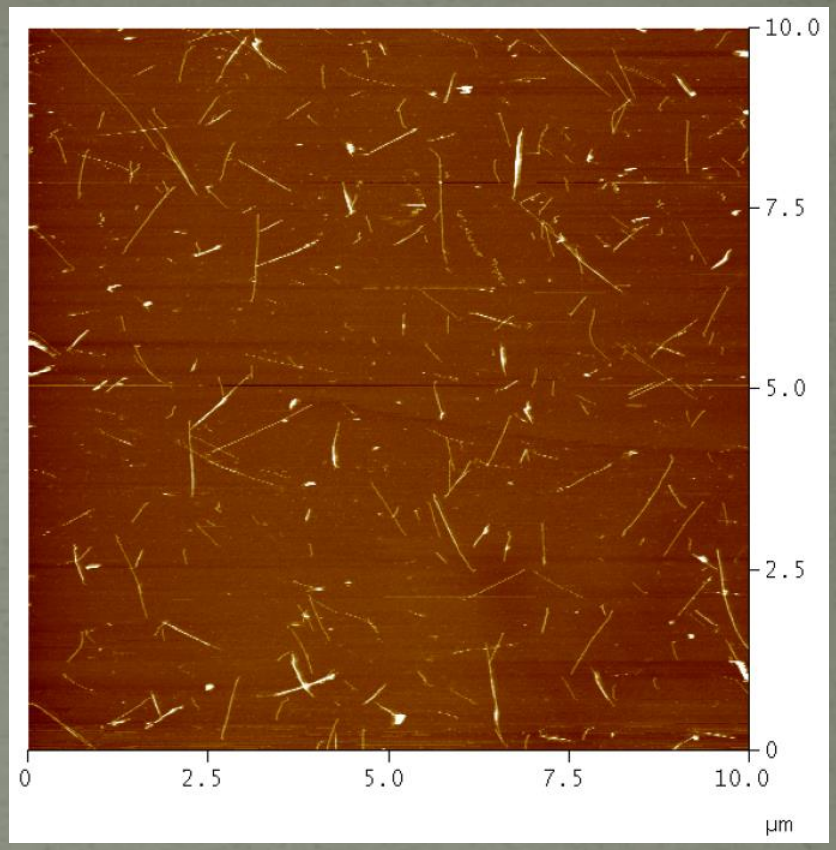

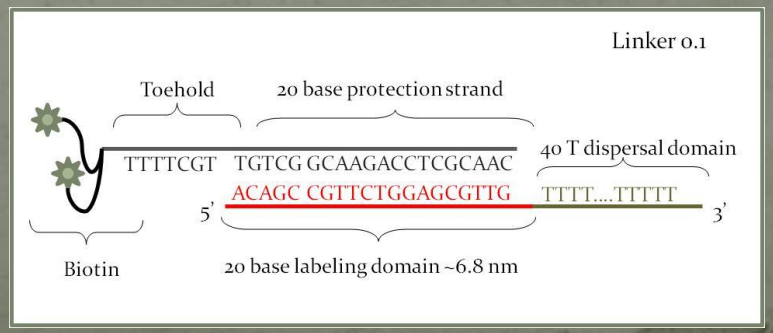

2nd Try

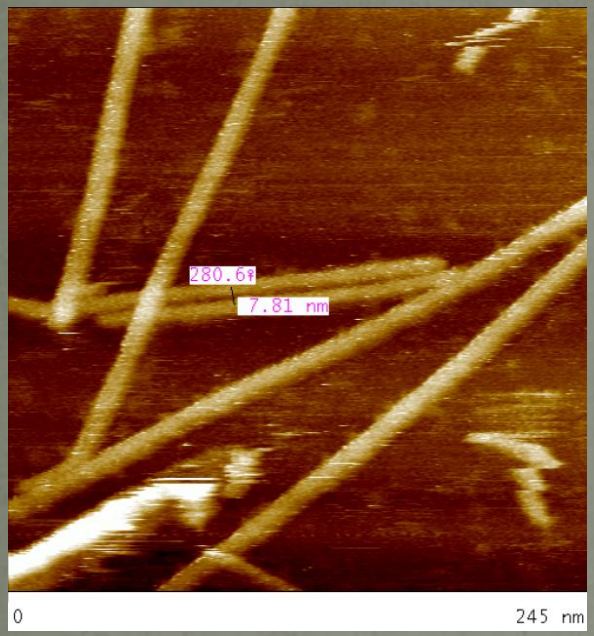

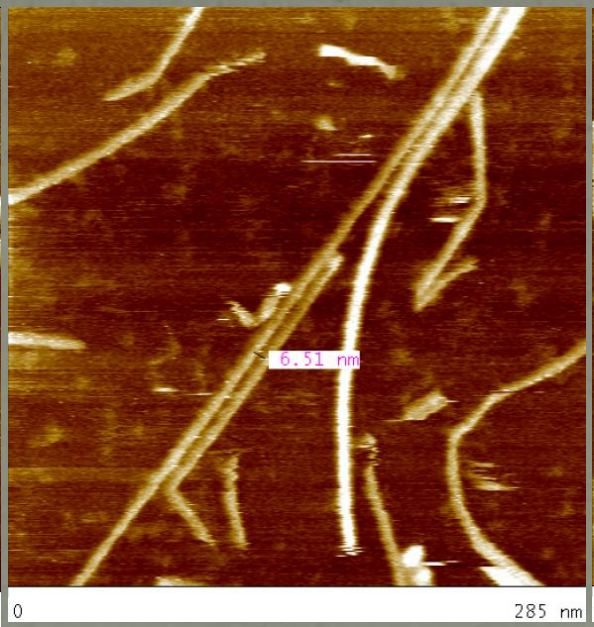

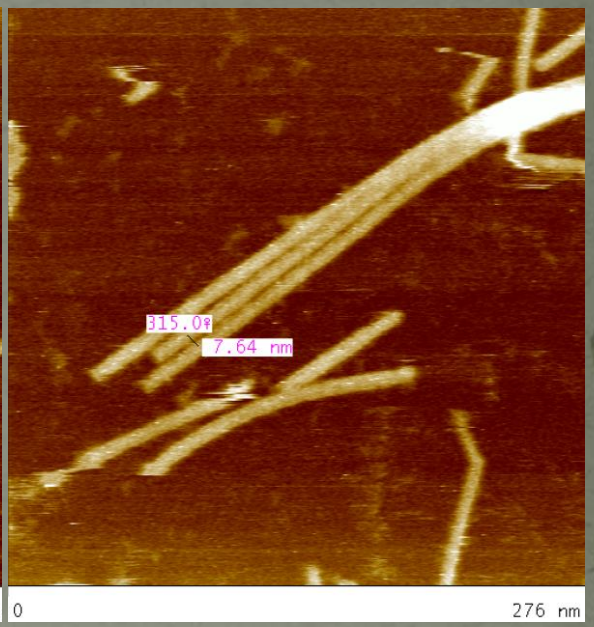

- 1 x TAE Mg++
- HipCo SWNT
- Had to change complex
- ~1 per 1 um x 1 um

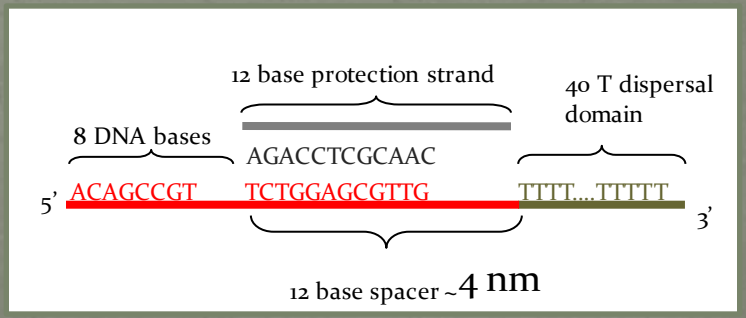

What's next?

- Use the 0.1 linker with 1x TAE Mg++
- Understand the role of the biotins (if any at all)
- Understand toehold energetics
- Examine pitch control with variable width spacers
- Revisit salt and pH issues
- Why useful?
  - Nanoscale physics – interesting coupled optical, mechanical, electronic and magnetic effects
  - Incorporation into bulk materials
  - Use in conjunction with other bulk alignment methods (LB trough, CNT forest, shear flows) to have wafer scale alignment with controlled pitch
    - Separated CNT forests
    - Crossbar arrays

Major challenge in achieving continued scaling of silicon based semiconductor devices

ITRS 2007 - Challenges

Year	2007	2010	2013	2016
Technology Node (nm)	65	45	32	22
MPU Gate Length (nm)	25	18	13	9
Gate Control (3-σ, nm)	2.6	1.9	1.3	0.9
Required CDU (nm)	**0.31**	**0.23**	**0.16**	**0.11**

MPU=MultiProcessor Unit CDU=Critical Dimension Uniformity

- **Gate CDU must be 12% of final *etched* gate size (3-σ)**
- **Variability control becomes major roadmap concern**
- **No known solution for gate CD uniformity**

Solution: Low-Energy Electron Enhanced Etching (LE4) Damage-Free Fabrication Semiconductor Devices

Collaboration with
H. Patrick Gillis (UCLA and Systine)
Samir Anz (CalPoly Pomona and Systine)

Etch Technology Driven by Device Demands

1st Generation: **Critical dimension control requires anisotropic etching**

Wet Etching (tens of μm)

RIE : (sub-μm)

RIE=Reactive Ion Etching

2nd Generation: **Ion bombardment damage must be reduced**

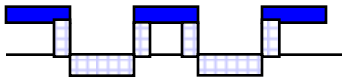

RIE

ICP, CAIBE

ICP = Inductively Coupled Plasma

CAIBE = Chemically Assisted Ion Beam Etching

Next Generation: **LE4 is anisotropic, damage-free, and smooth**

LE4

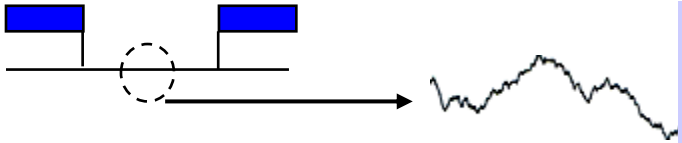

LE4 = Low Energy Electron Enhanced Etching

Damage-free anisotropic etching with smooth etched surface is required for advanced devices

Motivation: Paradigm Shift in Etching of Semiconductors Low-Energy Electron Enhanced Etching (LE4) For Damage-Free Fabrication

Current technology:
Ion-enhanced etching
2nm surface damage

Solution: low energy enhanced etching (LEEE=LE4) from DC discharge.
damage free etching extremely smooth surfaces with evem to 20 nm

20-nm Si Structures Etched by LE4

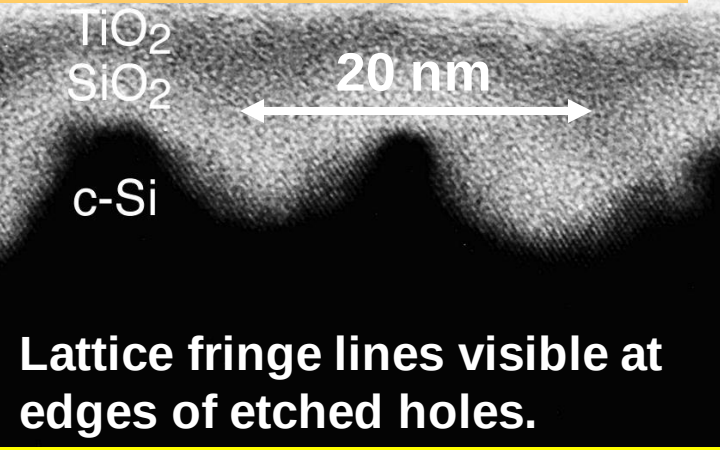

Lattice fringe lines visible at edges of etched holes.

Confirms that NO DAMAGE at crystal surface for LE4

LE4 Dramatically Reduces Line Edge Roughness

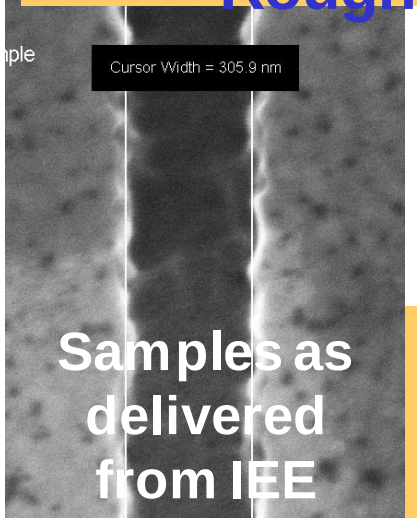

Samples as delivered from IEE

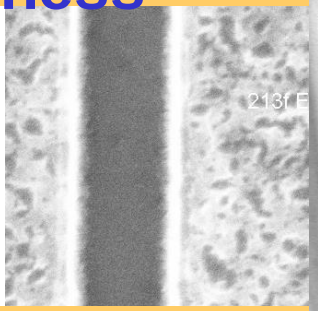

Samples after LE4 Etching

critical dimension (CD) control

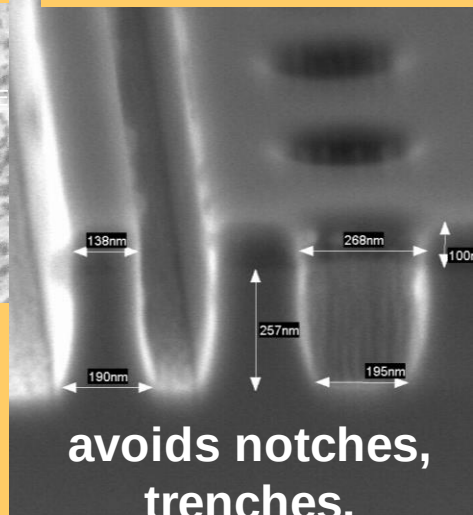

avoids notches, trenches.

Problem: to develop LE4 rationally need to Understand reaction mechanisms underlying LE4 etching

- LE4 eliminates damage due to ion bombardment (momentum transfer)
- **Mechanism for Low Energy Electrons is fundamentally different: LE4 *Chemically* etches atoms from the surface**
- Involves electronic excitations at surface (materials dependent thresholds)?
- Surface atoms removed by electron enhanced reaction product desorption?
- gas species, pressures, grid voltages all help selectively etch Si over SiO_2 and SiOxNy. Current LE4: 25:1 to 50:1 for Si:SiO_2 (best for IEE ~ 10:1).
- Now need modeling and process simulation of mechanisms for selective etching of any combination of Si, SiO_2, III-V, Nitride hard coating, photoresist, antireflective coating, Low K and High K materials.
- **Solution: Use theory and computation to deduce mechanism**

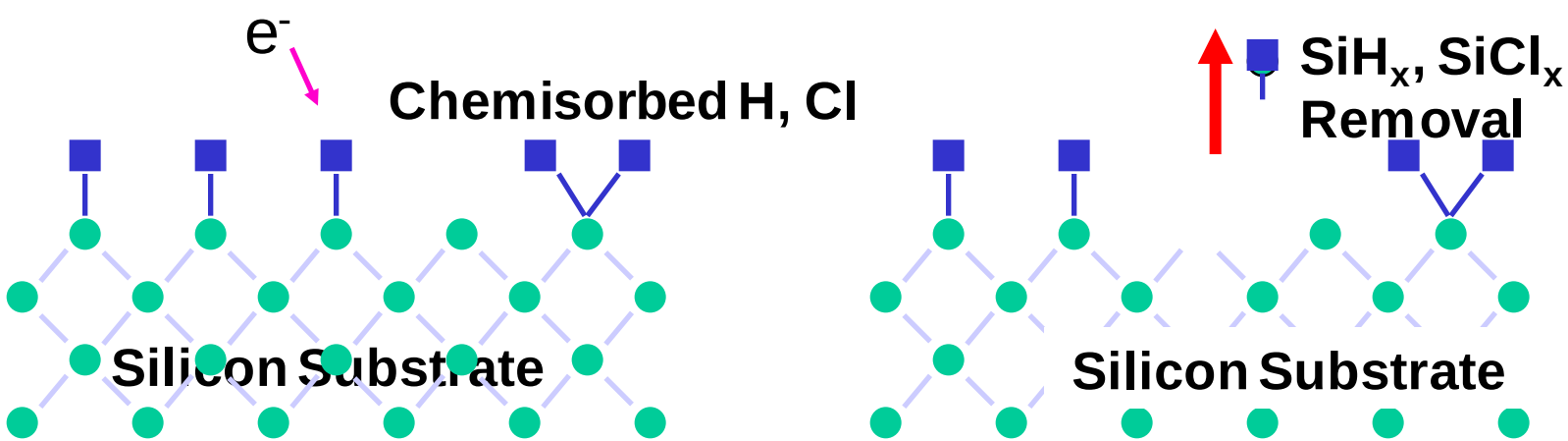

How can we simulate dynamical processes in complex systems with highly excited electronic states (~100s eV)

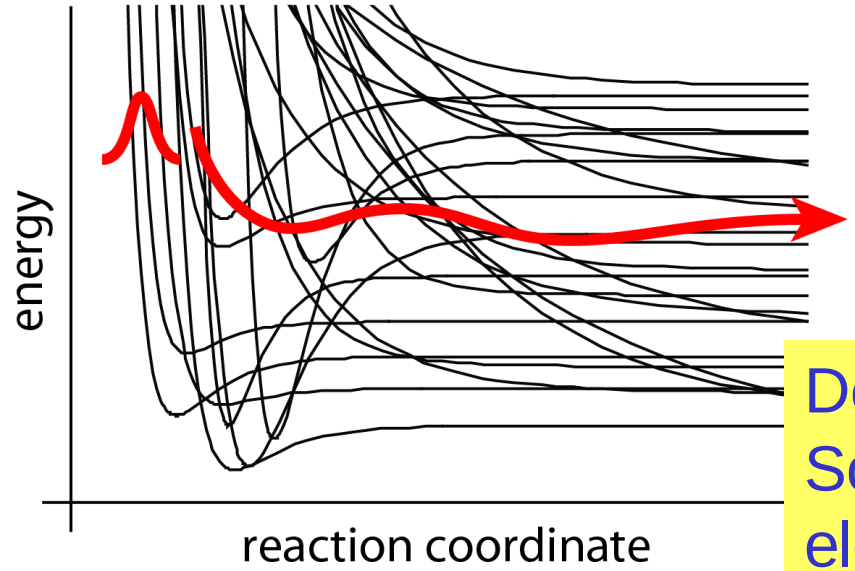

Cannot use normal QM: millions of lower electronic states, numerous curve crossings, 100 eV excess energy

Describe electron dynamics of Schrödinger Equation using the eFF: electron force field

1. Electrons represented by Gaussians.

$$\phi_i(r) \propto e^{-((r-r_i)/\rho_i)^2}$$

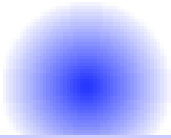

2. position and extent are continuous dynamical variables

3.Electronic wavefunction is Hartree Product.
No exchange, antisymmetry.

Key is Pauli exchange repulsion between same spin electrons

Add spin-dependent potential to describe how spin electrons repel each other (Pauli principle)

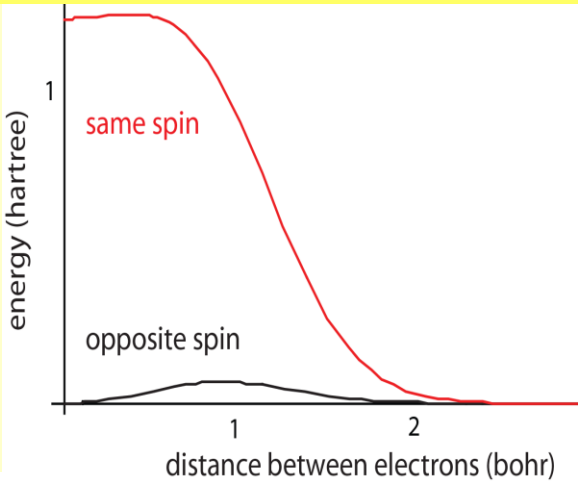

eFF leads to a reasonable (but not exact) geometries of of saturated hydrocarbons.

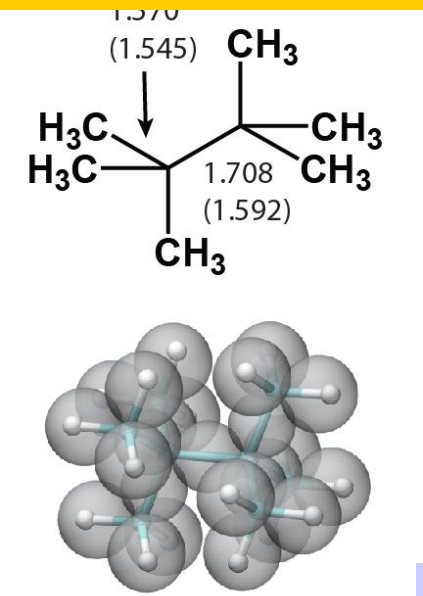

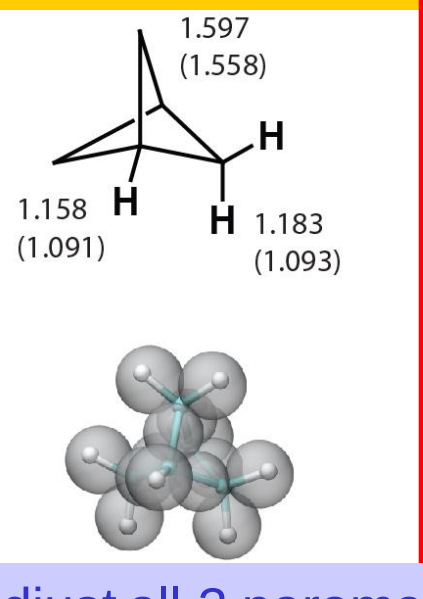

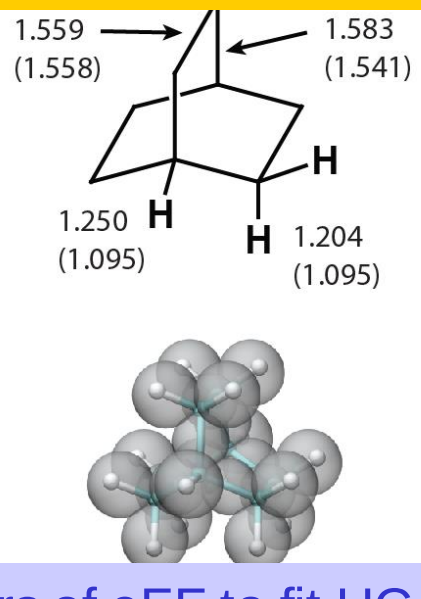

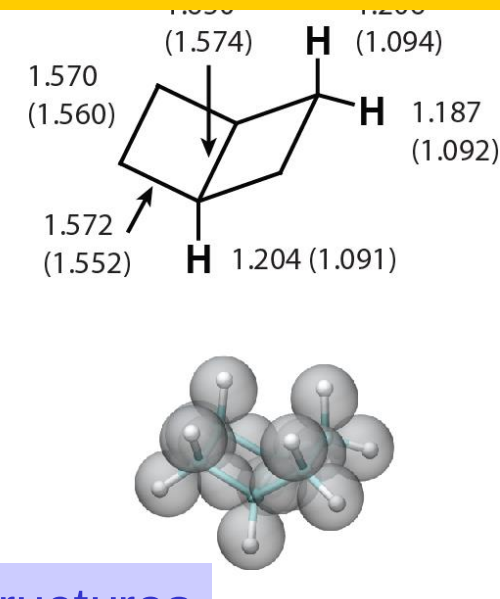

Adjust all 3 parameters of eFF to fit HC structures

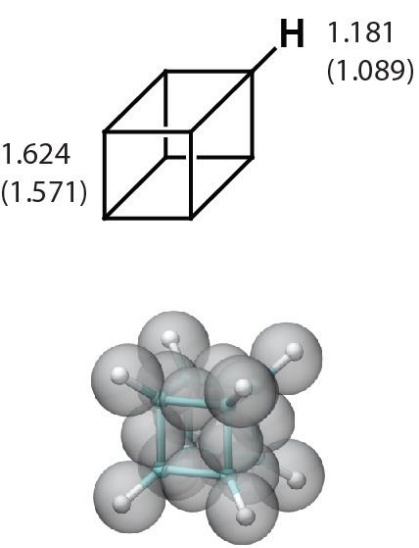

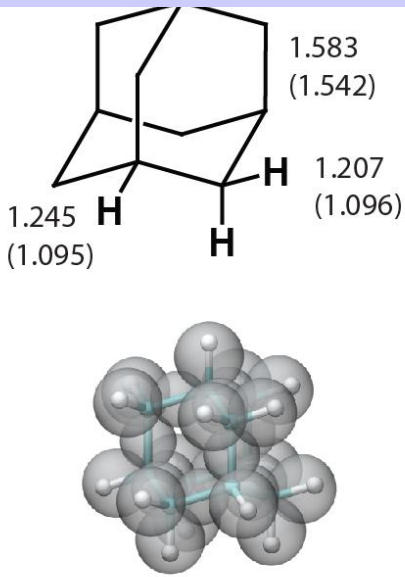

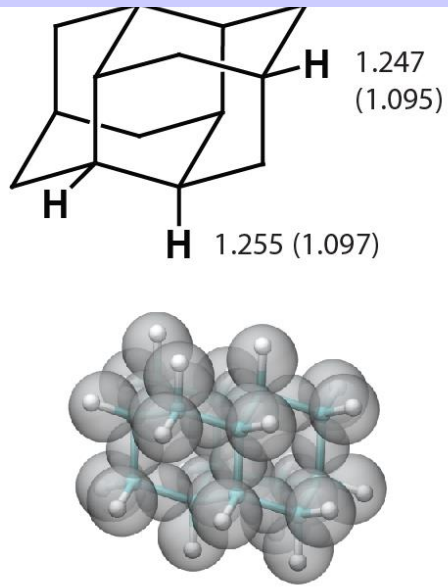

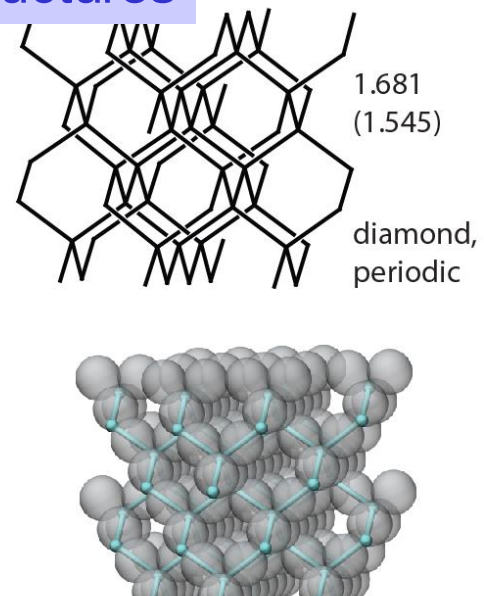

Electron densities in hydrocarbon bonds

CH bond in methane
Electron density (bohr^{-3})

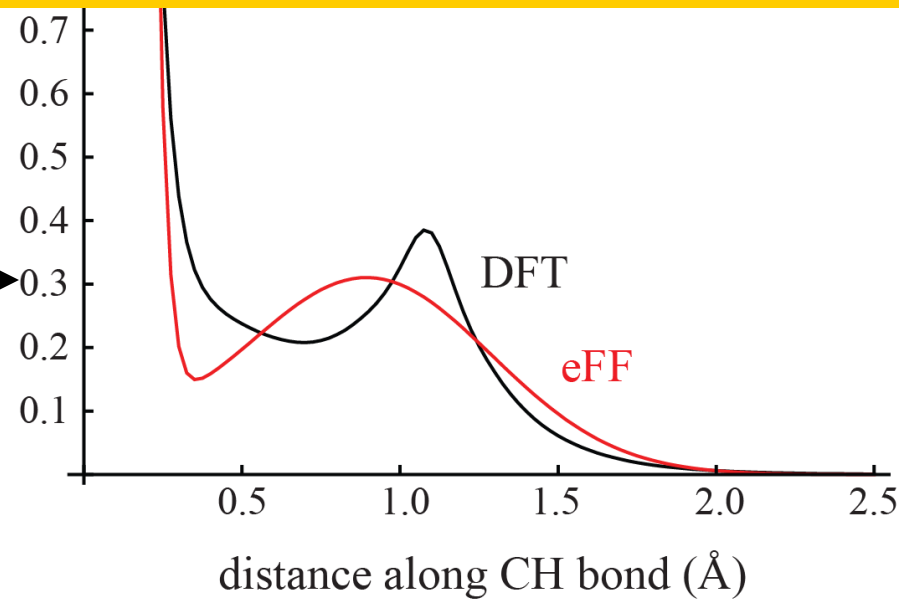

CC bond in ethane
Electron density (bohr^{-3})

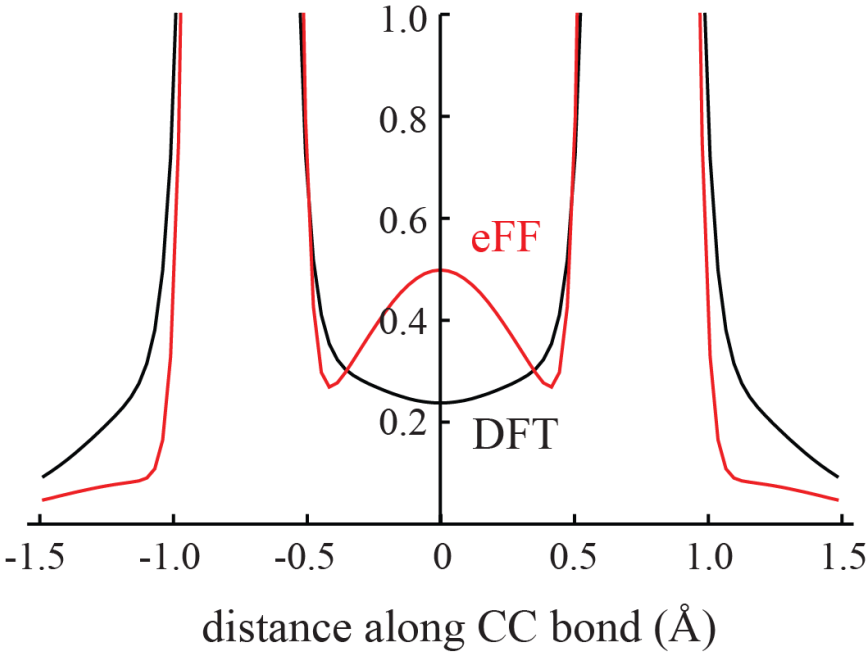

Good overlap between eFF and DFT electron densities

eFF = electron Force Field

Excited Electron Dynamics Modeling of Warm Dense Matter
Julius T. Su and William A. Goddard III, PRL **99,** 185003 (2007)

Simulations practical for 1,000,000 electrons!

eFF has just 3 parameters chosen to describe electron-electron interactions. Fitted to get structures of saturated hydrocarbons

Compare 300K EOS D2 Diamond Anvil experiments with eFF (no adjustable parameters)

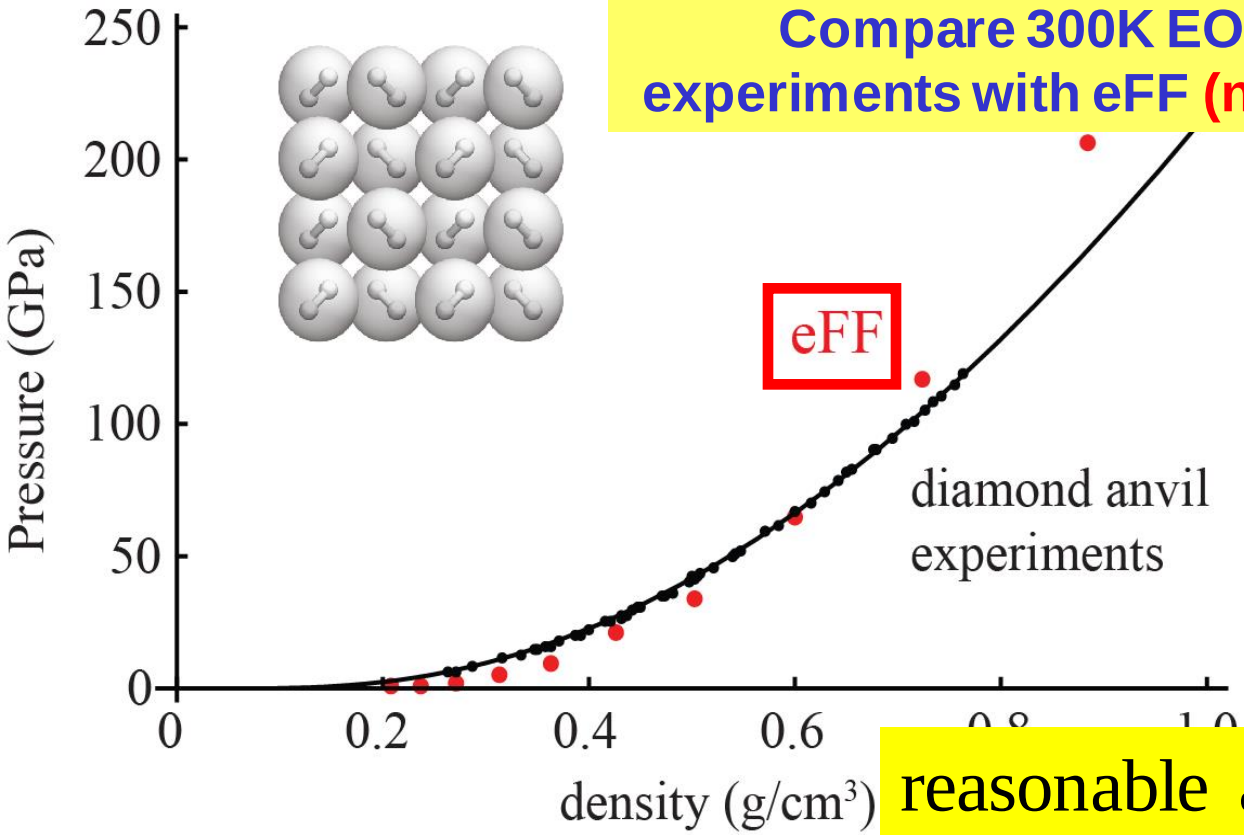

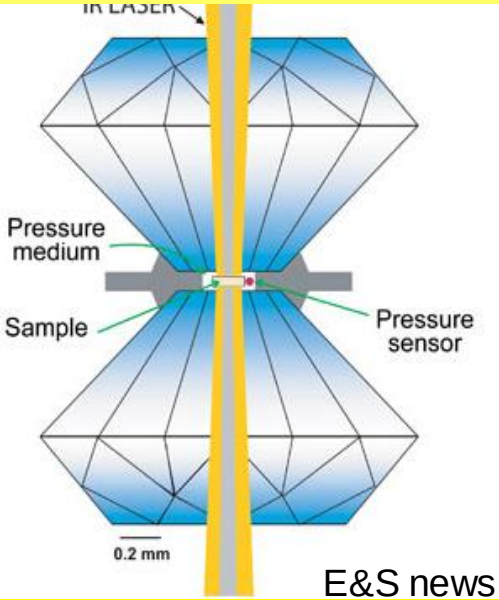

E&S news

reasonable agreement experiment

eFF (no adjustable parameters) reproduces Hugoniot for shock compression of D2

21100 K
Mostly atoms

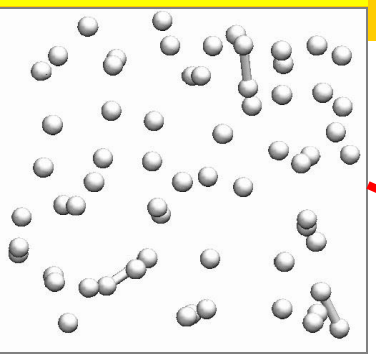

Transition 15400 K

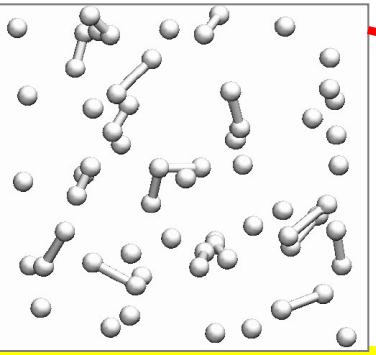

9100 K
Mostly molecules

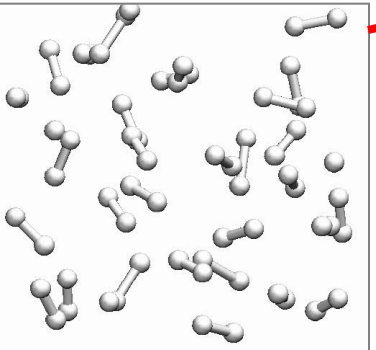

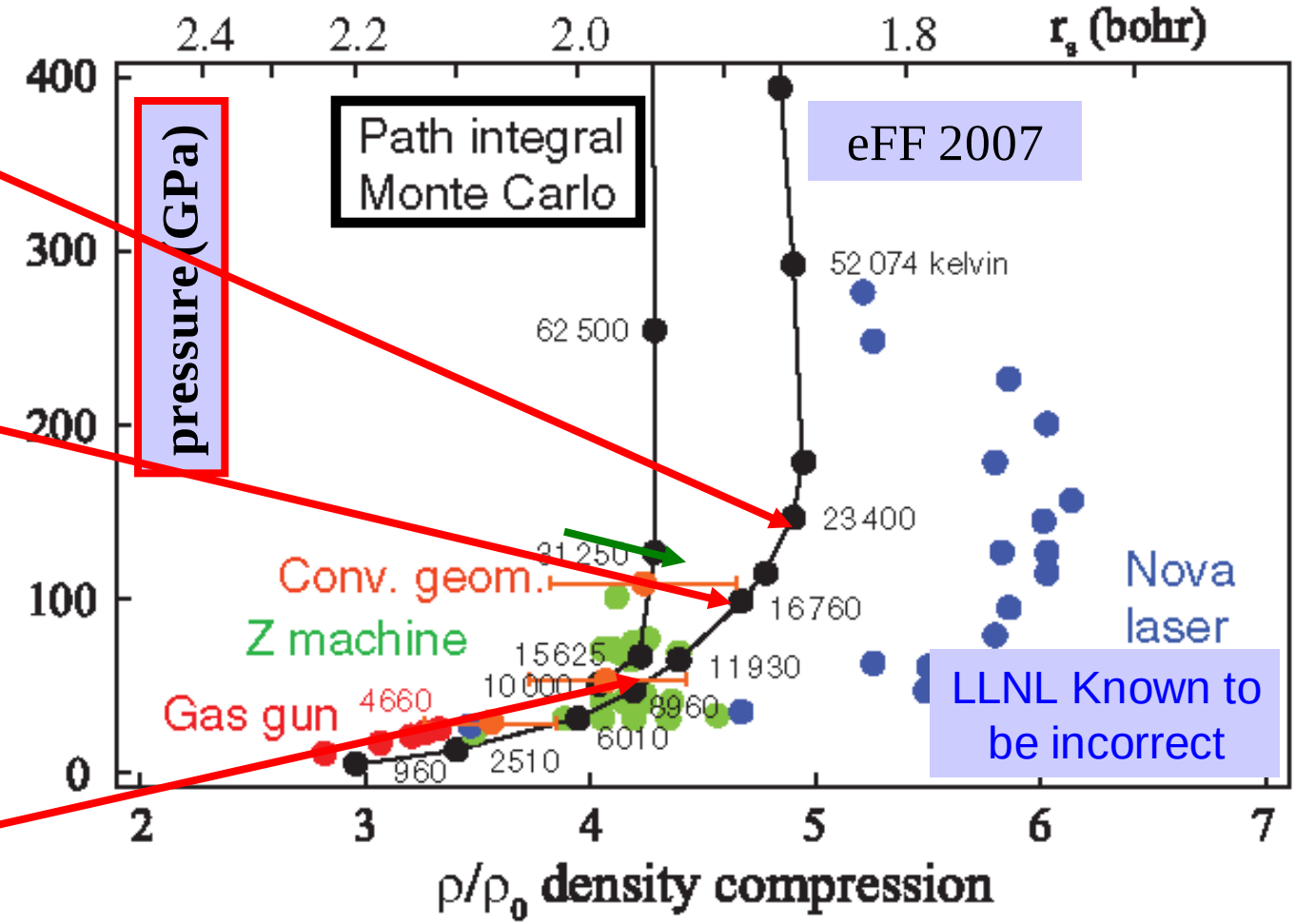

eFF New Paradigm (no adjustable parameters) describes dynamics of electrons, nuclei at short times for large system Su and Goddard PRL. **2007** 99:185003

eFF (no adjustable parameters) reproduces Hugoniot for shock compression of D2

21100 K
Mostly atoms

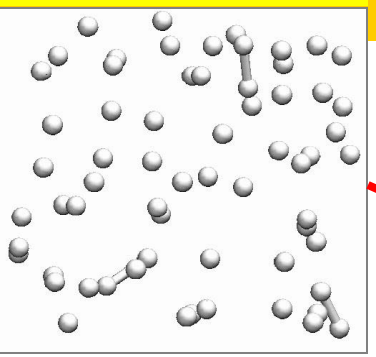

Transition 15400 K

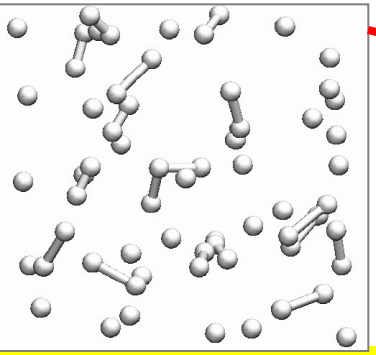

9100 K
Mostly molecules

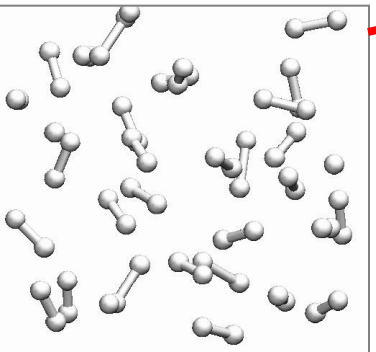

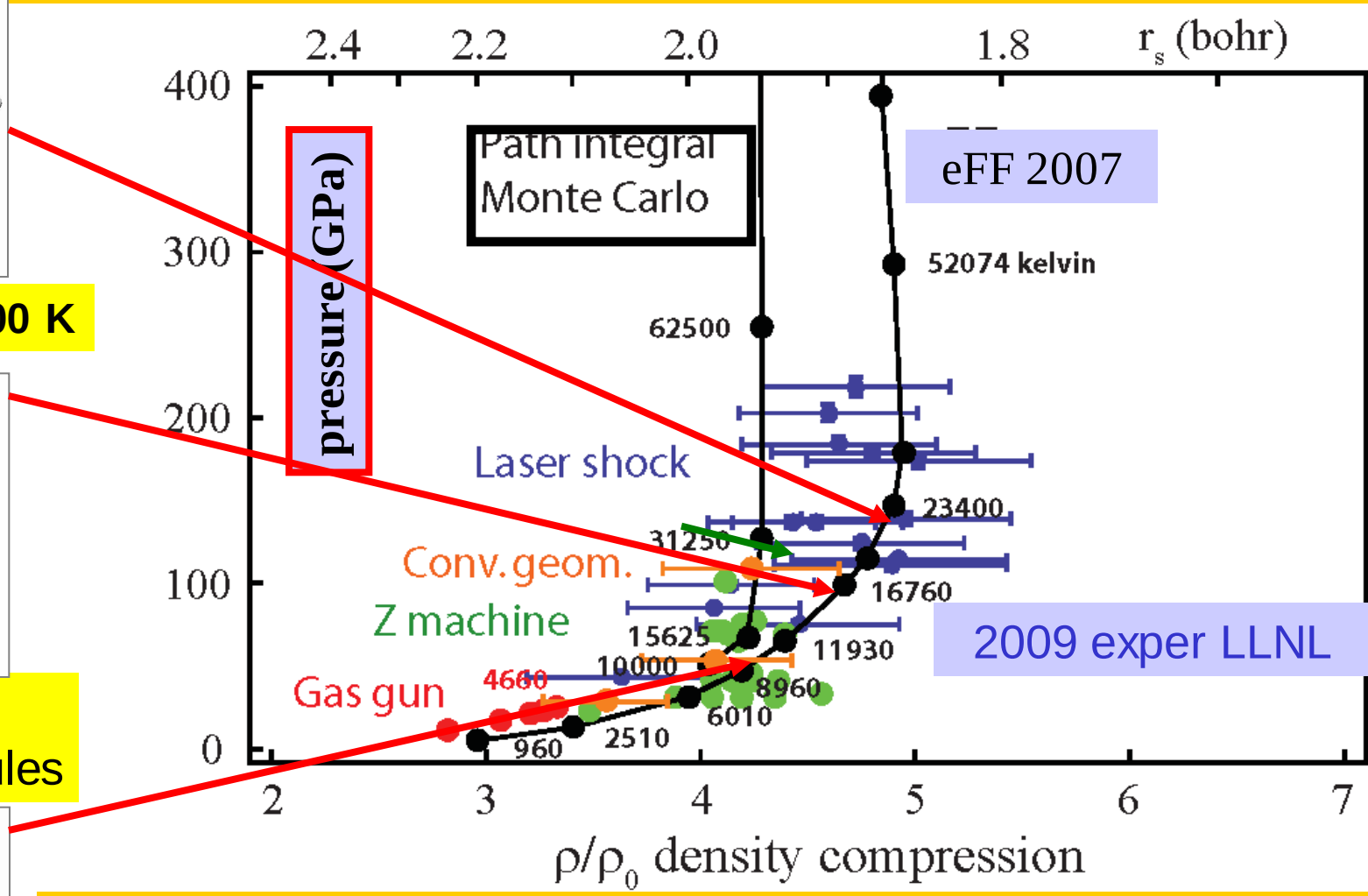

eFF New Paradigm (no adjustable parameters) describes dynamics of electrons, nuclei at short times for large system Su and Goddard PRL. **2007** 99:185003

Auger dissociation processes

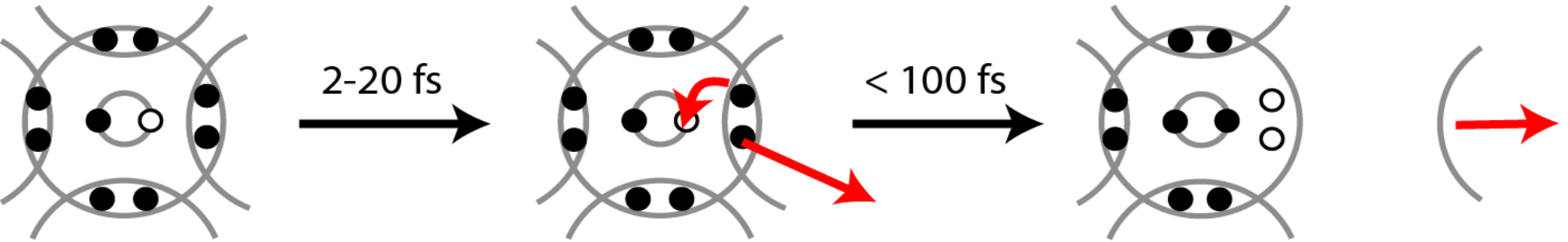

core hole filled,
2° electron ejected

two-hole state dynamics

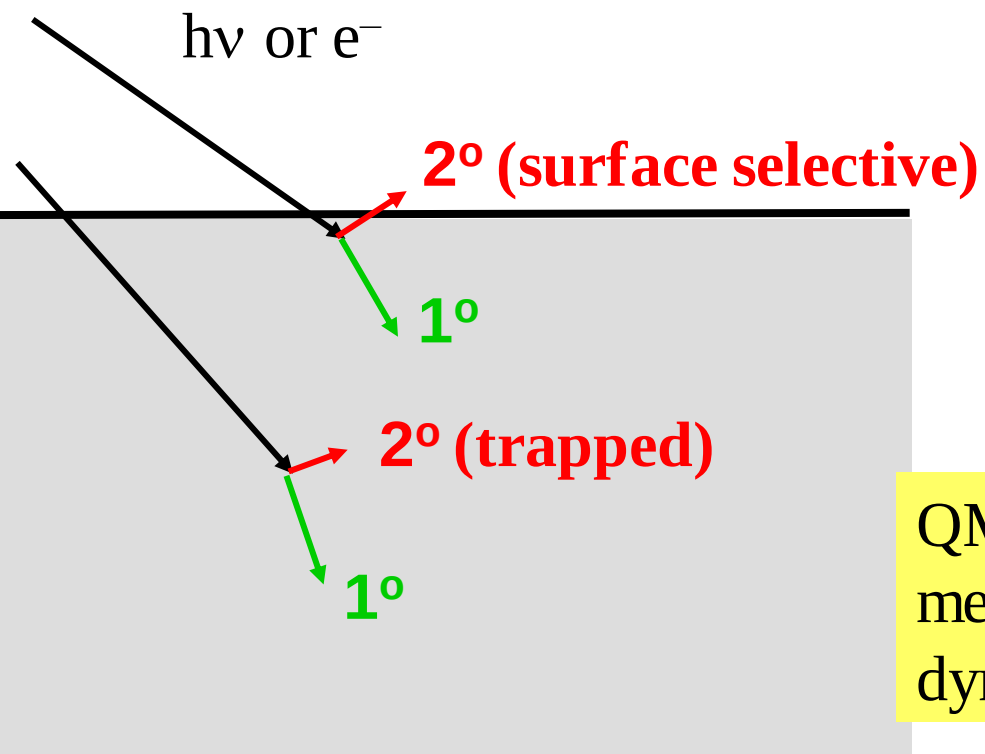

Key step in electron/photon stimulated desorption

QM can compute spectra, but no method to follow dissociation dynamics.

eFF Description of Auger Decay (Ionize C1s electron, follow decay as one electron fills hole and other is ejected)

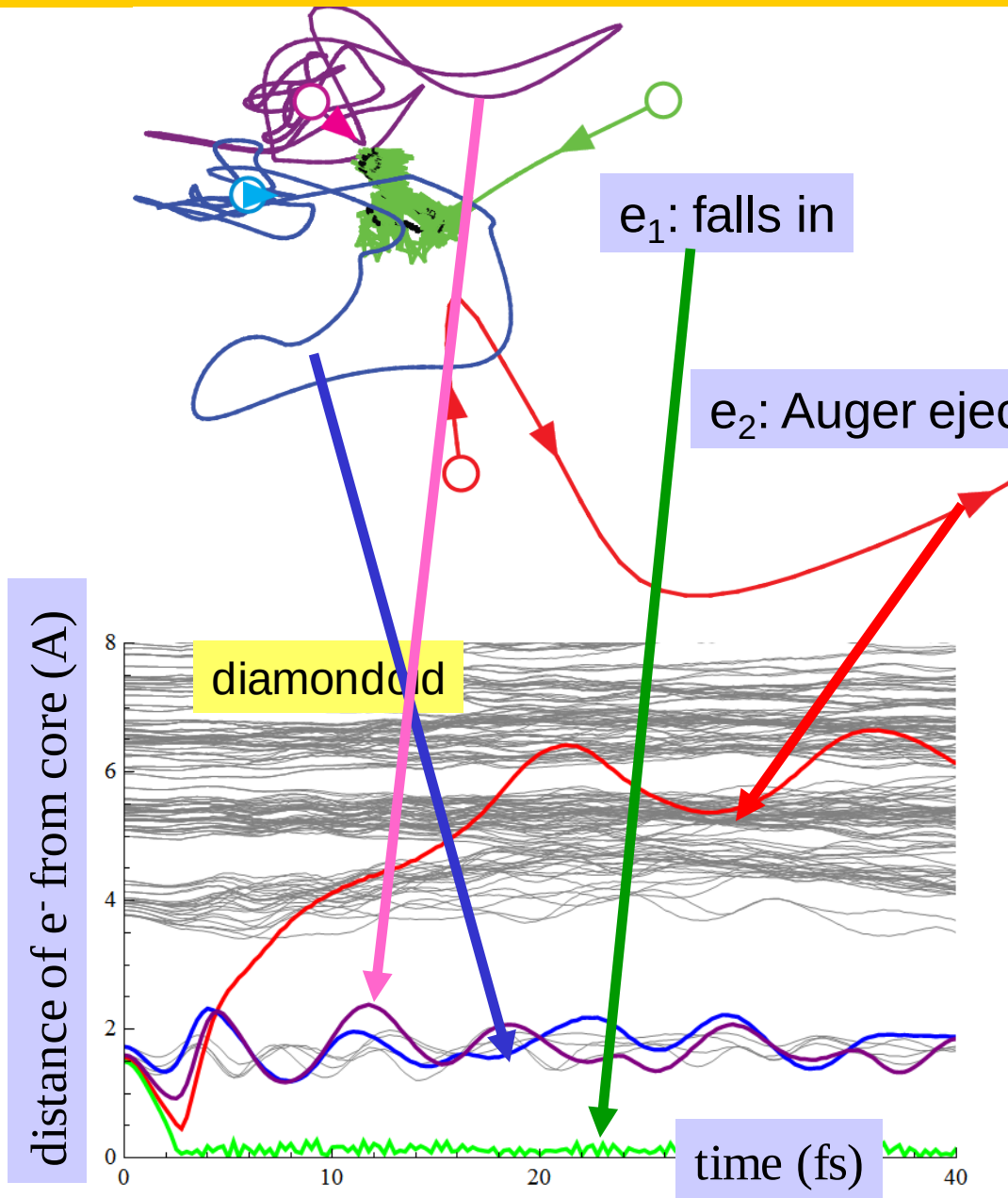

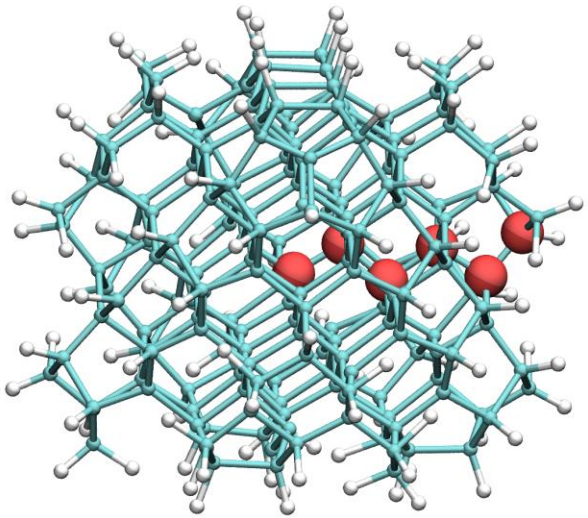

First 2fs, 4 electrons all move toward + charge of nucleus

Then green electron wins filling core hole at 2.9fs, while other 3 move away (Pauli Principle)

Then at 5-10 fs, red electron is kicked out while blue and purple electrons oscillate

Dynamics of the Auger process for 100 fs

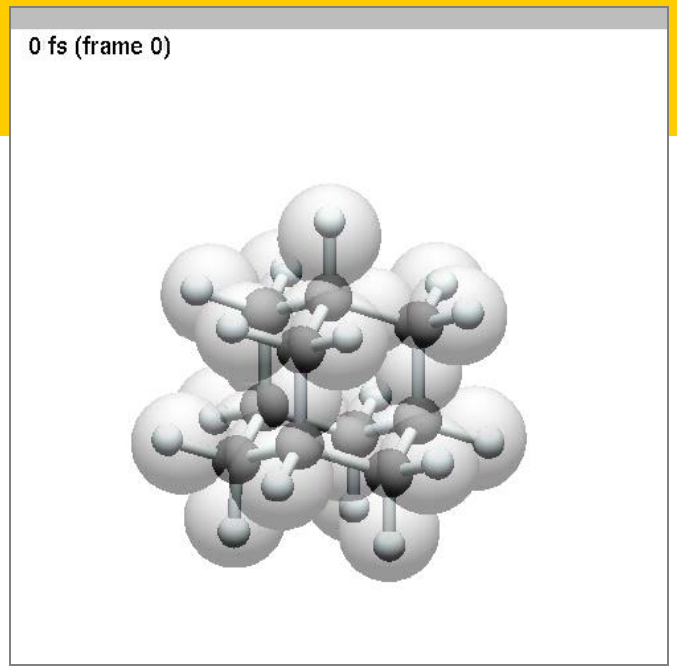

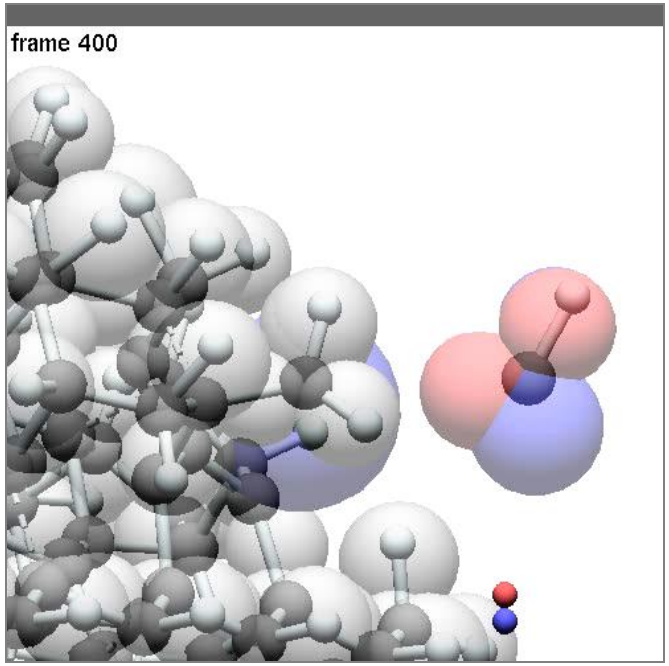

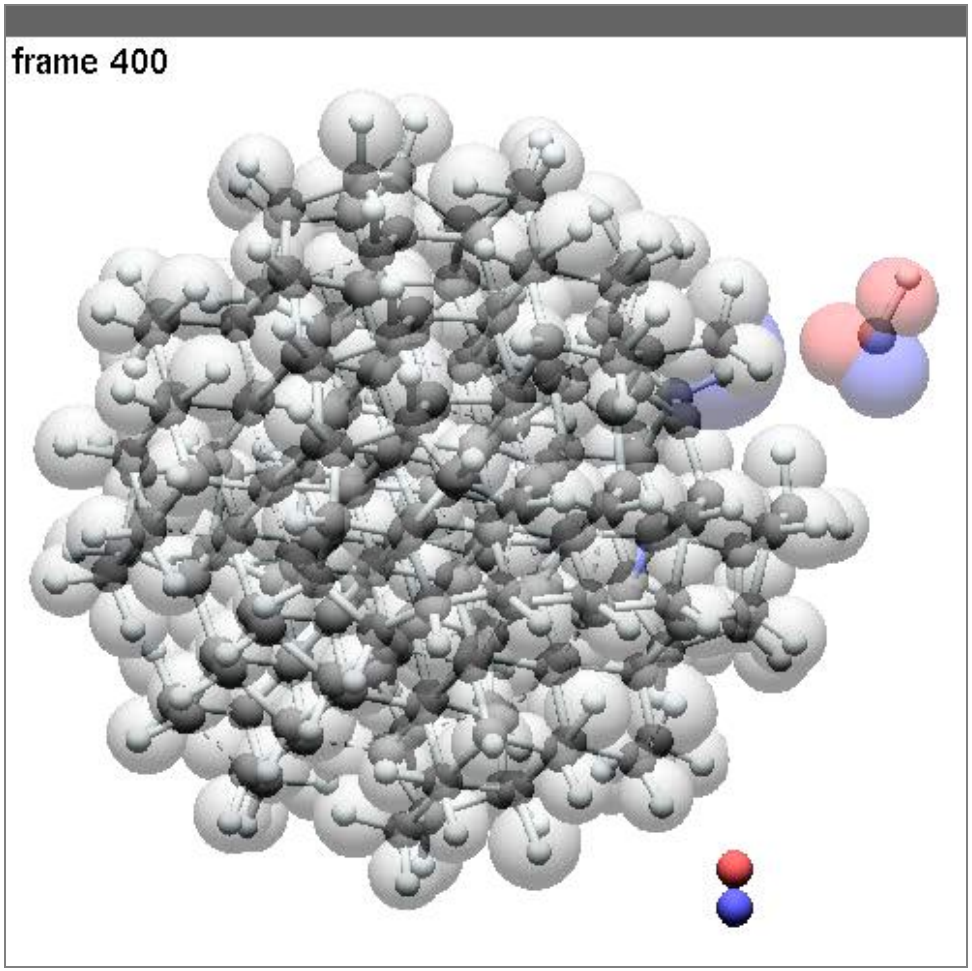

Photon-stimulated desorption of H on H-terminated diamond

Hoffman and Laikhtman, photon stimulated desorption – J. Phys. Conden. Mat. **2006** 18:S1517-S1546

Observation of indirect vs direct processes

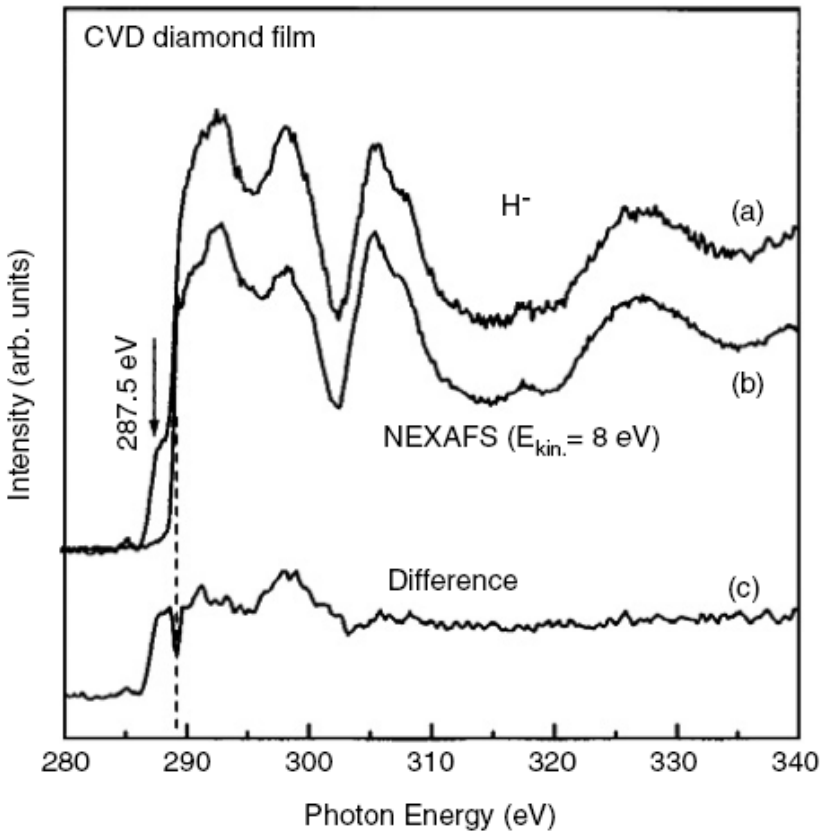

of H^- ions (both processes)

of slow electrons (indirect process)

Difference = ions from direct process

H^+ from direct Auger process at surface,
H^- from bulk process mediated by slow electrons
No measurement of H neutrals or CHn fragments

Origin of fragments after surface Auger excitation

Excite red atom (carbon of surface CH)

average # of fragments from each atom (>1000 trajectories)

Selective bond breaking:

7% CH_2 of adjacent site

13% CH of excited atom

86% H on excited atom

80% C of exited atom

82% Remote H (interstitial)

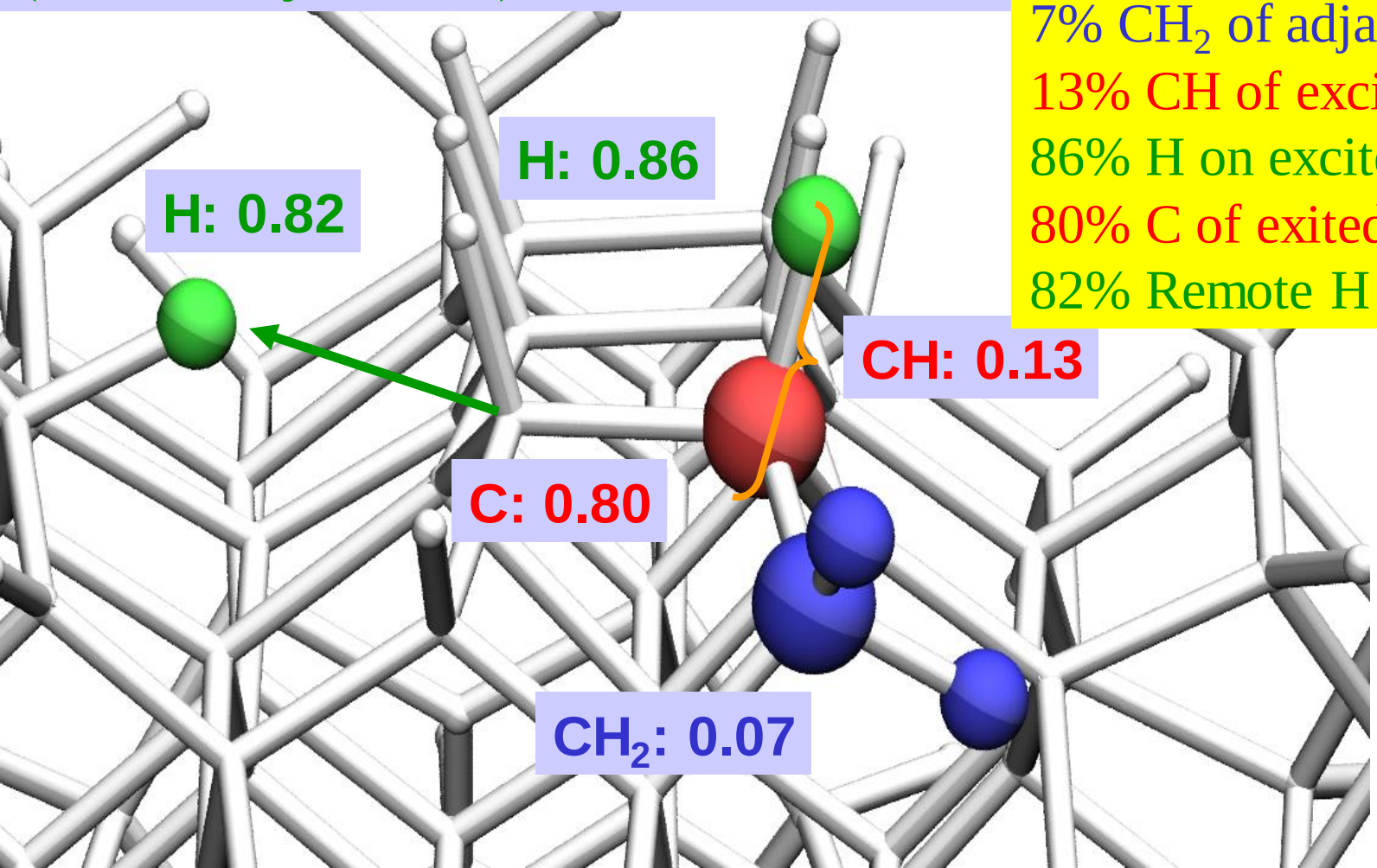

eFF finds Direct ejection of Proton, but 1/3 have electron hop on as leaving

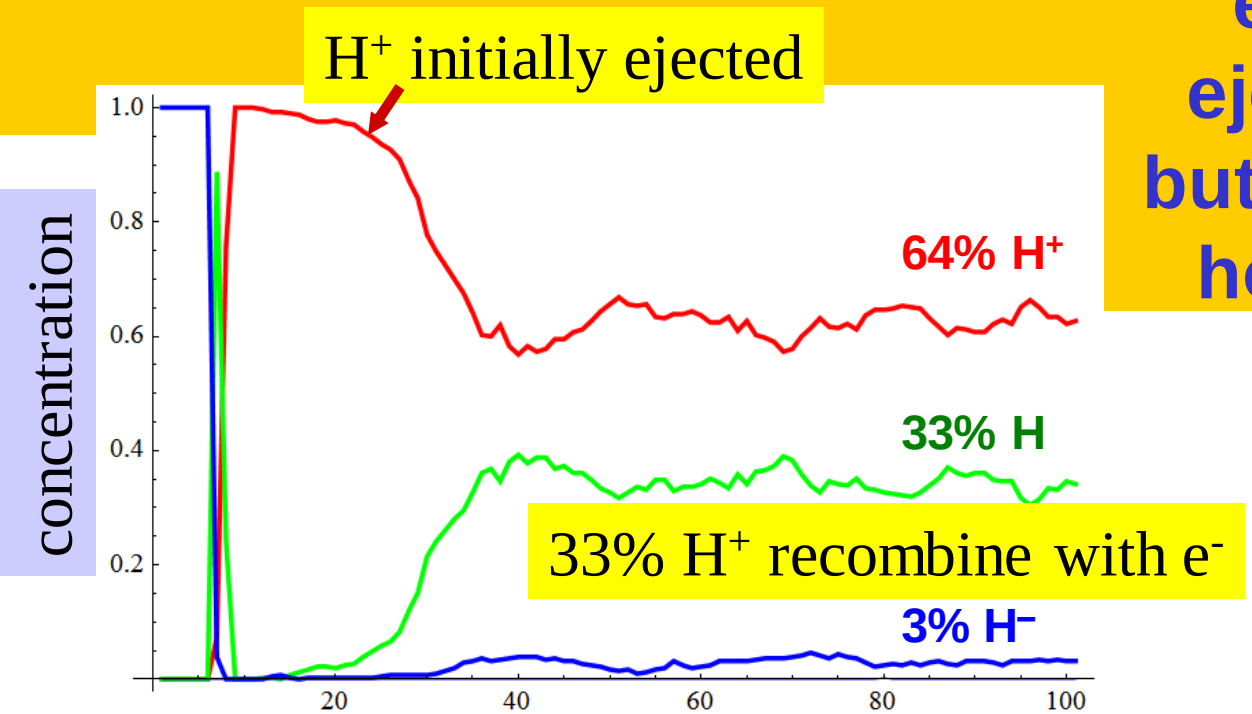

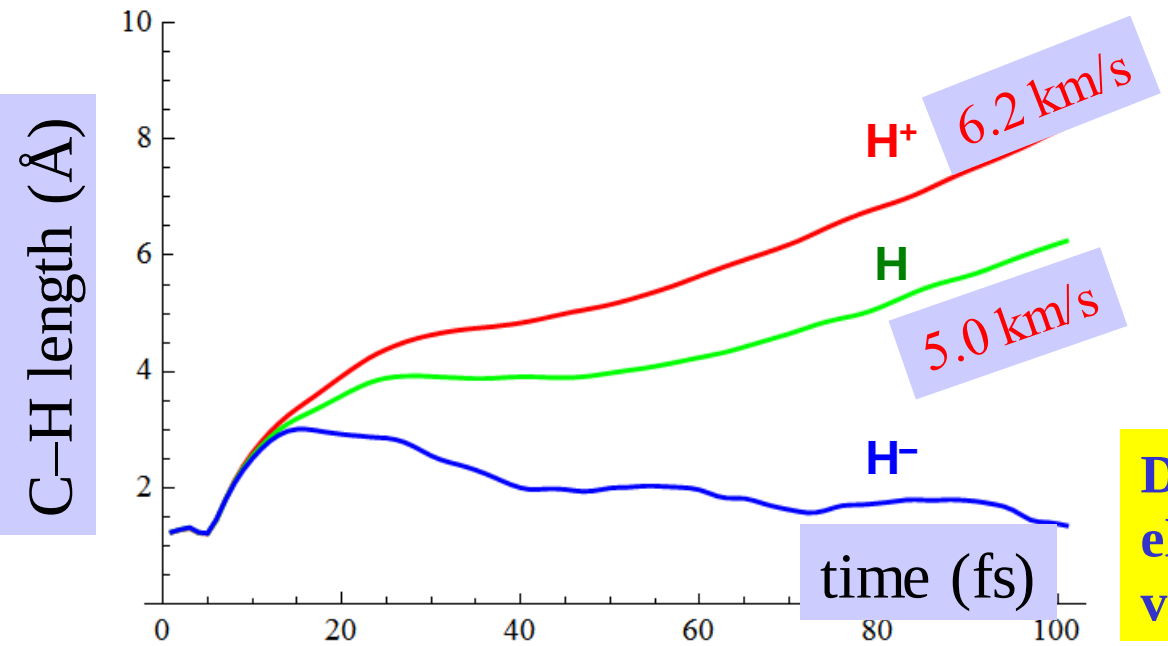

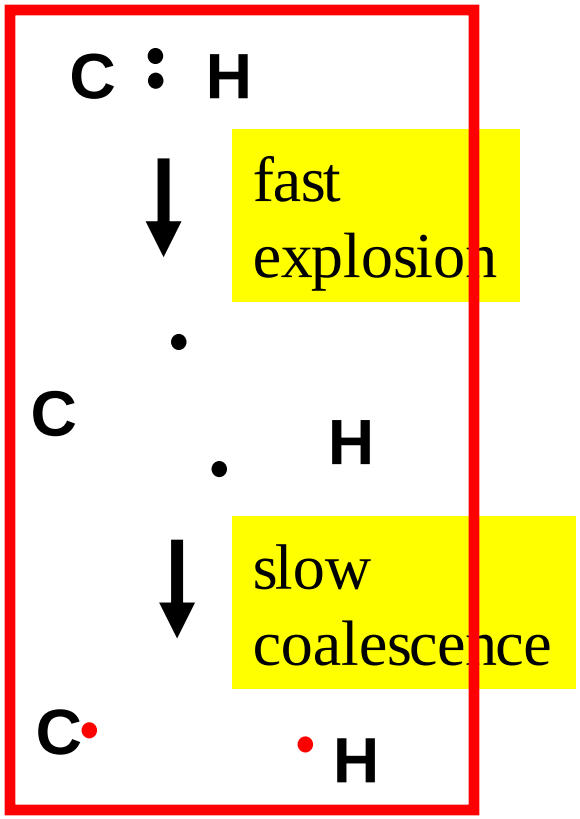

Do NOT eject both valence electrons as in KF, they remain in vicinity and control processes

Desorbed species from diamondoid nanoparticle

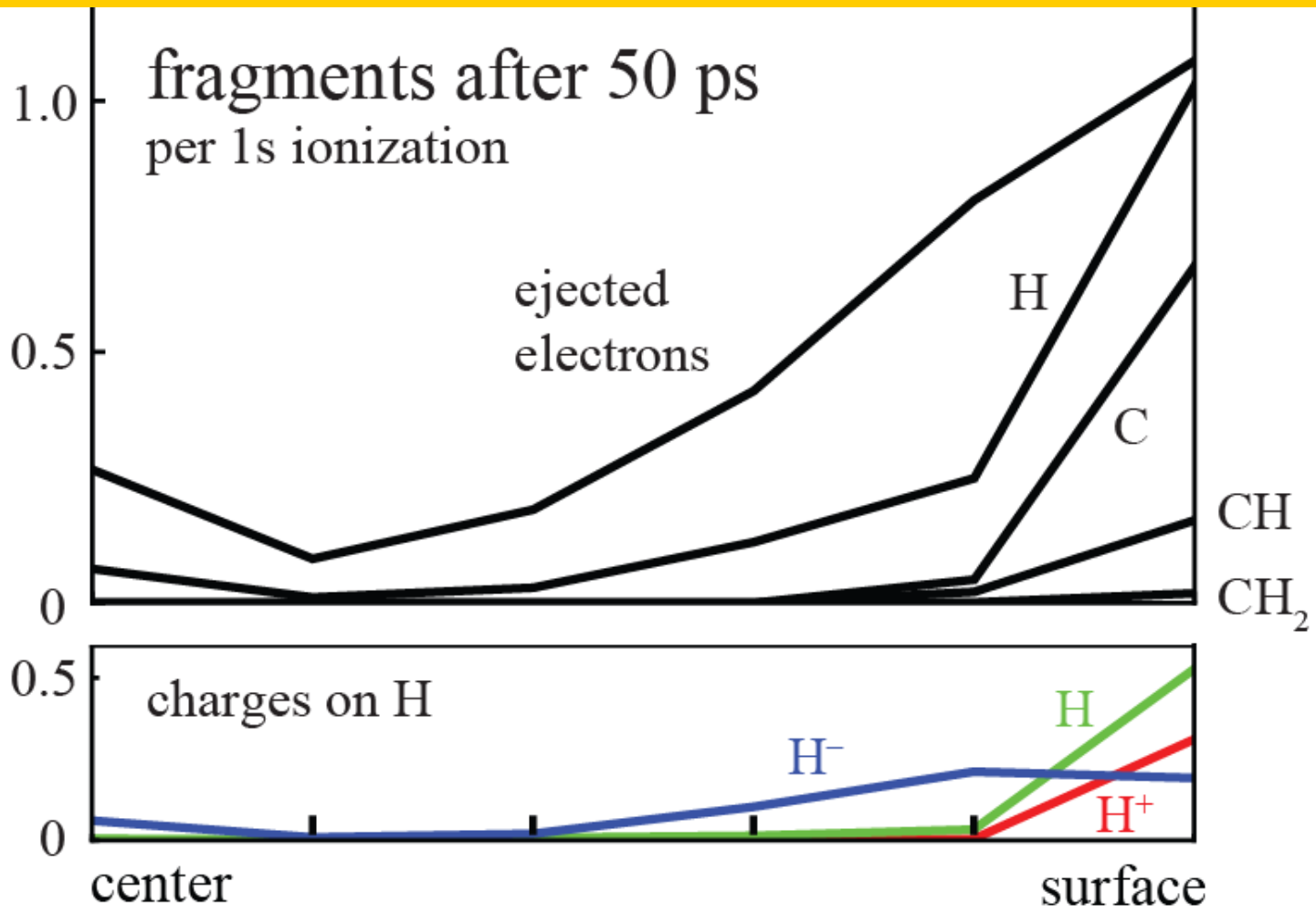

H/H^+ from surface excitations,

H^-/slow electrons from bulk excitations

CHn fragments only from surface ➔ smoothly etched surfaces

WATER NEEDS – Global Challenge

- **Contaminated groundwater**
- **Industrial wastewater**
- **Energy production**
- **Mineral recovery**
- **Ultrapure water**
- **Domestic wastewater**
- **Agricultural uses**
- **Drinking water**

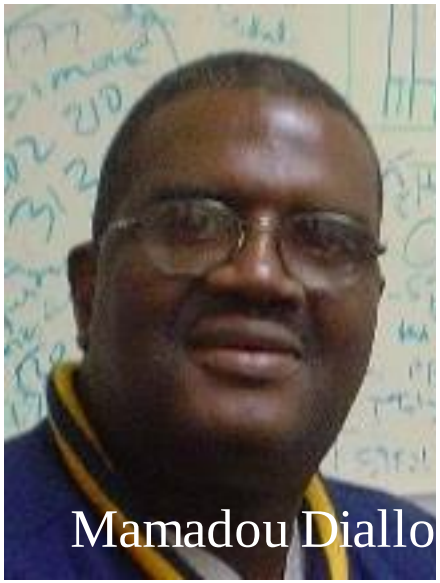

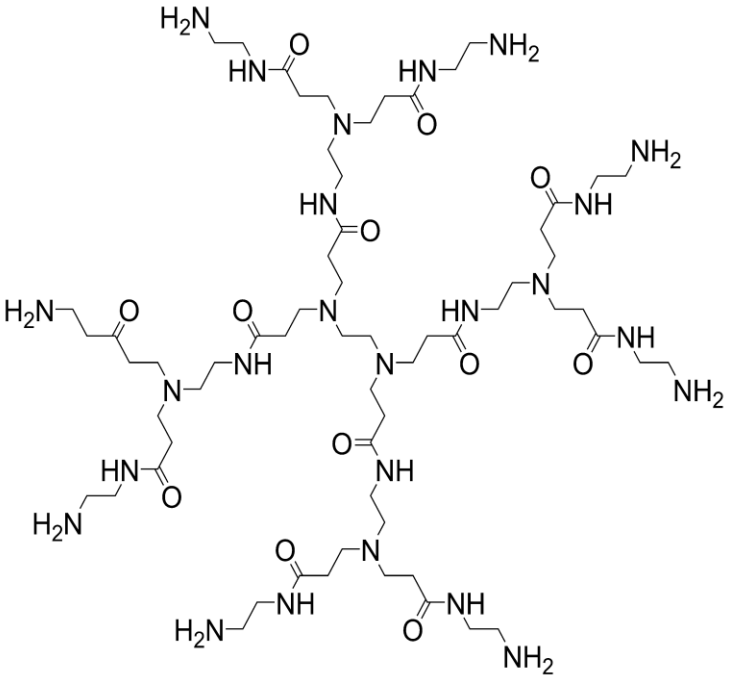

Solution: Water Treatment using Dendrimer Enhanced Filtration

old 036

Limitations of Current Technologies

Technology	Limitations
Reverse Osmosis (RO)	Non-selective; relatively high energy requirements, capital and O&M costs; limited water recovery; concentrated waste
Ion Exchange (IX)	Limited selectivity, not cost effective at high contaminant concentrations, high O&M costs, large waste volume
Microfiltration & Ultrafiltration (MF/UF)	Does not remove dissolved ions and small organic contaminants
Biological Treatment	Limited to biodegradable contaminants, not effective at high contaminant concentrations and volume, difficult to control

Caltech Solution:
Selective Encapsulation and Release/Destruction

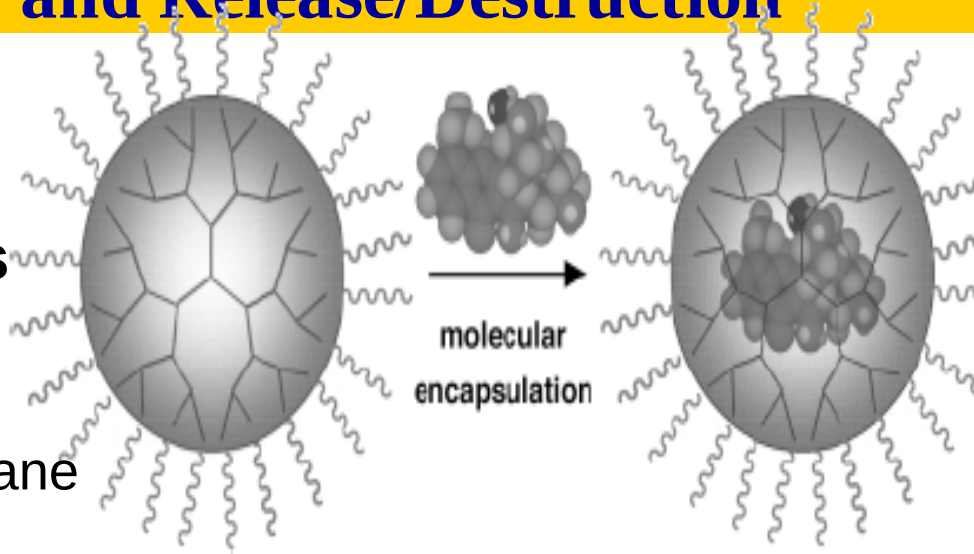

Low-cost dendrimer-like macromolecules (captymers with tunable contaminant binding sites

- Size allows for low pressure membrane (MF/UF) separation
- Easily integrated into existing treatment systems
- Scalable – for small and large scale applications
- Adaptable platform technology
  - Cations
  - Anions
  - Organic compounds
  - Water-borne bacteria and viruses
  - Catalysts for contaminants

What is special about dendrimer?
Can design in special chemical character inside or outside

Generation 4

64 primary amines on outside

plus 62 tertiary amines on inside

Plus 62 amides on inside

At pH> 10 the whole dendrimer is neutral

At pH ~ 7-8 get 64 protonated primary amines

At pH < 6 get also 62 protonated tertiary amines for a total charge of 126 on one molecule!

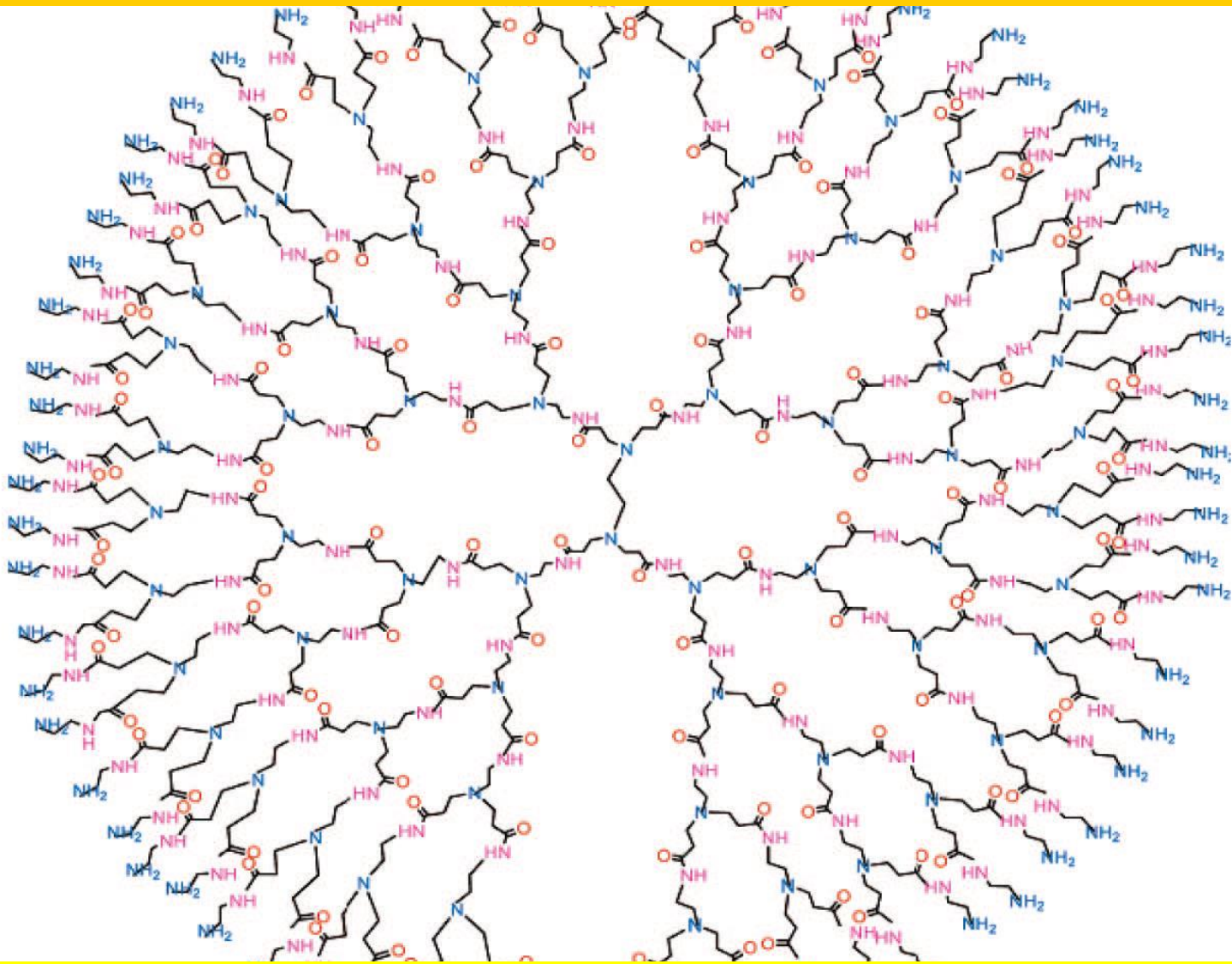

Can tune to bind metals (Cu, Fe, Cr, Hg, U, Pt) at one pH and the recover dendrimer by rejecting ions at another pH

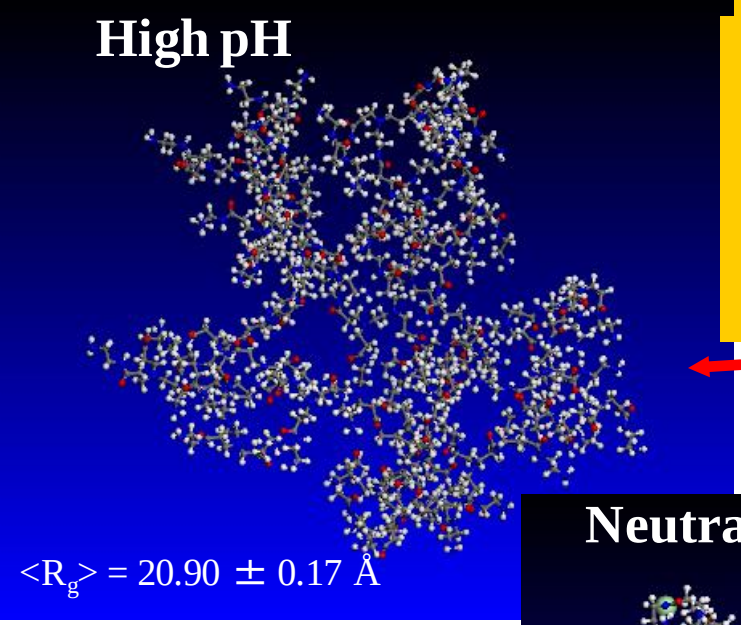

Actual structure from simulation

Oversimplified picture of dendrimer

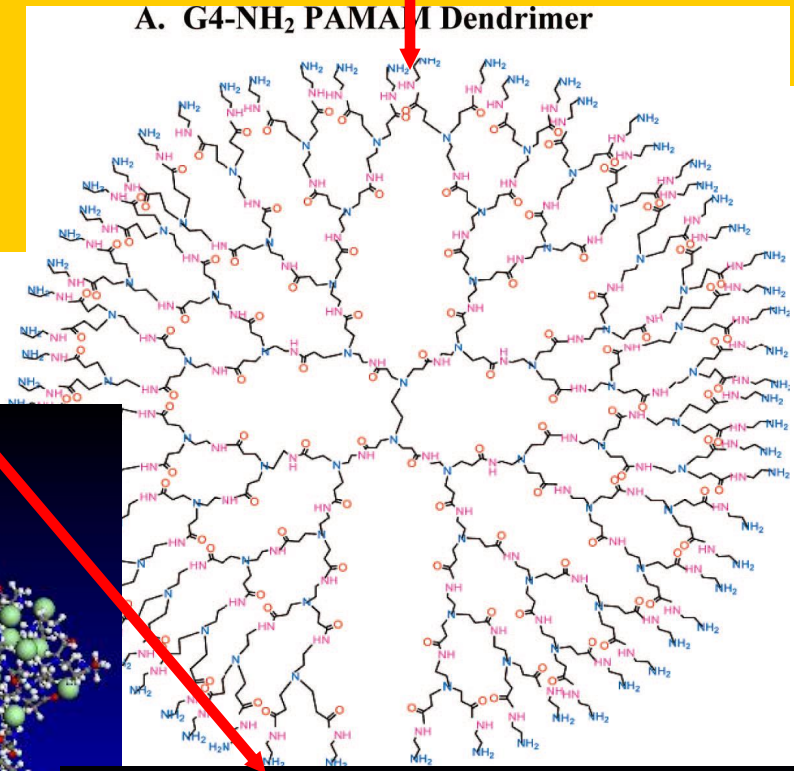

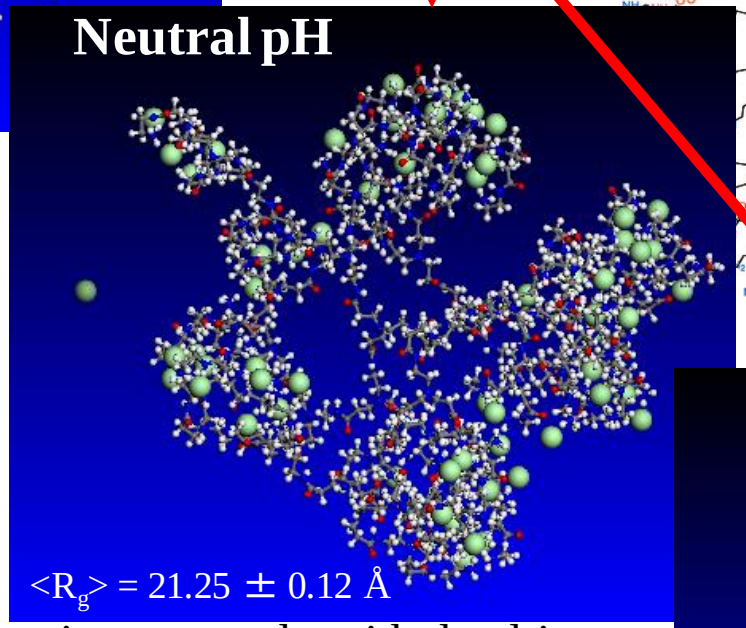

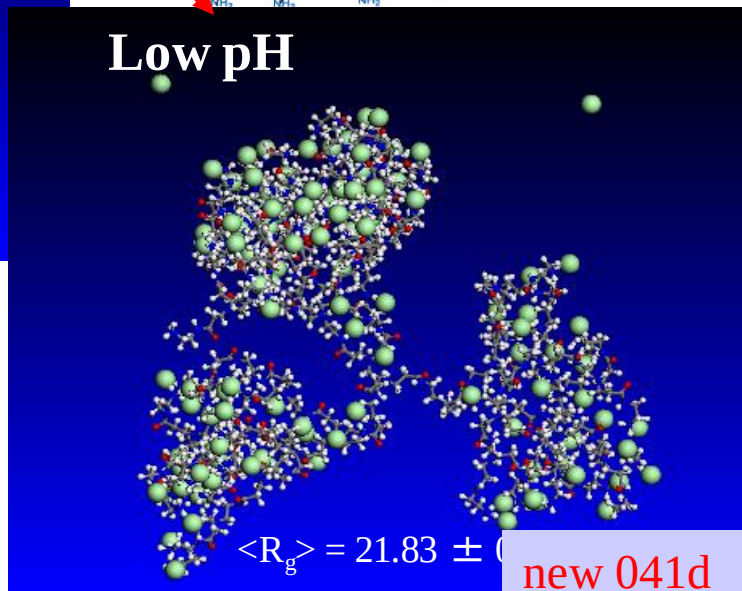

- ❑Size (Radius of gyration) of PAMAM remains essentially invariant as pH changes from 12 to 2.
- ❑This surprising result arises because:

1. Counterions (Cl-) associates strongly with dendrimer in vicinity of protons. Screening of counterions prevents the swelling of protonated dendrimer.
2. PAMAM backfolds locally at the periphery of dendrimer opening the surface and hollow interior.

new 041d

Process Schematic for Selective Encapsulation and Release of Contaminants (e.g., Anions) from Water

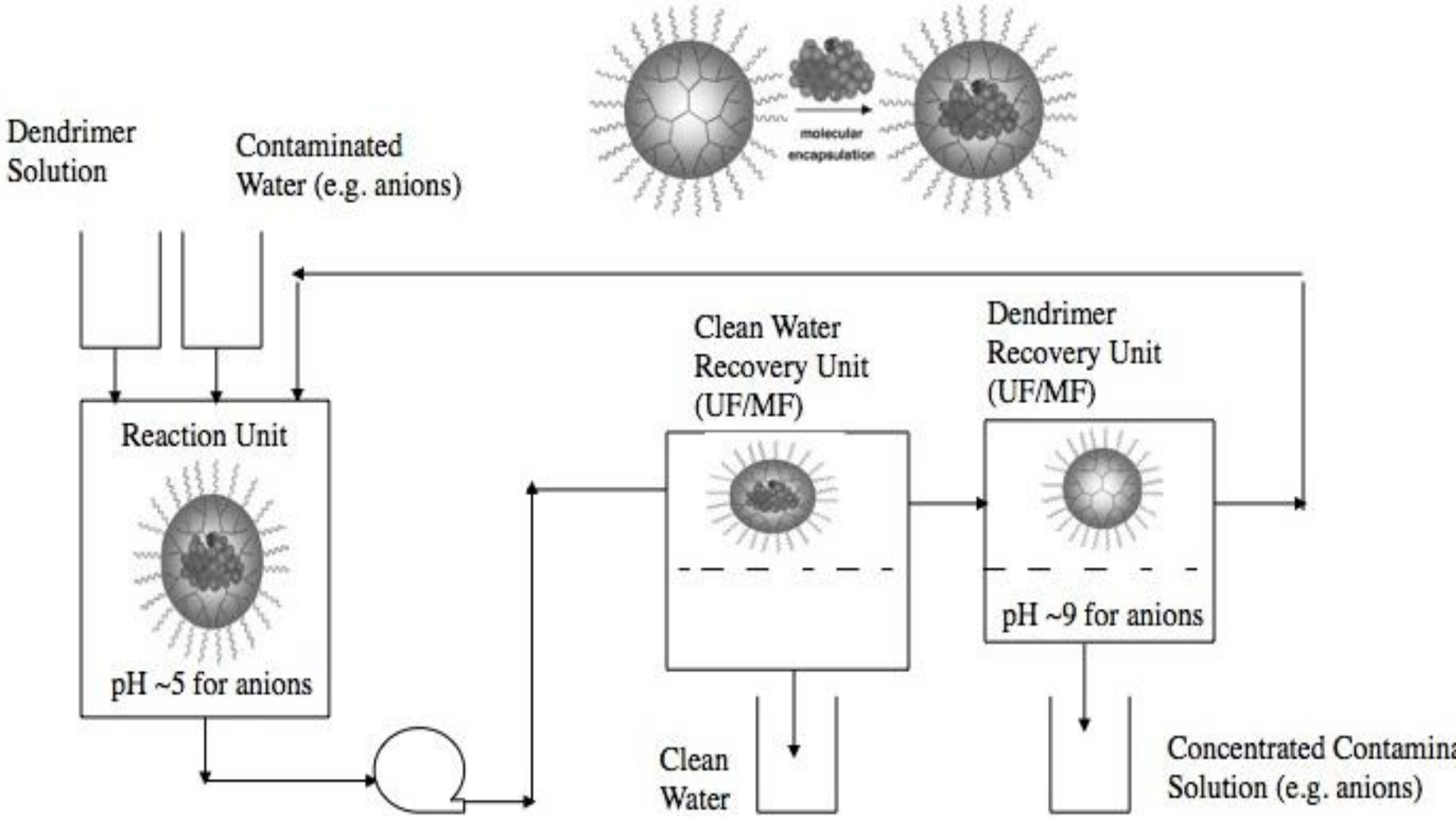

UF: Ultrafiltration MF: Microfiltration

CAPTYMER MEDIA VERSUS ION EXCHANGE RESIN: KEY DIFFERENTING FEATURES

A. Captymer IX Type Media

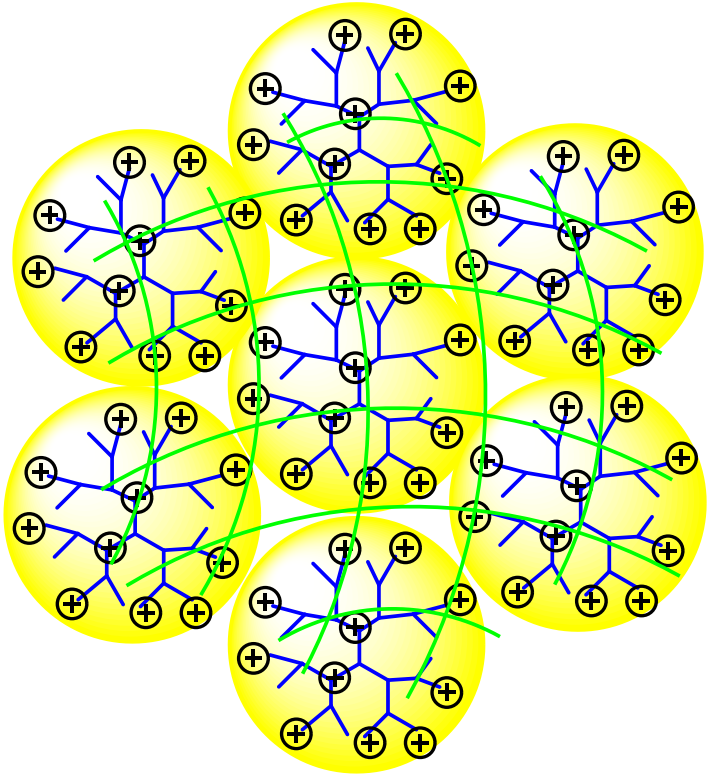

Porous network of hyperbranched macromolecules with large number of exchange sites dispersed throughout the network

B. Ion Exchange Resin Bead

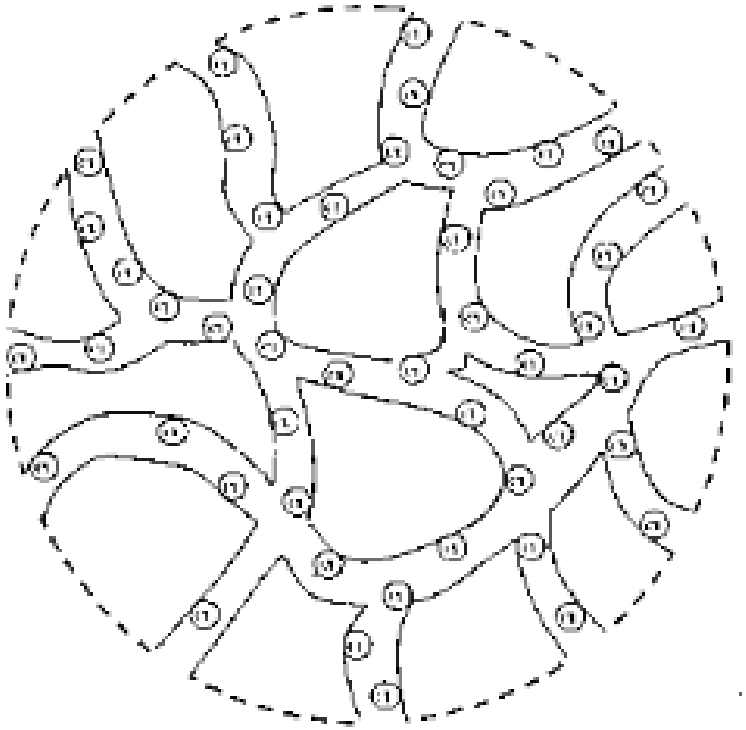

Macroporous copolymer bead with limited number of exchange sites fixed at selected positions within the bead

48

EXTRACTION OF SOLUTES FROM WATER BY SELECTIVE ENCAPSULATION

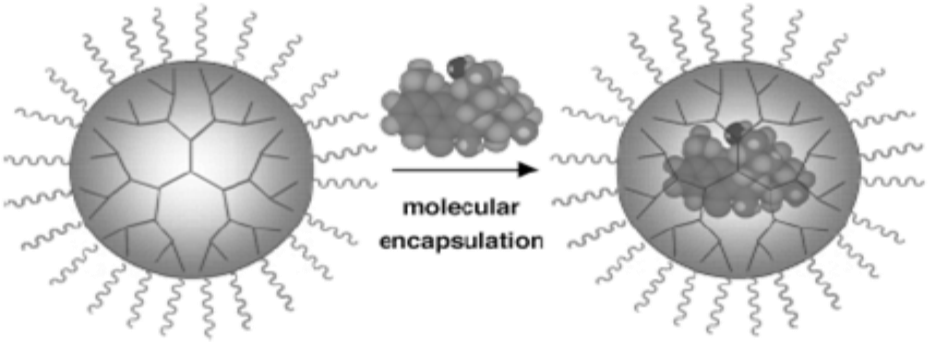

Captymer™: Branched macromolecules & particles (media) with tunable capture sites and multiple functionalities

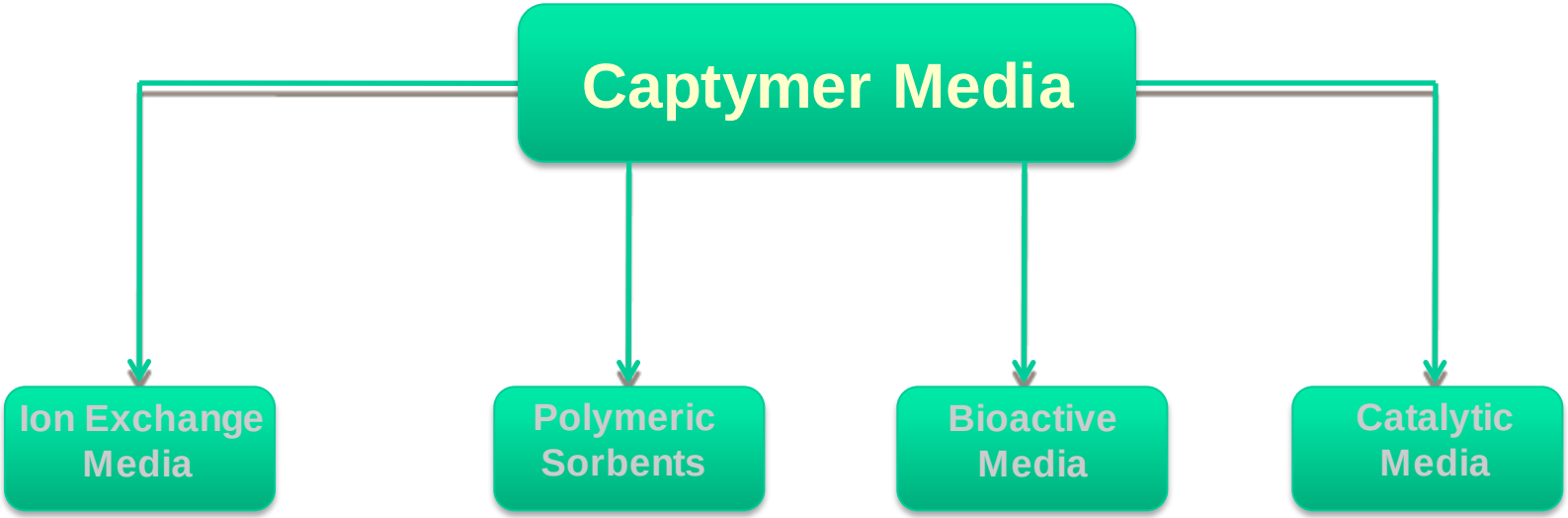

Metal Organic Frameworks (MOF) and Covalent Organic Frameworks (COF) for molecular storage and extraction (H_2, CH_4, CO_2, O2, H_2S)

Hydrogen storage systems

2010 Sang Soo Han

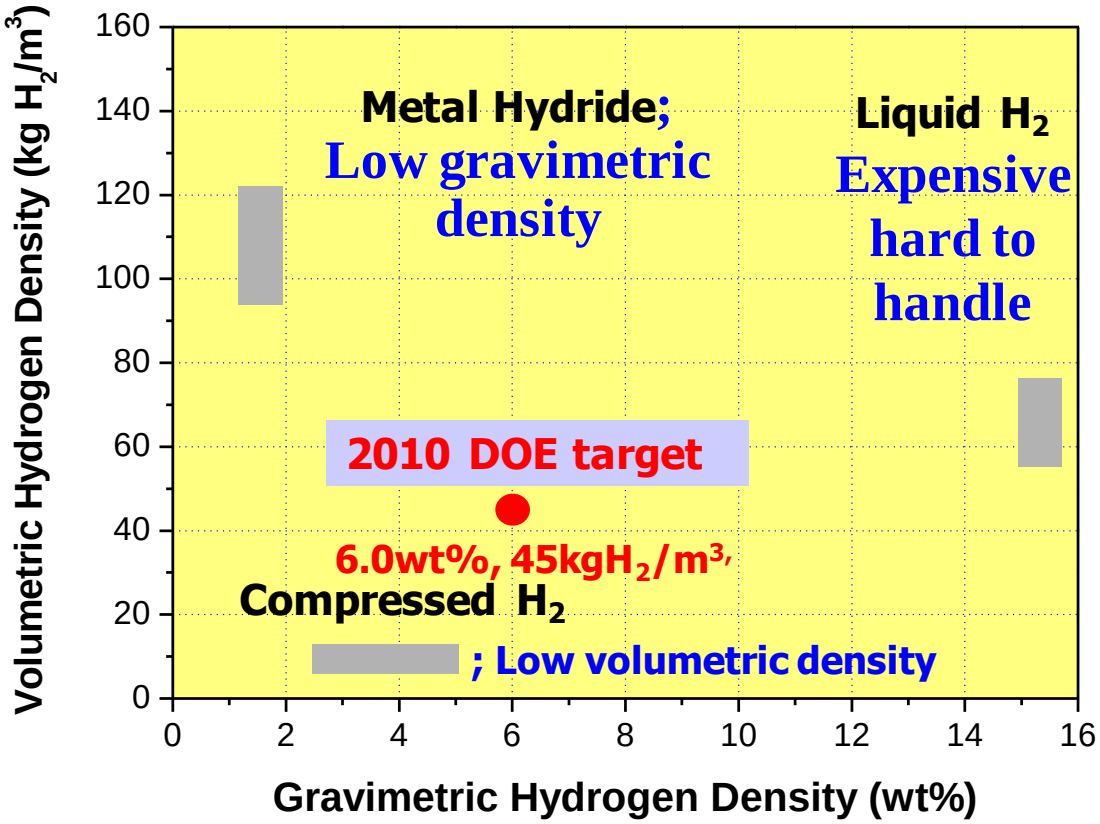

- High gravimetric/volumetric storage density
  (>6.0 wt%, >45 gH_2/L)
- Working condition
  (<100 bar, -30-85 ℃)
- Low cost and high chemical stability

New hydrogen storage medium is required

Metal Organic Framework (MOF)

- **Crystal structure** (M. D. Ward, Science, 300, 1104, ***2003***)

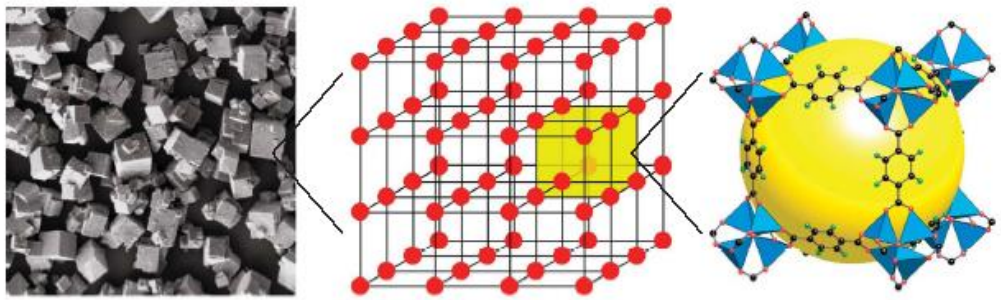

Cubic inside and out. The external shape of microscopic MOF-5 crystals (**left**) reflects their well-defined cubic lattice (**middle**). The structure consists of $[OZn_4]^{6+}$ clusters and organic connectors, with persistent pores that are continuous in three dimensions (**right**).

- Organic linkers

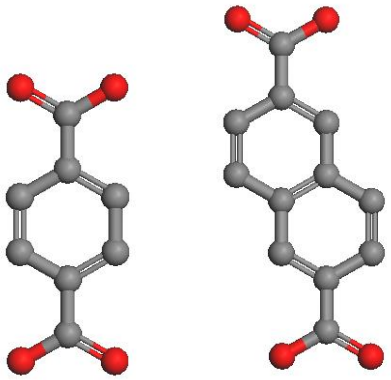

BDC (MOF-C6) **NDC (MOF-C10)**

- **Atomic structures of cubic MOFs in this work**

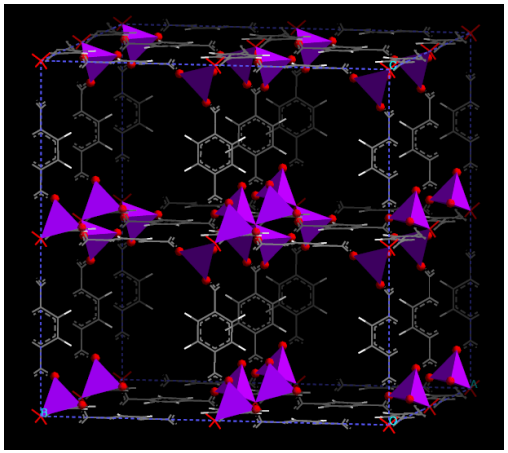

- Metallic node

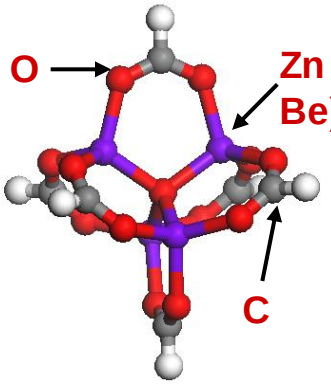

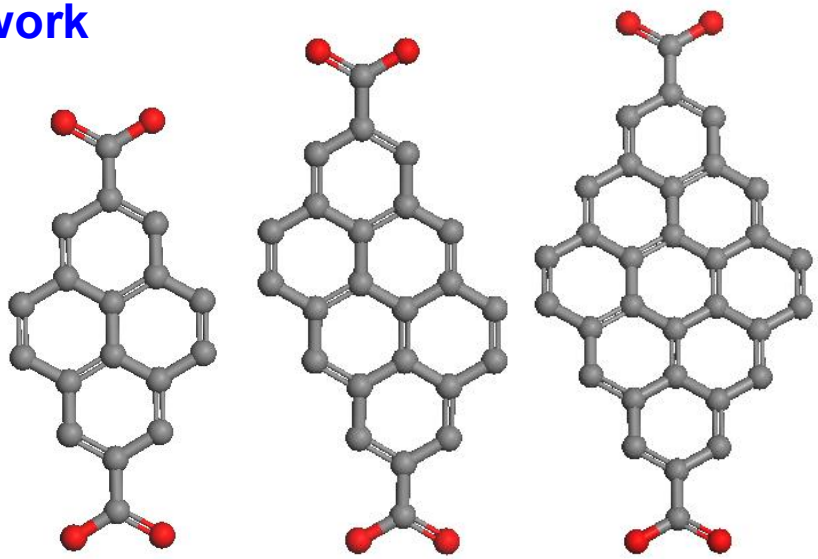

PDC (MOF-C16) **PDC1 (MOF-C22)** **PDC2 (MOF-C30)**

To assess performance must predict binding of H_2 as function of Temperature and Pressure

Use Grand Canonical Monte Carlo (GCMC) method to predict the amount of H_2 bound at various pressures and temperatures

GC-MC method:

In GC-MC the chemical potential (μ) is fixed while the number of molecules fluctuates. Equilibrium is achieved when the temperature and chemical potential of the gas inside the framework are equal to free gas outside.

We start with the pure framework (no H_2) as the starting configuration, each subsequent configuration is generated by one of four moves:

1. A molecule is created at a random position. The new configuration is accepted with probability P

$$P = \min\left[1; \exp\left(-\frac{\Delta E}{kT} - \ln\frac{(N_i+1)kT}{V}\right)\right]$$

2. A random molecule is destroyed.
3. A random molecule is translated a random amount and kept with probability P
4. A random molecule is Rotated a random amount and kept with probability P

When converged have a Grand Canonical Ensemble of structures for the given μ, T, p

Validation of the developed force-field

- **Comparison of simulated and experimental isotherms for Zn-MOF-C6 at 77 K**

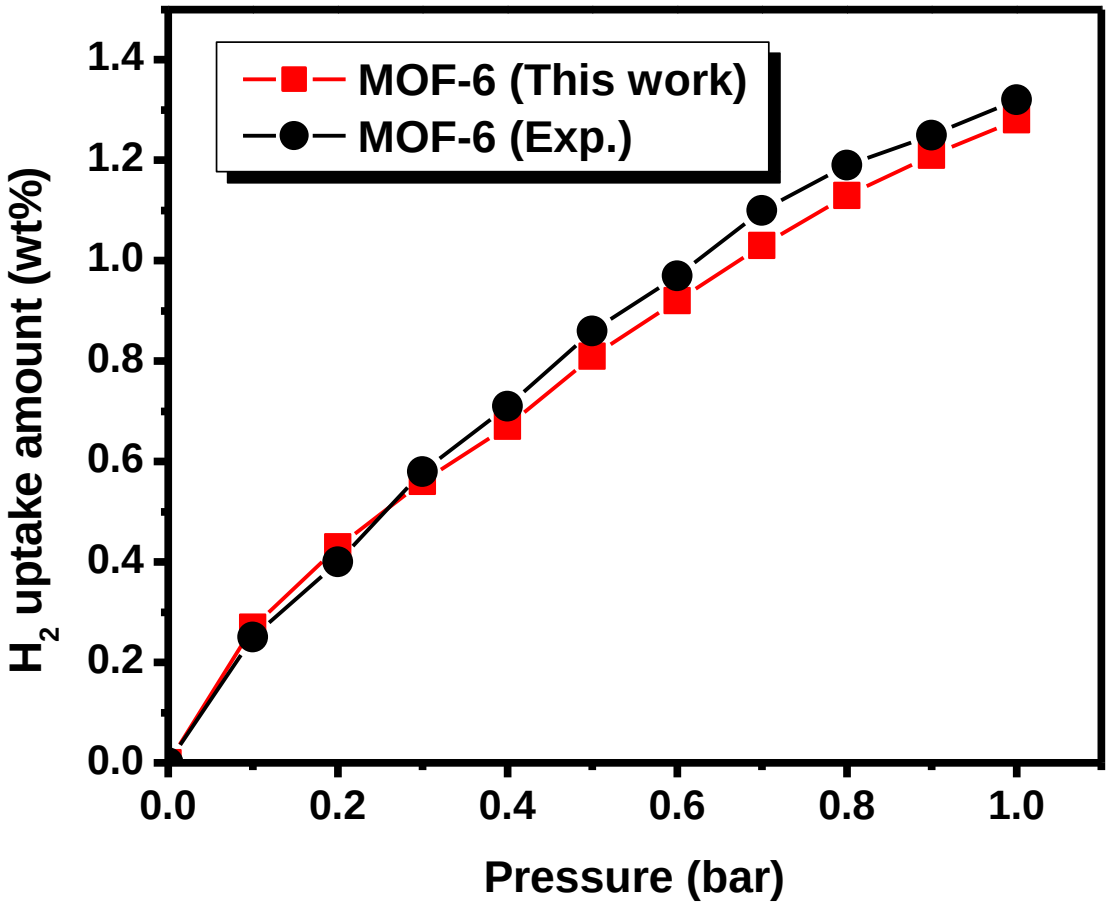

Good agreement with experiment

Rowsell et al., JACS 126 (2004) 5666.

Hydrogen storage in Li-doped Zn-MOF systems

At 300 K get up to 5.3%

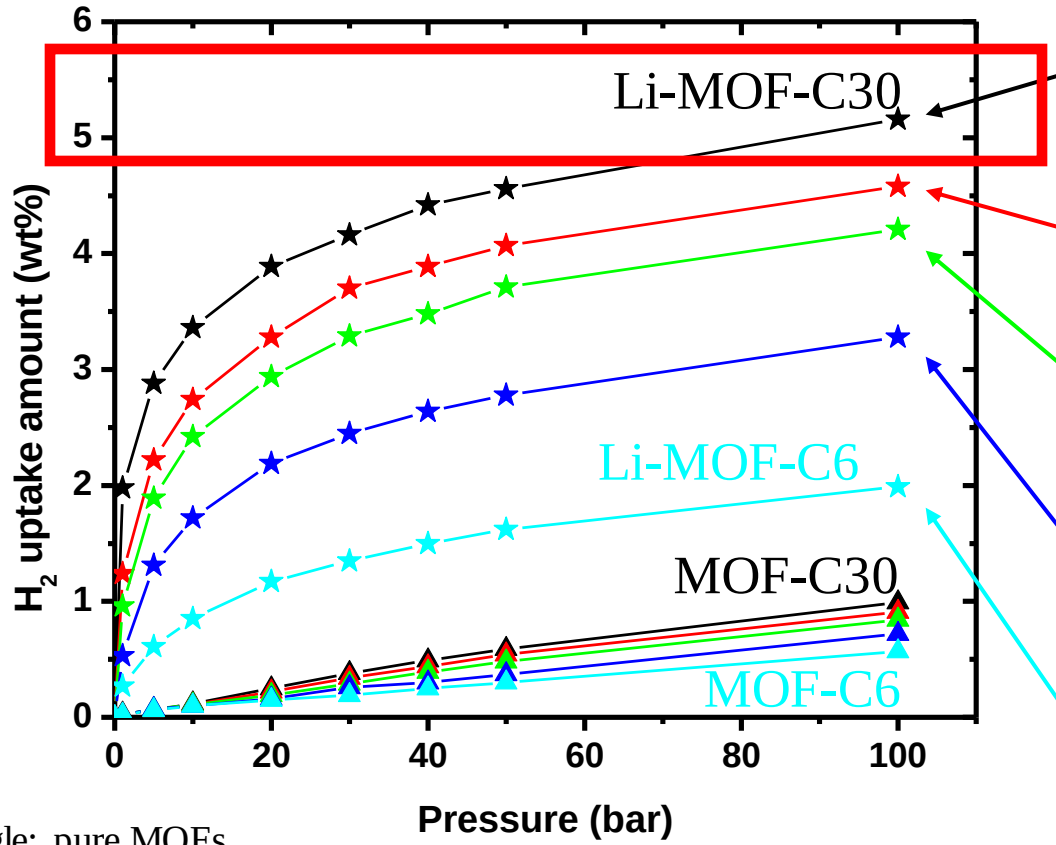

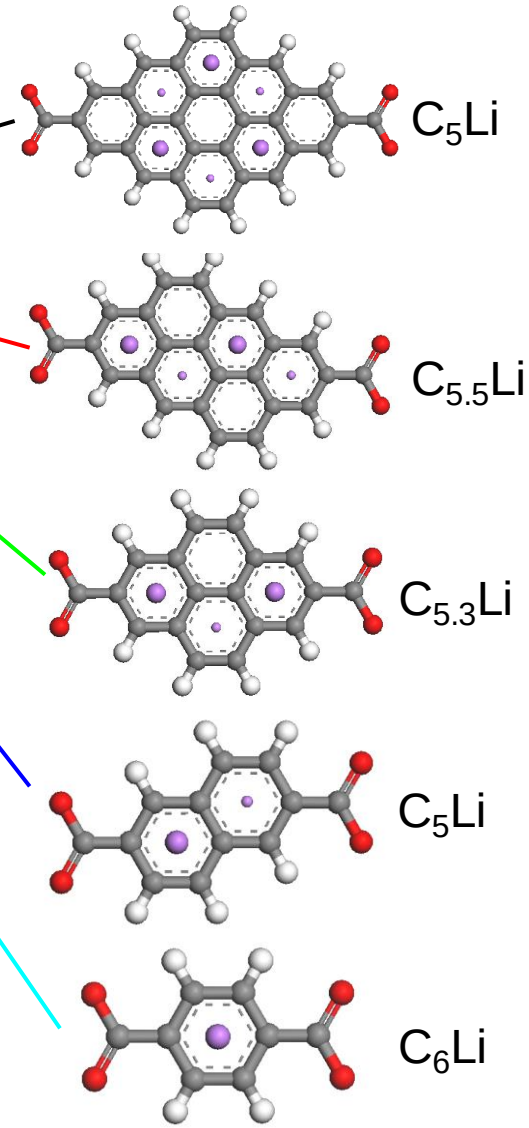

Triangle: pure MOFs,
Star: Li-doped MOFs
Cyan: MOF6,
Blue: MOF10,
Green: MOF16,
Red: MOF22,
Black: MOF30

old 073

Li Battery research: Hyungjun Kim, Hyun Woo Cho, Sang Soo Han, Yousong Jung

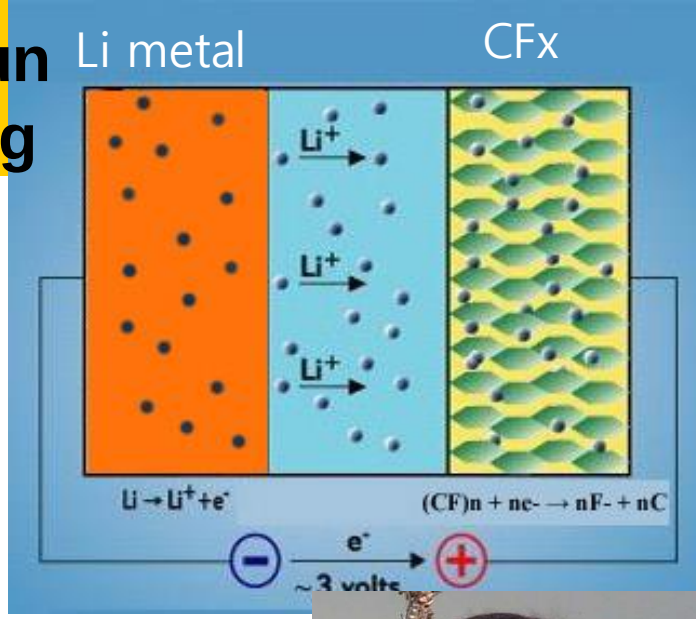

Li/CFx Primary Battery High energy density (theoretical specific energy of 2180 Wh/kg)

Long shelf life (self-discharge rate of 0.5% per year @RT)

Flat Discharge

Wide range of operating temperature

High safety and reliability

Issues:

Structures and energetics of Li/CFx phases

Migration barriers within Li/CFx phases

Structure and properties at the **solid electrolyte interface** (SIE)

Barriers of charging and discharging

Use theory and simulation. Validate against current materials.

Develop improved materials using theory and then experiment

Charge transfer processes at Graphite-Electrolyte interface
Solvation Sheath Structure of Li+ in nonaqueous electrolytes

Migration pathway of bulk solvated Li+ into intercalation in interior of graphene sheets

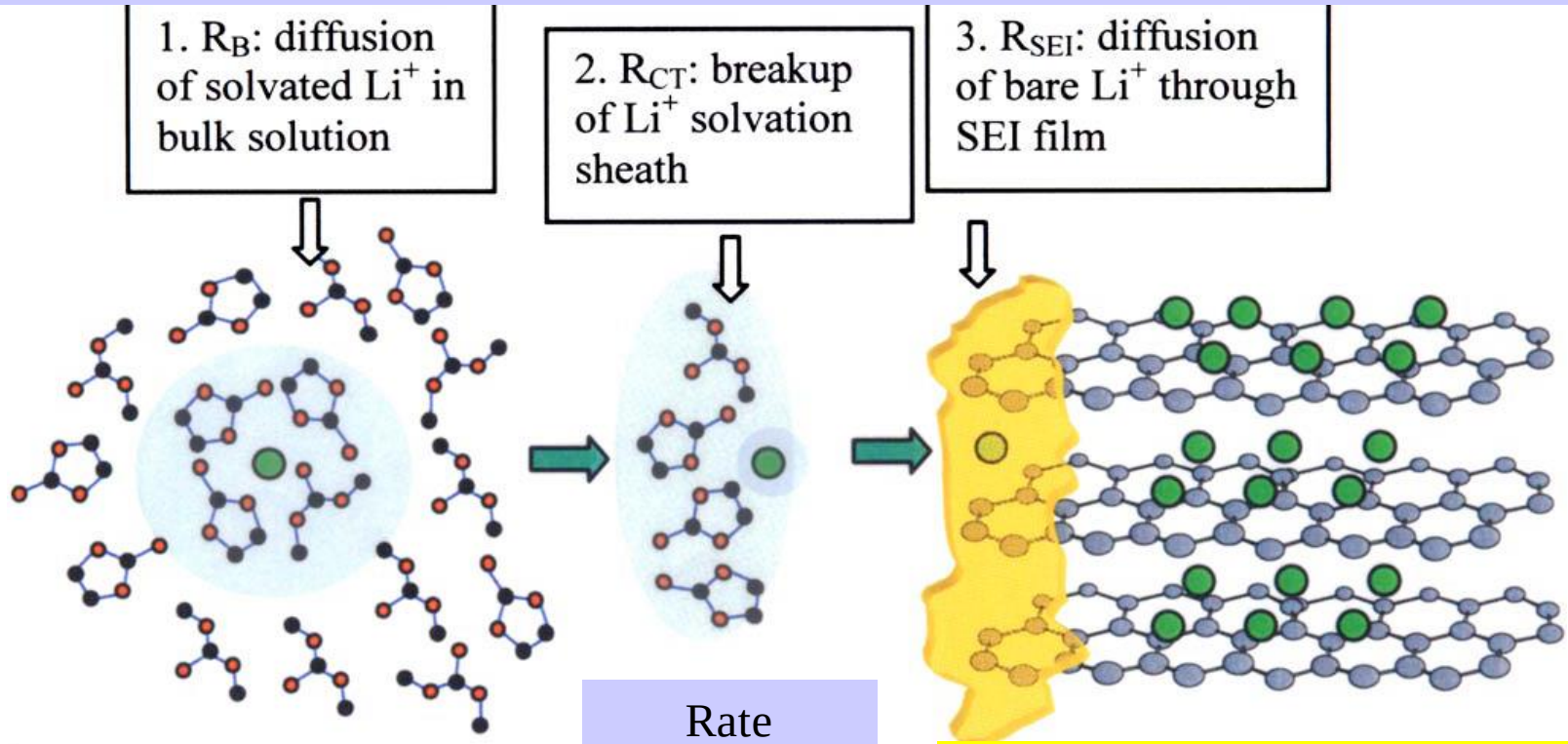

Rate determining step

We are using the ReaxFF reactive force field, trained with QM to describe the dynamics and structure as SEI is formed

From Kang Xu, J. Electrochem. Soc. 154 A162 (2007)

Comparison between Experiment and QM theory

Experimental Formation of SEI film

- **$EC + 2\,e^- + Li^+ \rightarrow C_2H_4\uparrow + (CO_3Li)^-$ (1)**
- **$(CO_3Li)^- + Li^+ \rightarrow Li_2CO_3$ at low EC concentration (2)**
- **$(CO_3Li)^- + Li^+ + EC \rightarrow (CH_2OCO_2Li)_2$ at low EC concentration (3)**

[Ref.] Aurbach et al. JPC(B) **1997**, *101*, 2195. and Langmuir **1999**, *15*, 2947.

- Our calculations predict all of these reactions.

Reaction (1): complex 16

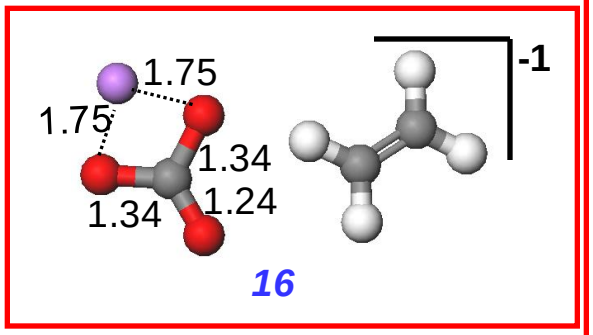

Reaction (2): complex 17

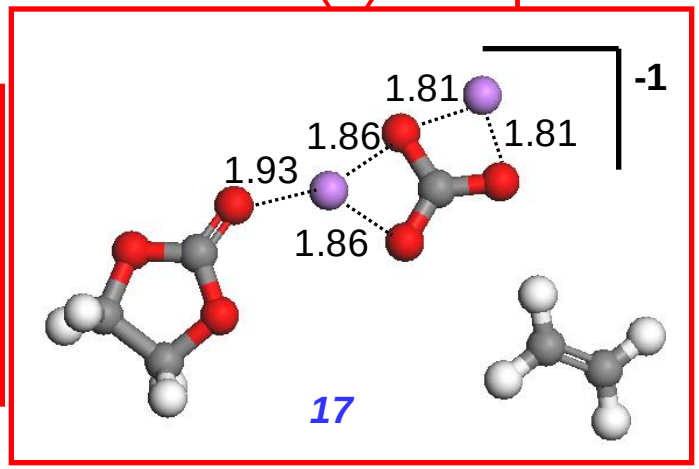

Reaction (2): complex 13

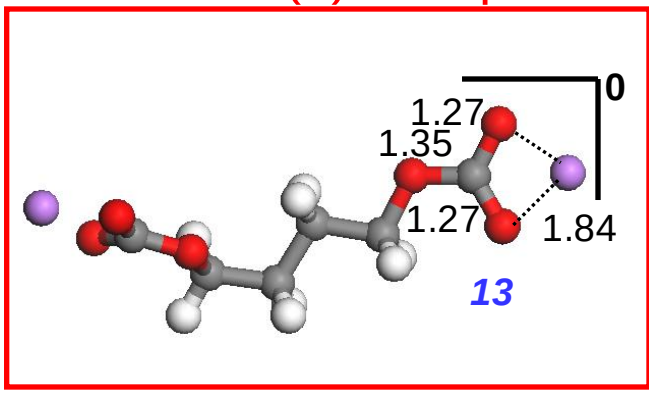

Superconducting Tc; A Story of Punctuated Evolution
All Serendipity

Discovery is made. Then all combinations tried. Then stagnation until next discovery.
Theory has never successfully predicted a new higher temperature material.
Embarrassing situation for Theorists.
To ensure progress we need to learn the fundamental mechanism in terms of the atomistic interactions

Temperature [K]

140
120
100
80
60
40

HgBaCaCuO
Today
TlSrBaCuO
$BiCaSrCu_2O_9$
$YBa_2Cu_3O_7$
77 K LN_2
Cuprate Era
A15 Metal Alloy Era
Metal Era
$LaBaCuO_4$
Nb_3Ge
Theoretical Limit (Anderson limit)
NbN
V_3Si
Pb
Nb
Nb_3Sn
NbC
Hg
4.2K LHe

1900 1920 1940 1960 1980 2000 2020

Year of Discovery

BCS Theory (1957)

Essential characteristic of all cuprate superconductors is oxidation (doping)

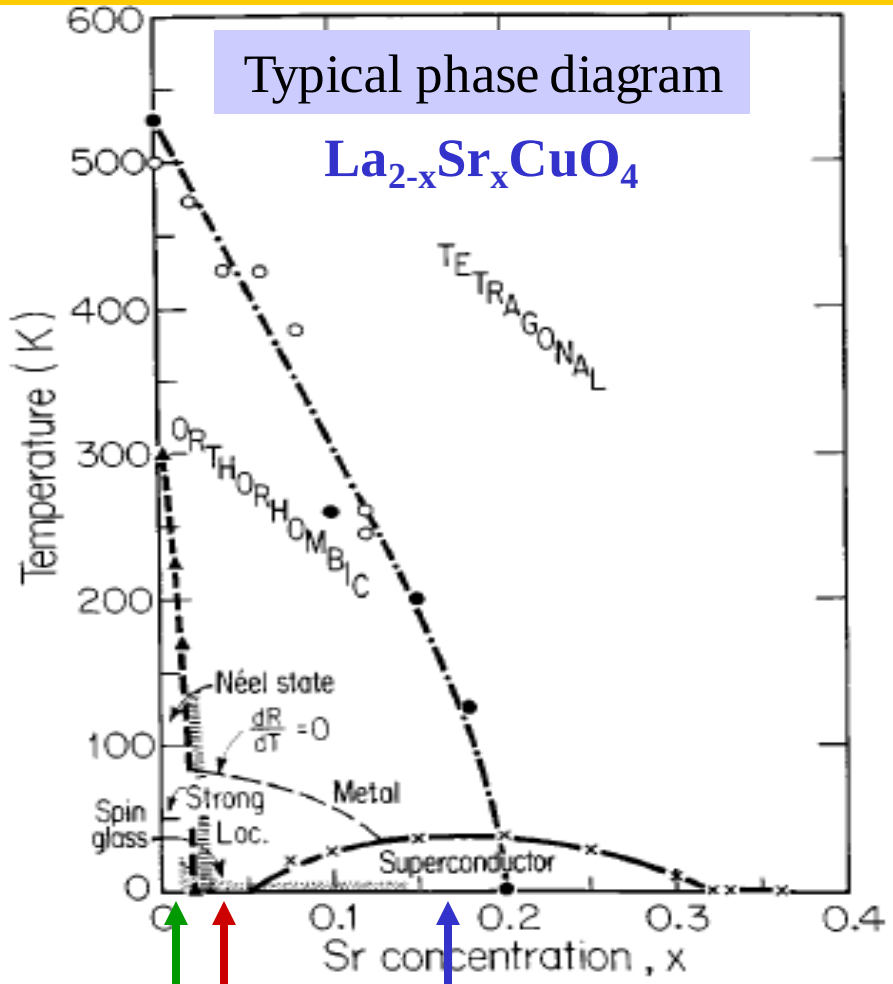

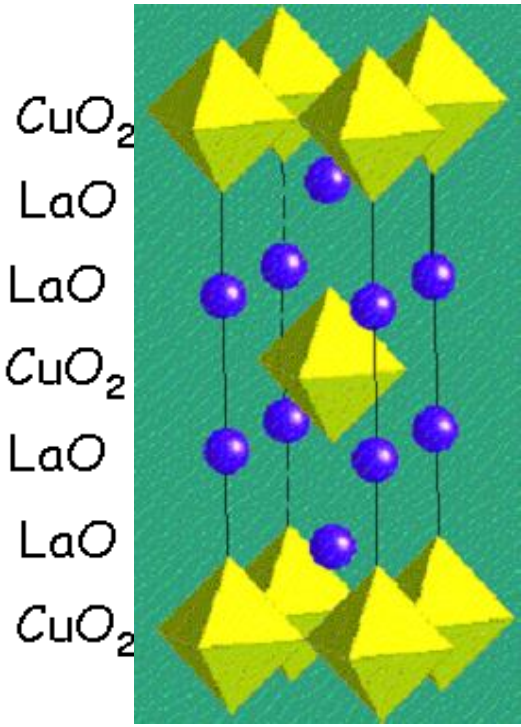

Superconductor: $0.05 < x < 0.32$

Spin Glass: $0.02 < x < 0.05$

Antiferromagnetic: $0 < x < 0.02$

Minimum doping to obtain superconductivity, $x > 0.05$.
Optimum doping for highest Tc=35K at $x \sim 0.15$.
Maximum doping above which the superconductivity disappears and the system becomes a normal metal.

Summary: Central Characteristics of cuprate superconductors, square CuO_2 lattice, 16% holes

CuO_2 plane

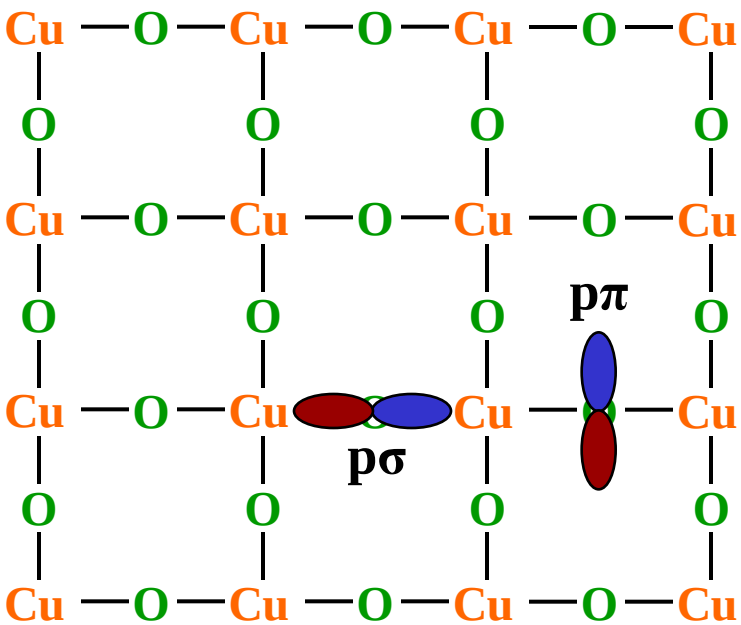

La_2CuO_4 (Undoped): La^{3+}, Sr^{2+}, O^{2-}, Cu^{2+}
d^9 Cu^{2+} → spin, with antiferromagnetic coupling

Doping (oxidation) $La_{2-x}Sr_xCuO_4$:
Hole → x Cu^{3+} and 1 – x Cu^{2+}, Or
Hole → x O^- and 4 – x O^{2-}

$YBa_2Cu_3O_7$:
Y^{3+}, Ba^{2+}, O^{2-} → 1 Cu^{3+} and 2 Cu^{2+}, Or
Y^{3+}, Ba^{2+}, Cu^{2+} → 1 O^- and 6 O^{2-}

Where are the Doped Holes?

Cu^{III} or d^8: Anderson, Science **235**, 1196 (1987), but **Cu^{II} → Cu^{III} IP = 36.83 eV**
O pσ: Emery, Phys. Rev. Lett. **58**, 2794 (1987).
O pπ: Goddard et al., Science **239**, 896, 899 (1988).
O pσ: Freeman et al. (1987), Mattheiss (1987), Pickett (1989).

All wrong: based on simple QM (LDA) or clusters (Cu_3O_8)

Basis for all theories of cuprate superconductors
LDA Band calculations of La_2CuO_4

LDA and PBE lead to a half filled band; predicting that La_2CuO_4 is metallic!

This is Fundamentally Wrong

Experimental Band Gap is 2 eV

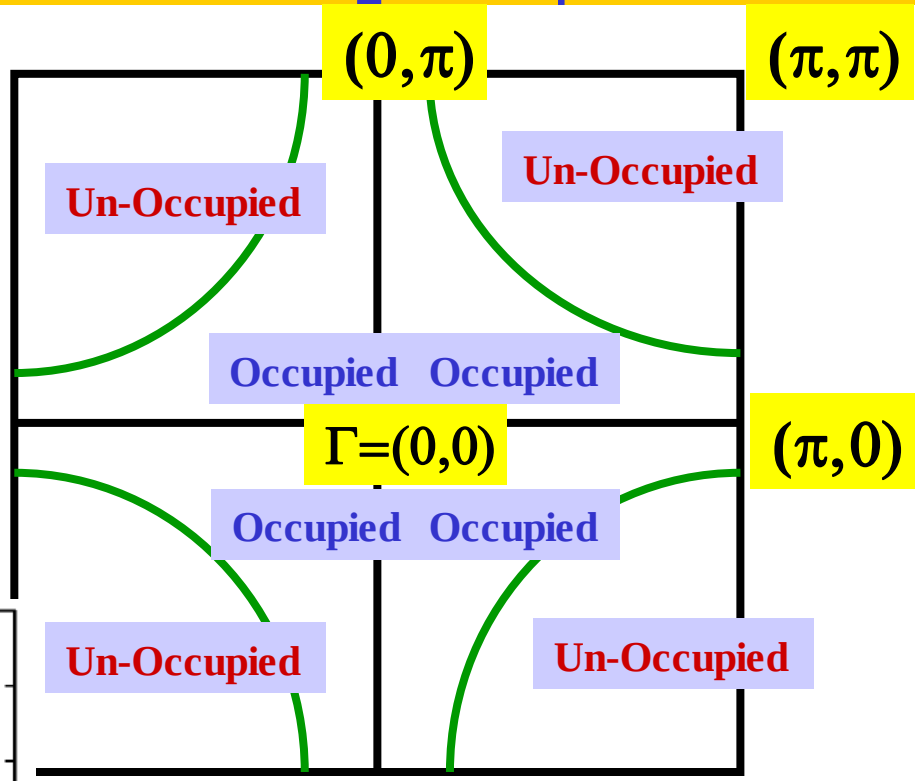

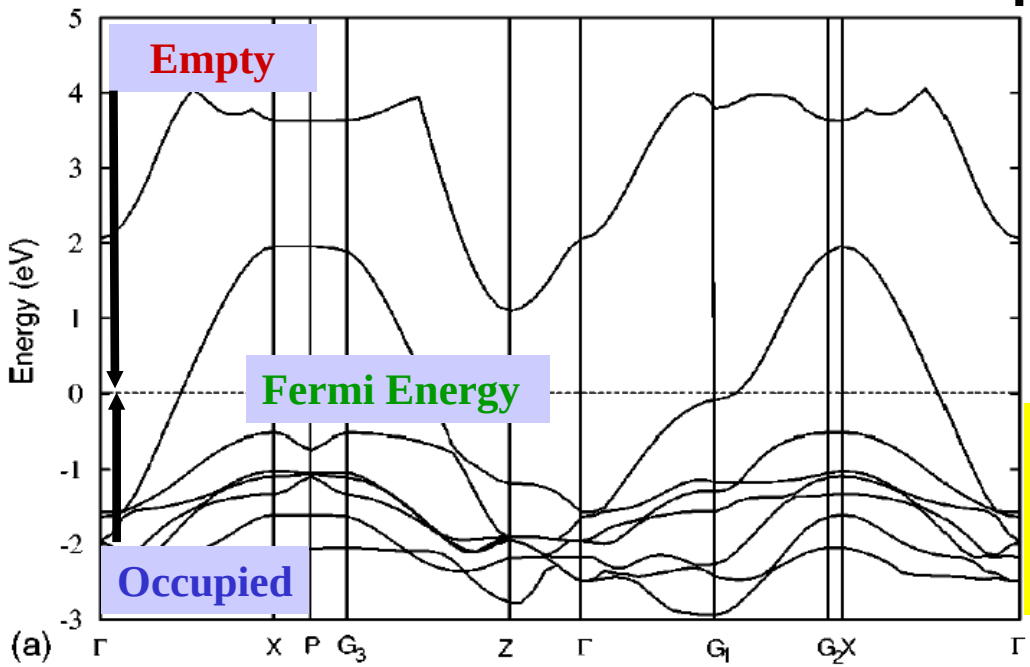

LDA: Freeman 1987,
Mattheiss 1987,
Pickett (1989)

Perry, Tahir-Kheli, Goddard
Phys. Rev. B **63**,144510(2001)
B3LYP recalculation of band structure

U-B3LYP calculations of La_2CuO_4

U-B3LYP leads to an insulator (2eV band gap) with a doubled unit cell (one with up-spin Cu and the other down-spin)

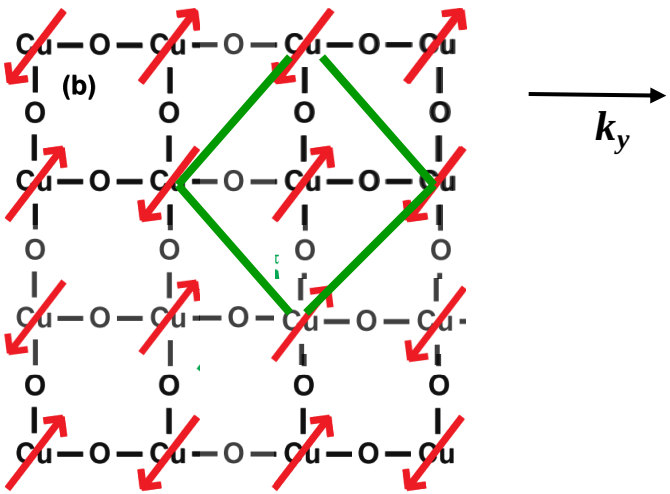

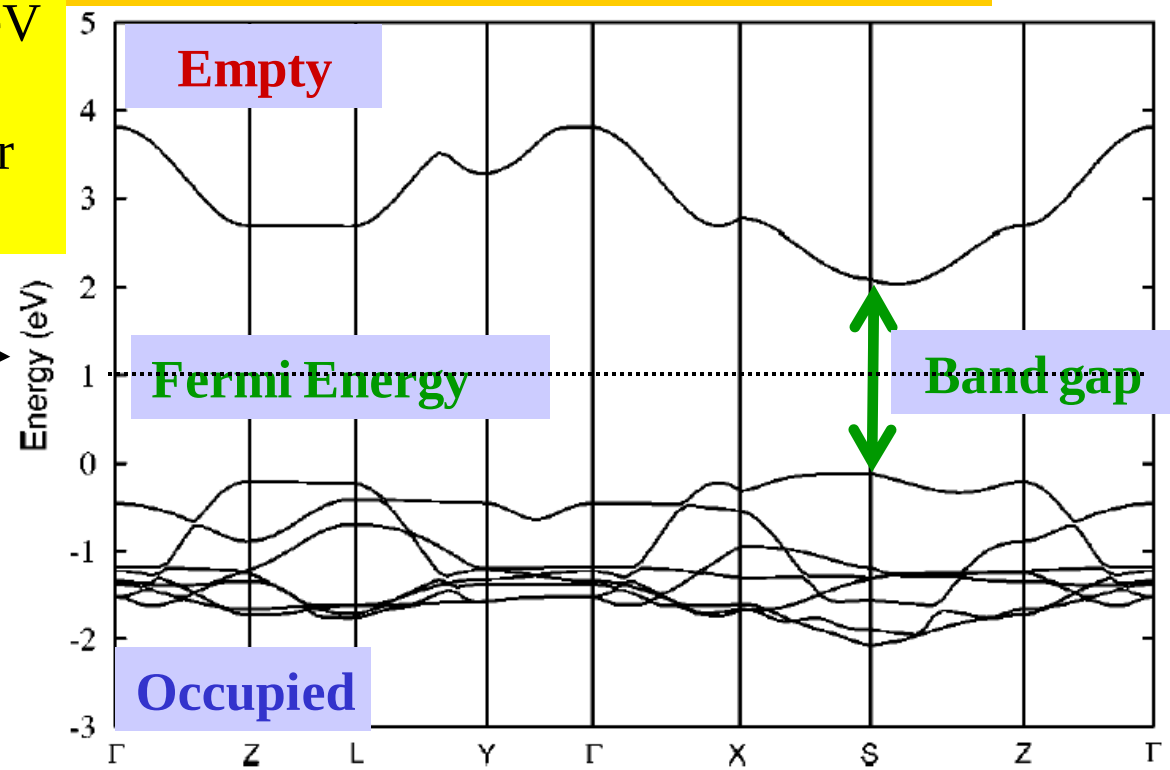

Method	Gap (eV)	Authors
LDA	0.0	Freeman et al. 1987, Mattheiss 1987, Pickett 1989
PBE	0.0	Tahir-Kheli and Goddard, 2006
PW91	0.0	Tahir-Kheli and Goddard, 2006
Hartree-Fock	17.0	Harrison et al. 1999
B3LYP (unrestricted)	2.0	Perry, Tahir-Kheli, Goddard *Phys. Rev. B* **63**,144510(2001)
Experiment	2.0	(Ginder et al. 1988)

Doping La→Sr ➔ hole out of CuO_2 plane the

The Plaquette Polaron

The Plaquette Polaron state is localized on the four-site Cu plaquette above the Sr. It ha apical O pz, Cu dz^2, and planar O pσ character over the plane of four Cu atoms. The Plaquette Polaron state is calculated to be **0.065** eV per 8 formula units above the apical polaron state this is 0.008 eV = 0.2 kcal/mol per Cu in the $La_{0.875}Sr_{0.125}CuO_4$ cell.

The apical O below the Sr shifts up 0.1 Å to a Cu – O bond distance of 2.50 Å (seen in Sr XAFS) leading to a plaquette state.

The apical O below the plaquette Cu distance optimizes to a Cu – O bond distance of 2.29 Å.

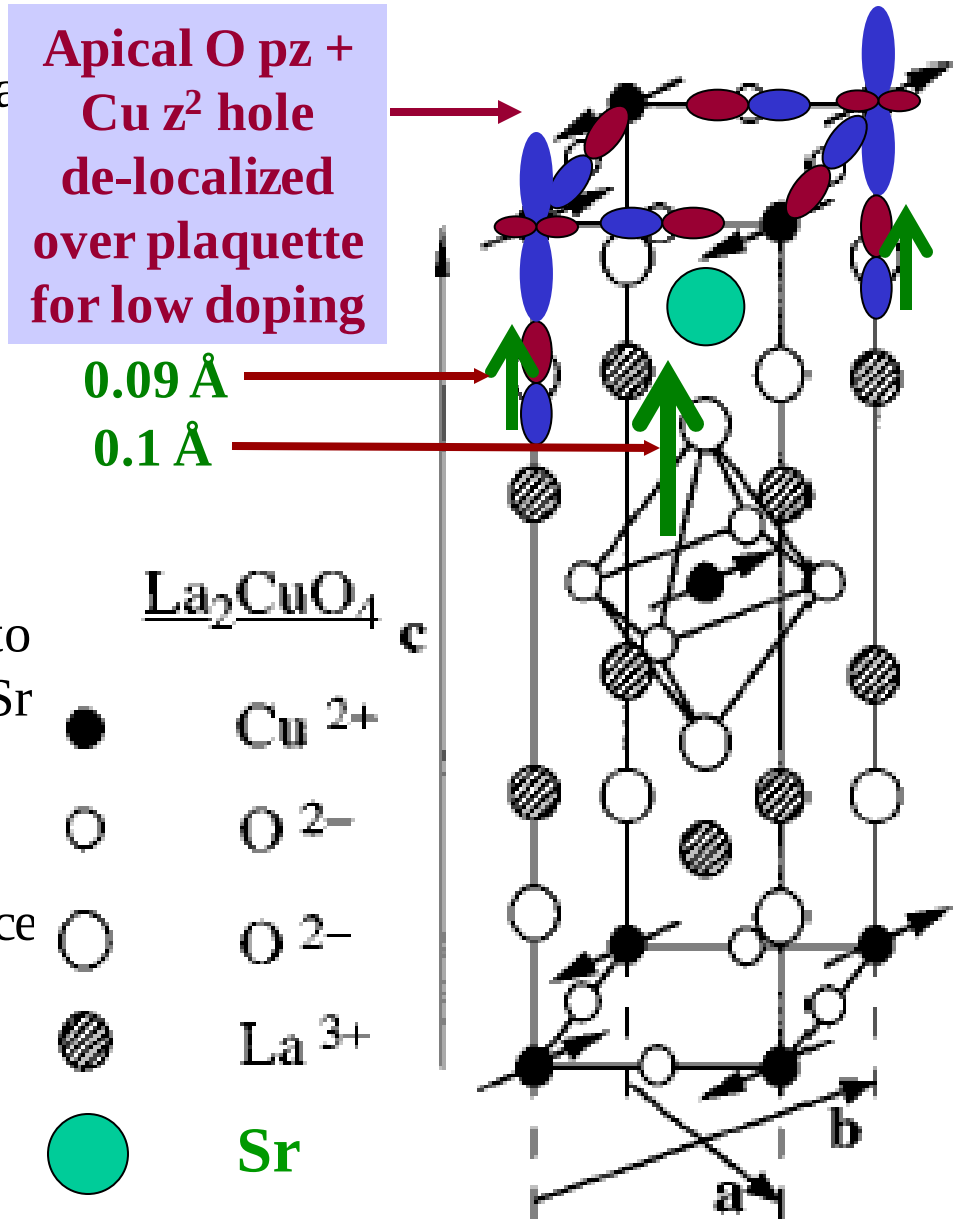

We obtain 3 types of Electrons

1. "Undoped" Cu AF d^9 sites
2. 4-site polarons (out of plane)
   - Two types of polarons
     a) Surface polarons (neighboring) AF d^9 sites
     b) Interior polarons (surrounded by other polarons)
3. x2-y2/pσ band electrons inside the percolating polaron swath (the "Doped" Cu sites)

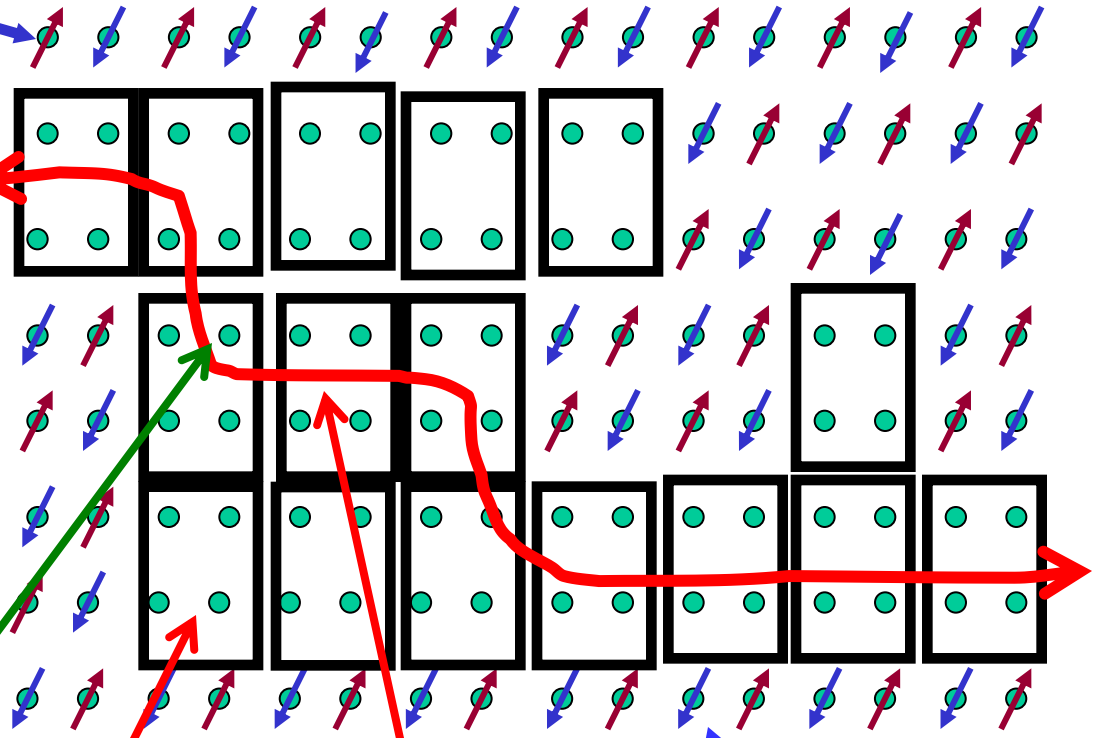

x2-y2/pσ band

Surface Polaron

Interior Polaron

d^9 AF

Assume Optimal T_c ➔ Maximum Surface Polarons per Volume

1000 x 1000 lattice
200 ensembles

S_p / Ω_{total}

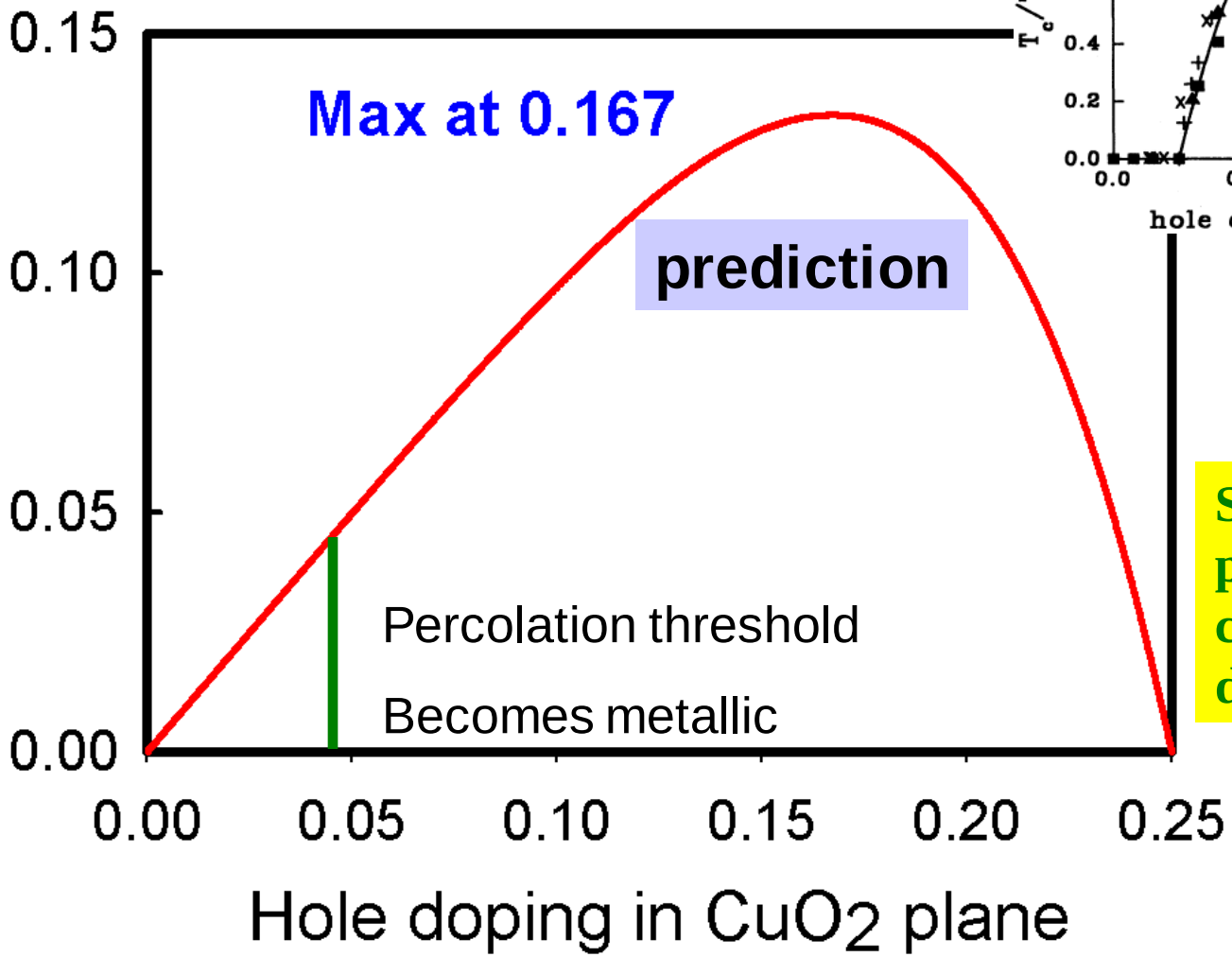

experiment

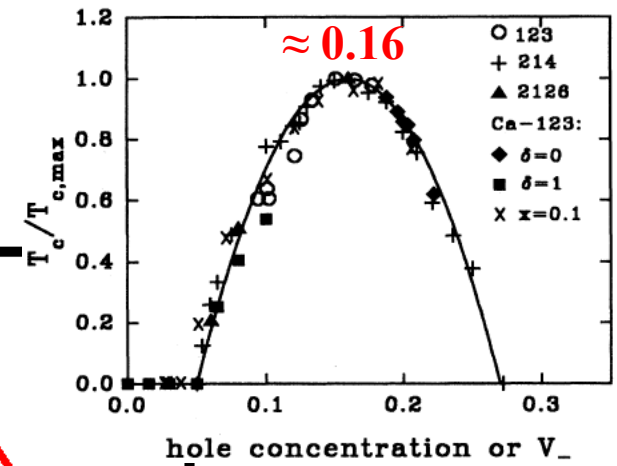

Surface area of pairing leads to correct optimal doping

Cuprate Superconductivity Puzzles
Must all be explained by any correct theory

Exp. Couples to Electron Spin

Neutron spin incommensurability

Neutron spin ω/T scaling

(expect ω/J_{dd} or ω/E_F)

Cu, O different NMR relaxations

Superconductivity

Phase transition to superconductivity

$Dx^2–y^2$ Gap Symmetry

Evolution of Tc with doping

Co-existence of magnetism and superconductivity

Exp. Couples to Electron Charge

Linear Resistivity $\rho \sim T$

Drude scattering $1/\tau \sim \max(\omega,T)$

Excess Mid-IR absorption

Low temperature resistivity $\sim \log(T)$

Negative Magnetoresistance low T

"Semi-conducting" c-axis resistivity

Hall Effect $\sim 1/T$ (expect ~ constant)

Hall Effect $R_H \sim$ const for field in CuO_2 plane.

Photoemission Pseudogap

Photoemission Background Large

A successful theory must explain experiments from each category. Previous theories leave many of the very puzzling properties unexplained. The chiral plaquette paradigm based on out-of-plane holes explains all of these

Chiral plaquette polaron theory of cuprate superconductivity

Tahir-Kheli, Goddard; Phys. Rev. B **76**: 014514 (**2007**)

Explains each of these phenomena

Universal Thermopower for cuprates as a function of hole doping (at 290K) explained by CPPP

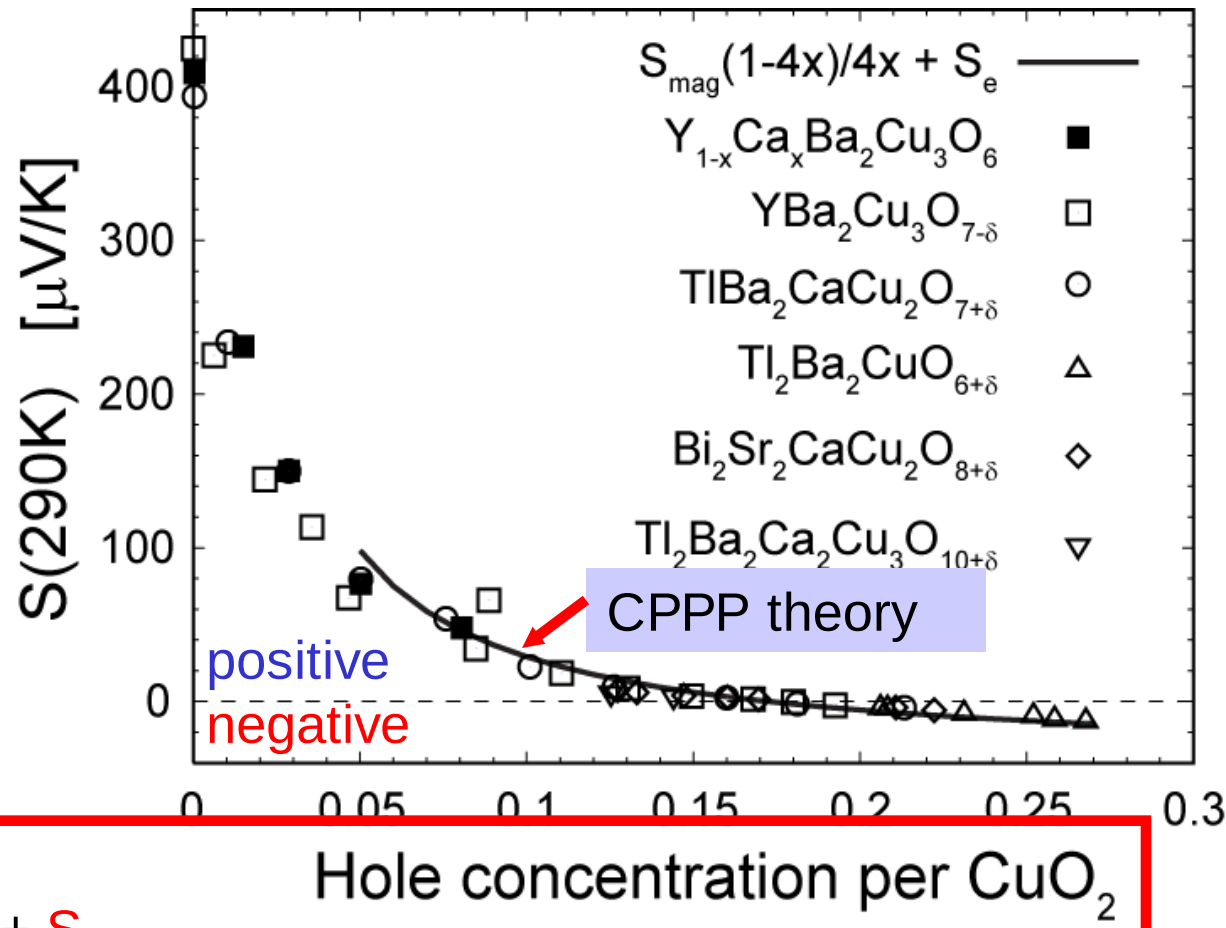

CPPP theory

$S(290K) = S_{magnon}[(1-4x)/4x] + S_e$,

The first term in the expression arises from the magnon drag effect while the second term is the electronic thermopower contribution.

Se = −12.5 μV/K Mott formula

Smagnon = 27.6 μV/K is adjusted to fit experiment

Estimate of Maximum Tc

Chemical Physics Letters 472 (2009) 153–165

To estimate Tc, use the formula from BCS theory $T_c = 1.13\ \hbar\omega_D \exp(-1/N(0)V)$

$\hbar\omega_D$ is Debye energy,

N(0) is the density of states at the Fermi level, and

V is the strength of the attractive coupling.

In CPPP, the Debye energy is replaced by the scale of the energy splitting between opposite chirality plaquettes.

For a plaquette surrounded on all four sides by d^9 spins get

~ $2J_{dd}$ = 0.26 eV ~ 3000K.

Expect range from $J_{dd}/2$ for one-side with d^9 spin neighbors to $3J_{dd}/2$ for case with three-side interfacing d^9 spin neighbors

Assume exponential term is ~ 1/10 as for A15 superconductors (Tc ~ 23K)

Expect that Maximum Tc for a cuprate superconductor is in range of $0.05J_{dd}$ to $0.15J_{dd}$ or 150K to 450K.

Current maximum of 138K may be $0.05J_{dd}$ case.

Expect that Tc of ~ 300K might be attainable..

Using 100x100 supercell, self-consistent calculations for 100 random 16% doping cases we adjusted the d^9-plaquette coupling to give gap ➔ Tc ~138K, then we chose specific doping patterns and calculate Tc. We have found cases with Tc > 200K. We expect to predict optimum doping structure to have Tc > 200K. May be a challenge to synthesize.

G-Protein Coupled Receptors (GPCR)

Histamine binds here, extracellular

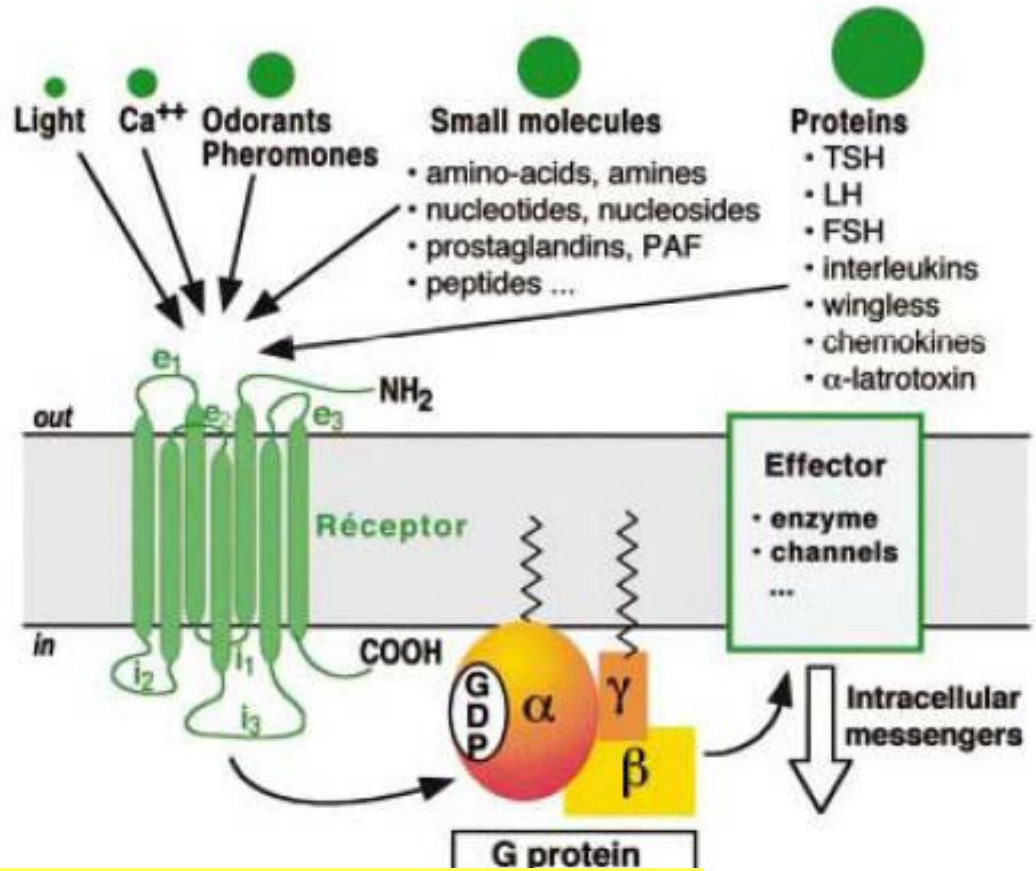

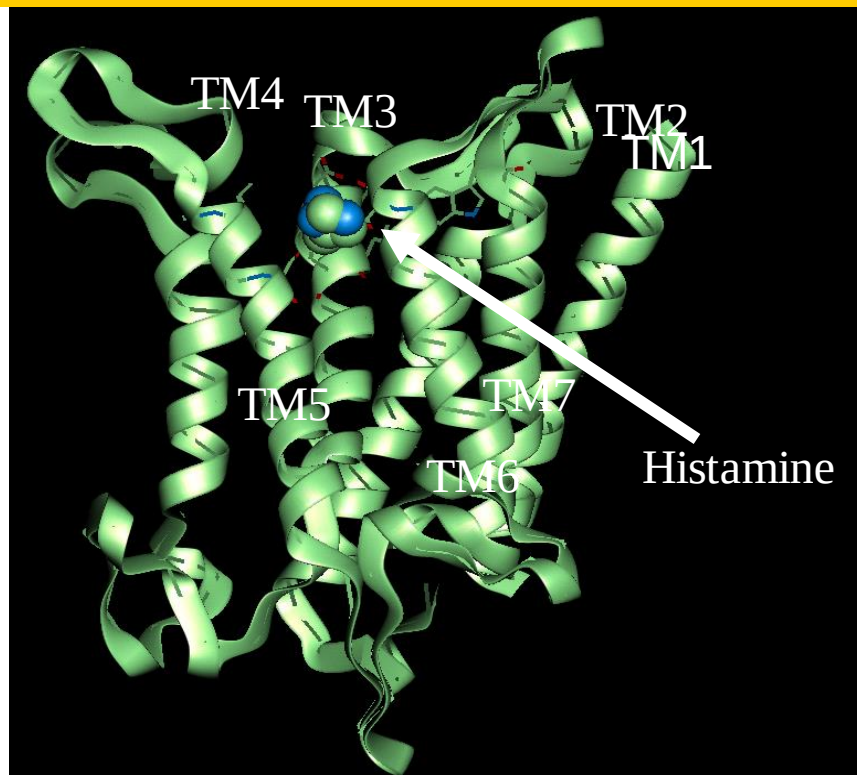

Causes intracellular signal

GPCR Sensors (smell, taste, vision, Pain)

GPCR signaling (acetylcholine, serotonin, bradykinin, adrenoceptors, LPA, S1P1, chemokine Dopamine

7 Transmembrane domains
extracellular Ligand binds
Transduces signal into cell by activating intracellular G protein

Predicting 3D structures of GPCRs: GEnSeMBLE

Start with sequence

```
MNGTEGPNFYVPFSNKTGVVRSPF
EAPQYYLAEPWQFSMLAAYMFLLI
MLGFPINFLTLYVTVQHKKLRTPL
NYILLNLAVADLFMVFGGFTTTLY
TSLHGYFVFGPTGCNLEGFFATLG
```

PredicTM → find the TM regions

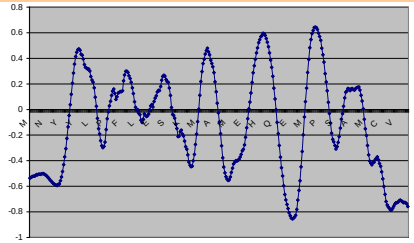

Find hydrophobic centers and place on a plane

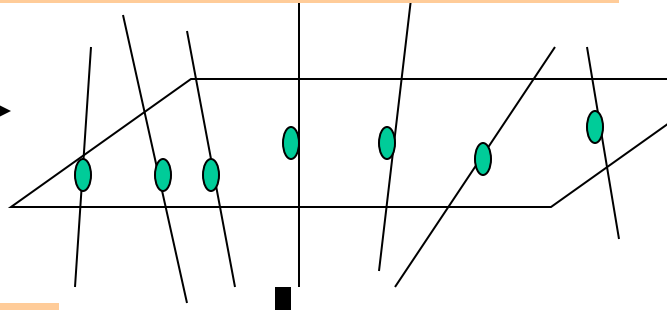

OptHelix: optimize helices (may be kinked).

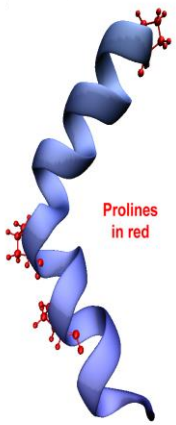

BiHelix Method: Sample 35,000,000 Rotations, select best 10

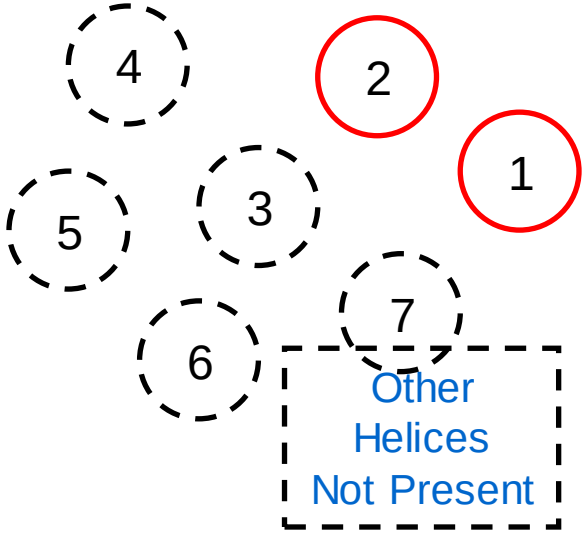

CombiHelix: Build top combinations from BiHelix to obtain an ensemble of 7-TM bundles

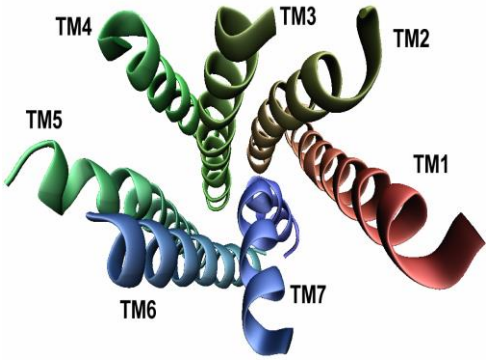

Templates used in GEnSeMBLE

Choose z position based on hydrophobic center to be aligned at z=0 of bundle

Choose η (rotation of the helix from some standard reference) based on BiHelix

Get other four variables from templates of known structures

x, y positions within the plane

θ (tilt from z axis) φ (azimuthal angle of tilted helix

Templates:

Frog Rhodopsin (elect. diff. ~1998) used for MembStruk

Bovine Rhodopsin (xray ~2002)

Human β2 AR (xray 2007)

Turkey β1 AR (xray 2008)

Human adenosine (A2A) (xray 2008)

Human DP prostaglandin (MembStruk 2007)

Human MrgC11 (MembStruk 2007)

Human CCR1 (MembStruk 2007)

Want to consider all possible rotations of 7 helices: 30º increments ➔ 12^7 = 35,831,808 combinations Reduce to 1728 with BiHelix Sampling Method

BiHelix sampling

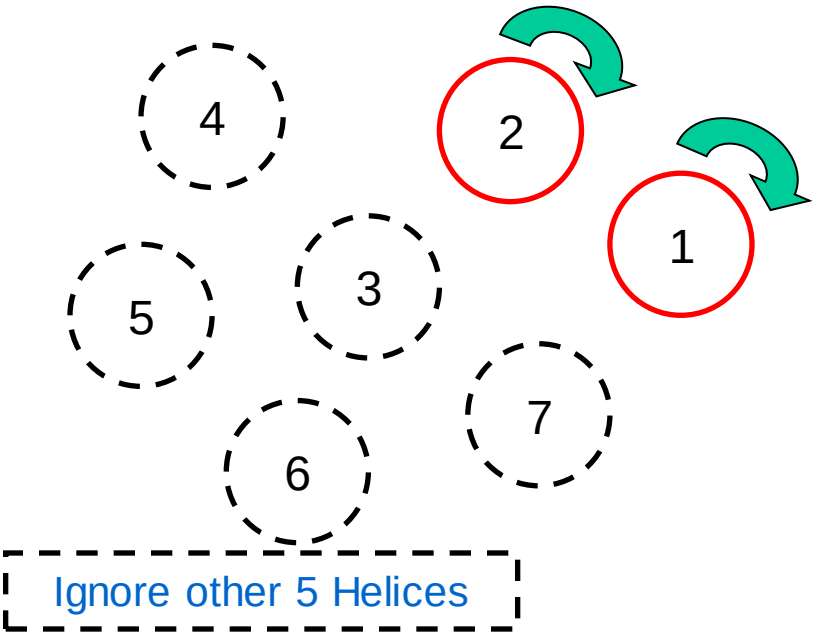

Have 12 interhelical contacts:

12,24,45,56,67,71,

31,32,34,35,36,37

For each pair consider all 12x12=144 combinations (30º increments)

For each pair Optimize side chains (SCREAM)

Combine these 12*144=1728 energies to estimate the total energy (valence + nonbond) for all 35 million packings

Choose best 1000 by total energy, construct 7 helix bundle, calculate total energy

Choose best 10 and minimize

Choose best 2 or 3 and do MD

BiHelix Predicted Packings for human β_2 AR

							Energy (kcal)	
H1	H2	H3	H4	H5	H6	H7	noSolv	Solven
0	0	0	0	0	0	0	153	51
90	0	0	0	0	0	0	220.5	129.3
0	0	0	30	0	0	0	256.2	158.1
0	0	0	120	0	0	0	262.5	167.7
0	0	0	0	270	0	0	270.6	190.7
120	0	0	0	0	0	0	315.7	205.8
90	0	0	30	0	0	0	329.8	241.2
90	0	0	0	270	0	0	337.2	265.5
90	0	0	120	0	0	0	340.2	284.5
0	0	0	30	270	0	0	361.5	283.5

Xray Structure

Select top 100 conformations from BiHelix analysis:

- Build the full 7-helix bundle with the specific rotations for each helix.
- Optimize side-chains using SCREAM.
- Calculate implicit membrane solvation energy.

This confirms that the crystal structure for modified human β2 AR is the most favorable for wild type. Of course it is inactive, but other low lying packings may be active

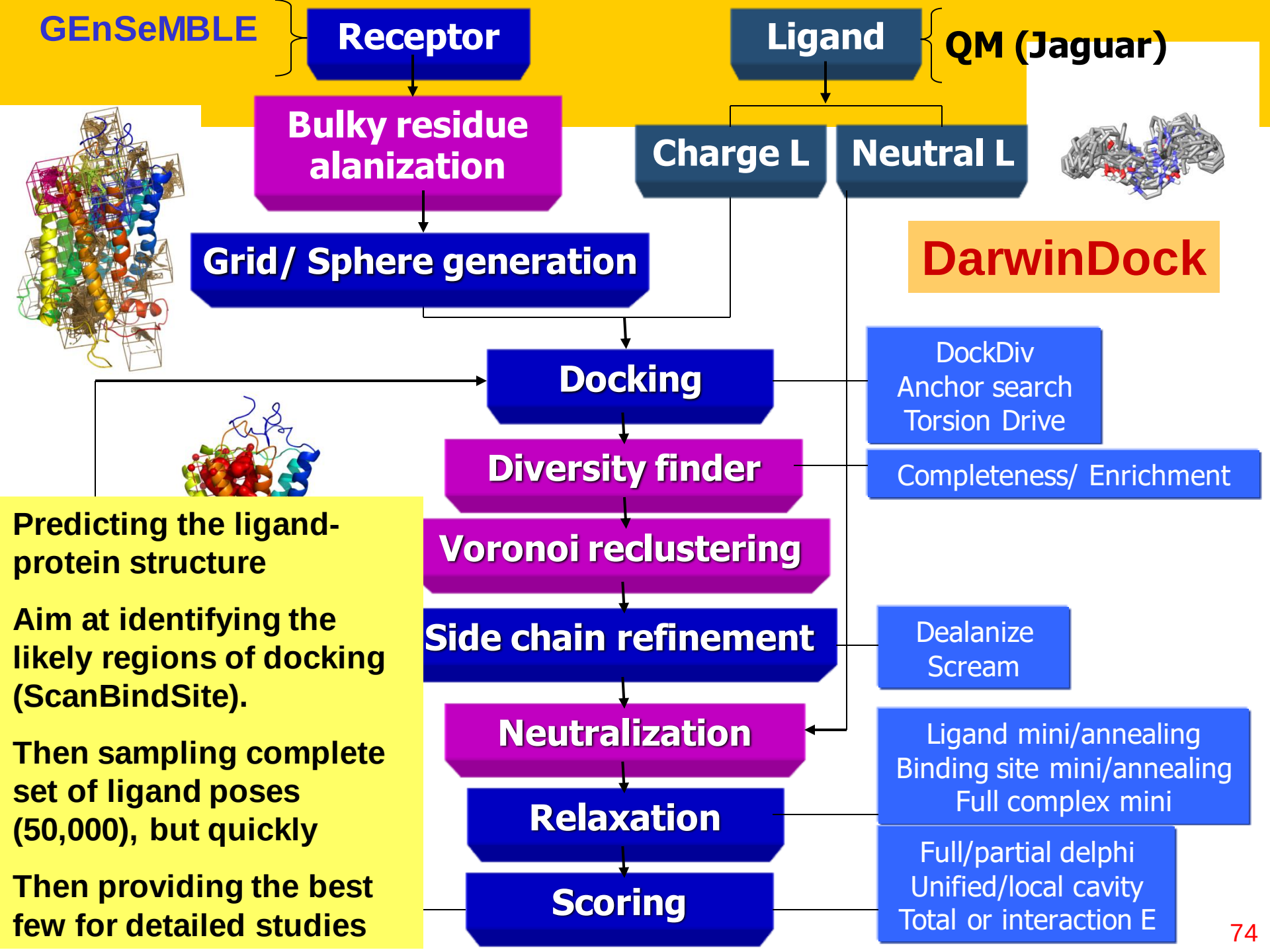
GEnSeMBLE
Receptor
Ligand
QM (Jaguar)
Bulky residue alanization
Charge L
Neutral L
Grid/ Sphere generation
DarwinDock
Docking
DockDiv
Anchor search
Torsion Drive
Diversity finder
Completeness/ Enrichment
Voronoi reclustering
Side chain refinement
Dealanize
Scream
Neutralization
Ligand mini/annealing
Binding site mini/annealing
Full complex mini
Relaxation
Full/partial delphi
Unified/local cavity
Total or interaction E
Scoring
Predicting the ligand-protein structure
Aim at identifying the likely regions of docking (ScanBindSite).
Then sampling complete set of ligand poses (50,000), but quickly
Then providing the best few for detailed studies

Example: Beta2 + Carazolol
predict ligand site to 0.3Å RMSD

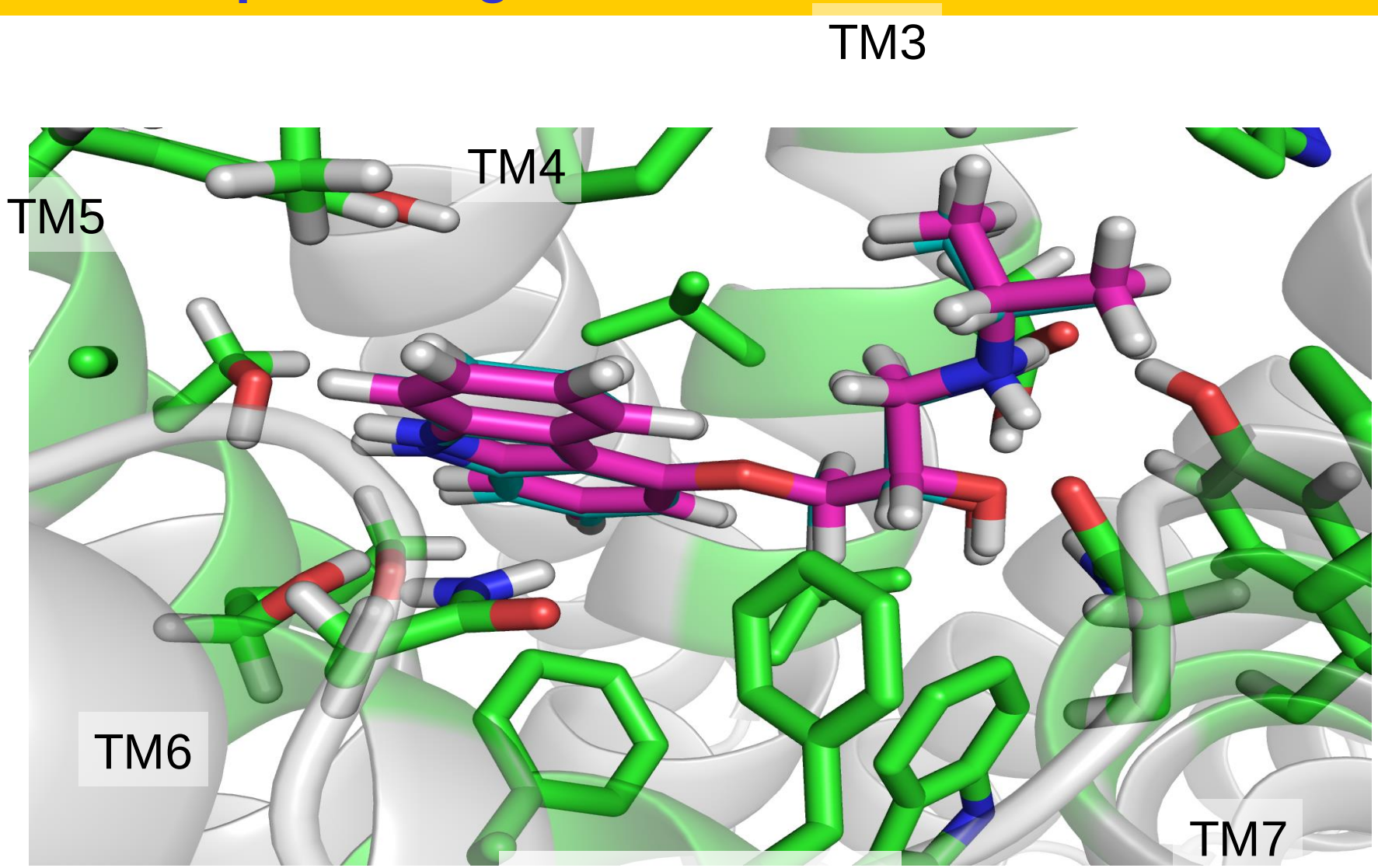

Pink = Predicted

Blue = Crystal

Use GEnSeMBLE (Monte Carlo Sampling) to find best 3 or 4 packings of 7 TM bundle
For each one use DarwinDock (Monte Carlo sampling) to find best binding site for each important ligand conformation.

Not practical to include explicit membrane and solvent for these calculations, which sample quadrillions of packings and 50,000 ligand positions for each packing.

After reducing the problem to a few packings and ligand positions it is practical to validate for full Protein-Ligand complex in infinite lipid bilayer + explicit water.
(40,000 to 60,000 atom MD at 300K for ~ 10 ns)

Cannot use MD to FIND the correct structure, but it can tell us tell us that we have the wrong structure

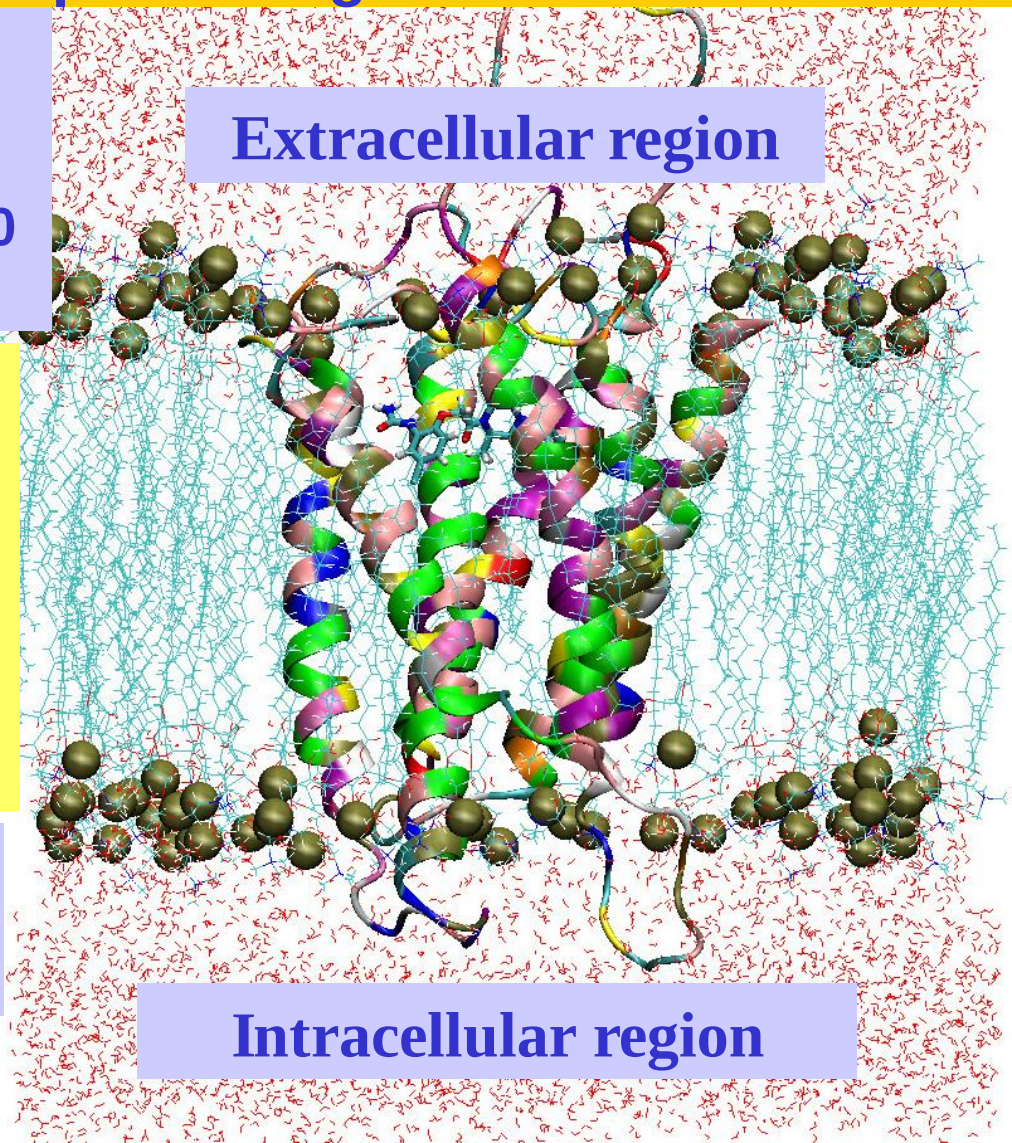

Various applications underway

- Cannabinoids (**CB1**, CB2)
- Chemokine receptors CCR1, CCR3, **CCR5**, CXCR3, **CXCR4**
- Dopamine **D1, D2, D3, D4, D5**
- Adrenergic receptors (**β1,2,3, α1A,B,D and α2A,B,C**)
- Histamine receptors (**H3**, **H1, H2, H4**)
- Urotensin II, Vasopressin,
- Prostaglandin (DP, EP1-4)
- GLP-1R for treatment of diabetes Type II
- Muscarinic acetylcholine receptors **M1**, M2, M3, M4, M5
- Serotonin receptors beyond 5HT2B,C
- LPA1-3,S1P-1
- Olfactory receptors - mouse and human
- Bitter and sweet receptors

Recent Publications

•Predicted 3D Structure Of The Human D2 Dopamine Receptor And The Binding Site And Binding Affinities For Agonists And Antagonists. *Proc. Natl. Acad. Sci. Usa* 101, 3815 (**2004**).

•Predicted 3D structure for the human β2 adrenergic receptor and its binding site for agonists and antagonists. *Proc. Natl. Acad. Sci. USA* 101, 2736-2741 (**2004**).

•Joyce Yao-chun Peng, Nagarajan Vaidehi, Spencer E. Hall, William A. Goddard III, **The Predicted 3D Structures of the Human M1 Muscarinic Acetylcholine Receptor with Agonist or Antagonist Bound**; *ChemMedChem*, 1 (8): 878-890 **(2006)**

•Maiti, P.K.; Pascal, T.A.; Vaidehi, N.; Goddard, W.A., **Understanding DNA based nanostructures**; *Journal of Nanoscience and Nanotechnology*, 7 (6): 1712-1720 Sp. Iss. (**2007**)

•Ryman-Rasmussen JP, Griffith A, Oloff S, Vaidehi N, Brown JT, Goddard WA, and Mailman RB, **Functional selectivity of dopamine D-1 receptor agonists in regulating the fate of internalized receptors**; *Neuropharmacology*, 52 (2): 562-575 (**2007**)

•William A. Goddard, III and Ravinder Abrol, **3-Dimensional Structures of G Protein-Coupled Receptors and Binding Sites of Agonists and Antagonists**; *Journal of Nutrition* 137: 1528S-1538S (**2007**)

Theory validated experimentally AFTER predictions

Vaidehi, Schlyer, Trabanino, Kochanny, Abrol, Koovakat, Dunning, Liang, Sharma, Fox, Floriano, Lopes de Mendonça, Pease, Goddard, Horuk; **Predictions of CCR1 chemokine receptor structure and BX 471 antagonist binding followed by experimental validation;** *Journal of Biological Chemistry* 281 (37): 27613-27620 (**2006**)

Heo JY, Han SK, Vaidehi N, Wendel J, Kekenes-Huskey P, Goddard WA, **Prediction of the 3D structure of FMRF-amide neuropeptides bound to the mouse MrgC11 GPCR and experimental validation**; *ChemBioChem*, **8** (13): 1527-1539 (**2007**)

Li YY, Zhu FQ, Vaidehi N, Goddard WA, **Prediction of the 3D structure and dynamics of human DP G-protein coupled receptor bound to an agonist and an antagonist**; *Journal of the American Chemical Society* **129** (35): 10720-10731 (**2007**)

Merck lead compound

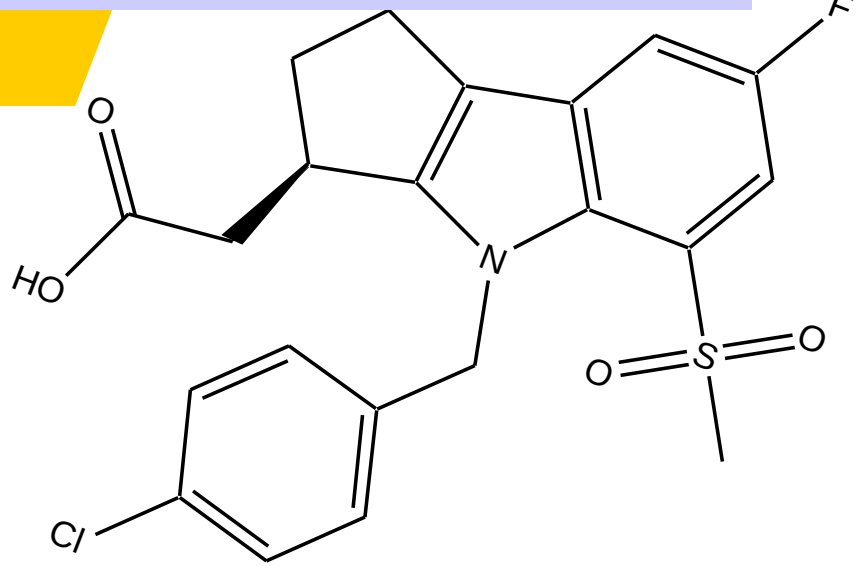

With Aventis we developed optimal derivatives for three scaffolds for human DP receptor antagonists

First we predicted the SAR for ~20 derivatives of the Merck compound. We did not have the data, but Aventis Lead Chemist did. We did well and were allowed to participate in lead optimization for 3 Aventis compounds

Three Aventis lead scaffolds

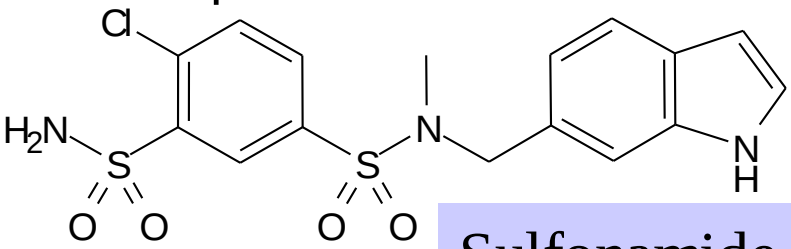

Sulfonamide

Pyrimidine

Success

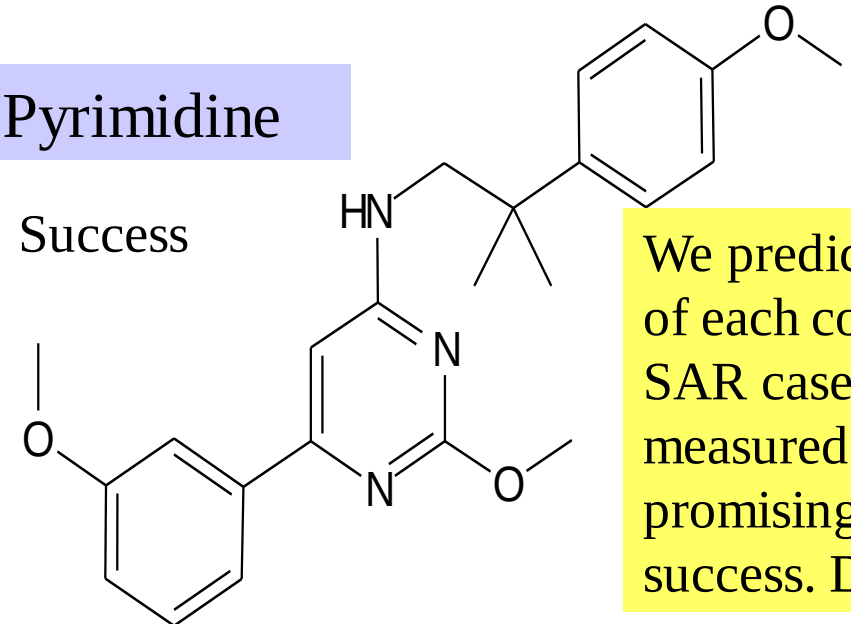

We predicted binding mode of each compound and 20 SAR case. Aventis measured the most promising ones. Obtained success. Drug in trials

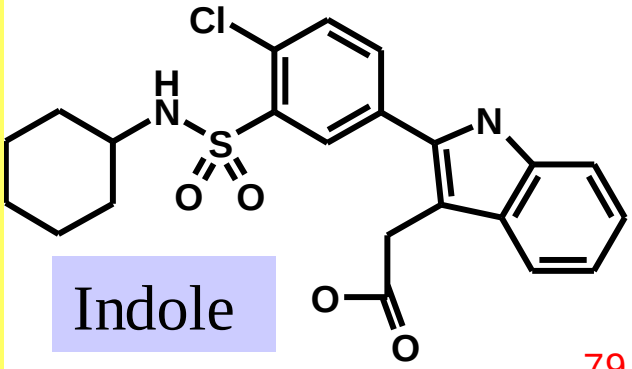

Indole

Predicted binding mode of Merck cyclopentanoindole antagonist in human DP receptor.

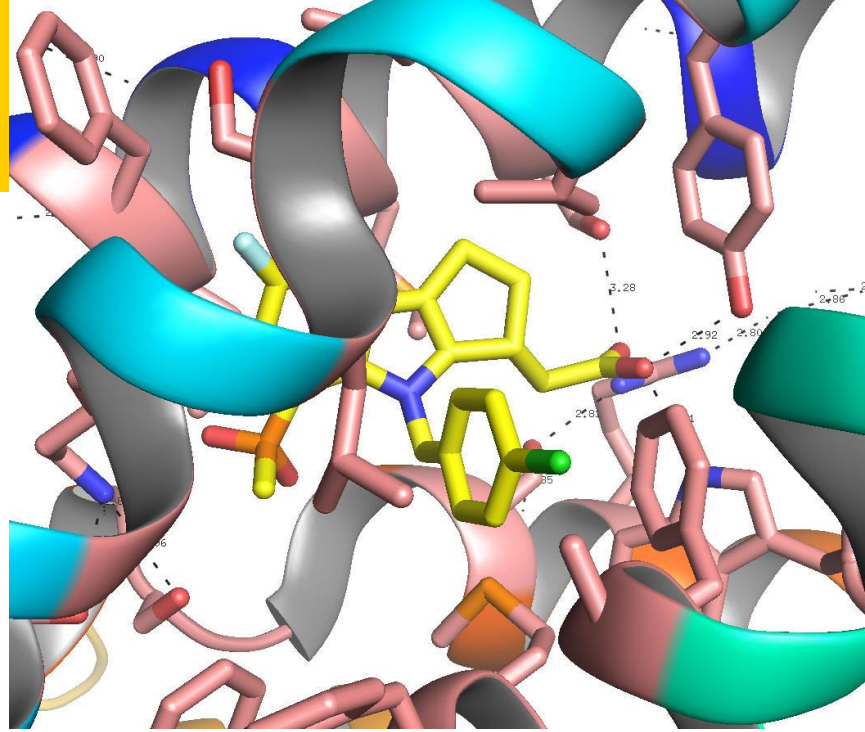

CORDAPTIVE™ (ER niacin/laropiprant), Formerly known as MK-0524A,

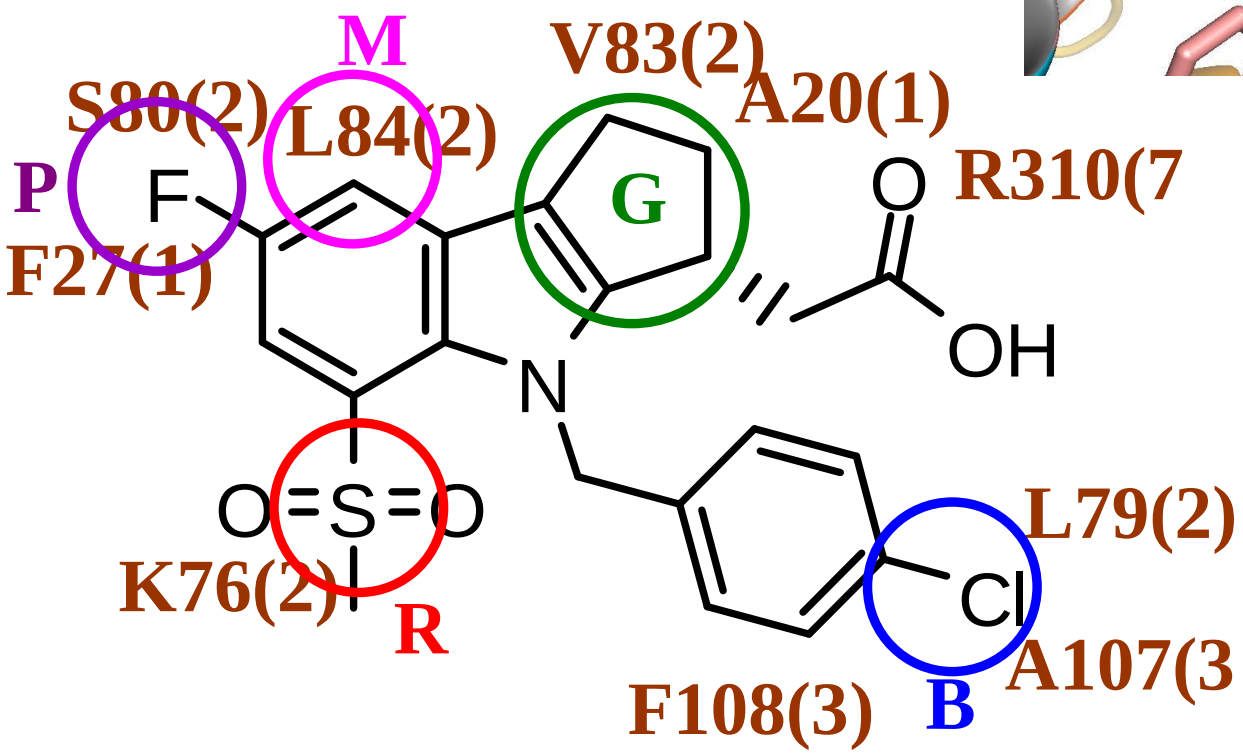

4 critical regions:
- carboxylic acid,
- cyclopentane ring,
- indole ring
- benzene ring.

SAR: structure activity relations for Merck CPI antagonist

Using our predicted binding mode, we predicted the binding energies of ~20 modified compounds. The 8 published later by Merck are shown

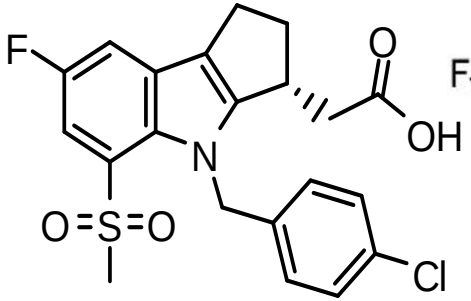

a) BE: -128.1 kcal/mol
Ki: 0.57± 0.17nM

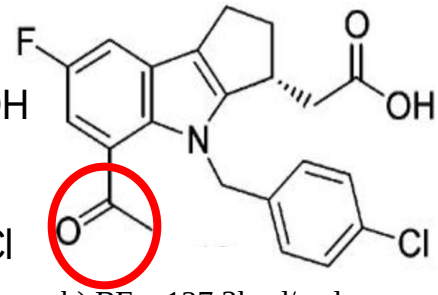

b) BE: -127.3kcal/mol
Ki: 1.1± 0.22nM

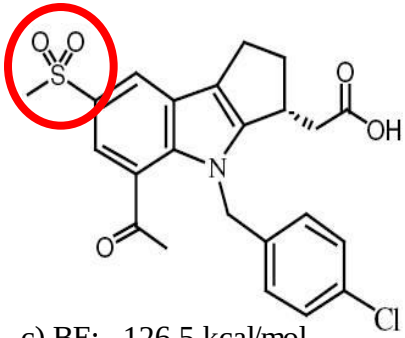

c) BE: -126.5 kcal/mol
Ki: 2.6± 0.7nM

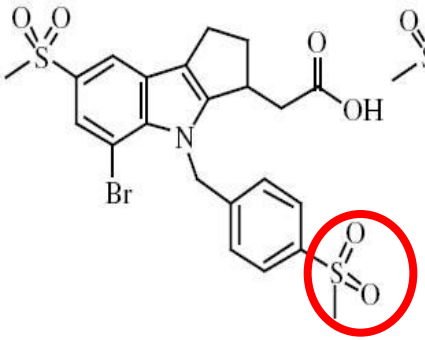

d) BE: -107.4 kcal/mol
Ki: 1900± 720nM

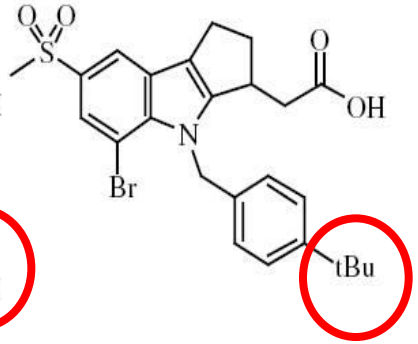

e) BE: -125.0 kcal/mol
Ki: 7.5± 1.0nM

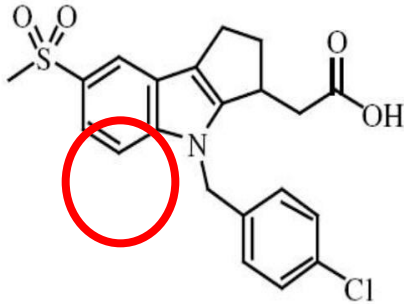

f) BE: -109.9 kcal/mol
Ki: 300± 95nM

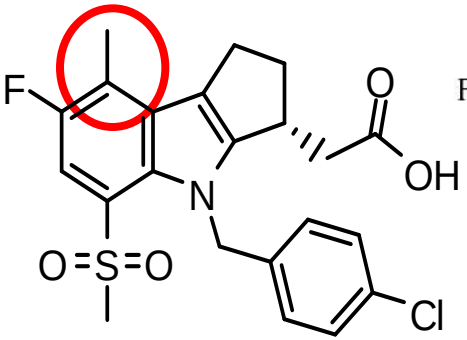

g) BE: -105.3 kcal/mol
Ki: >2000nM

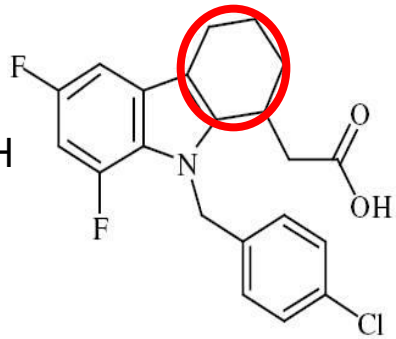

h) BE: -124.5kcal/mol
Ki: 11± 5.1nM

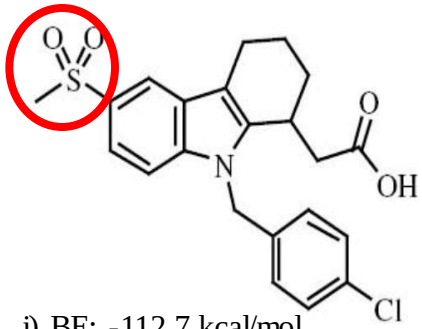

i) BE: -112.7 kcal/mol
Ki: 80± 6.6nM

Development of new selective antagonist for DP Receptor

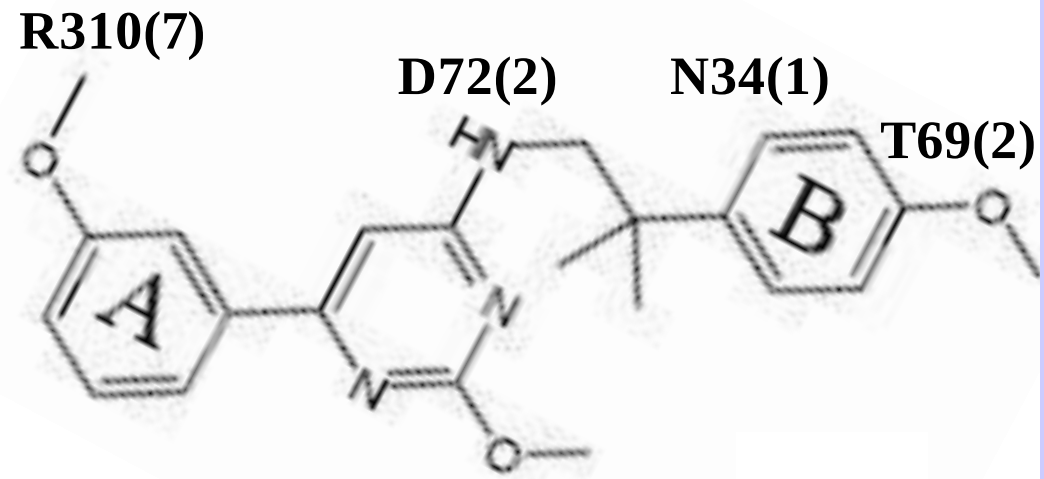

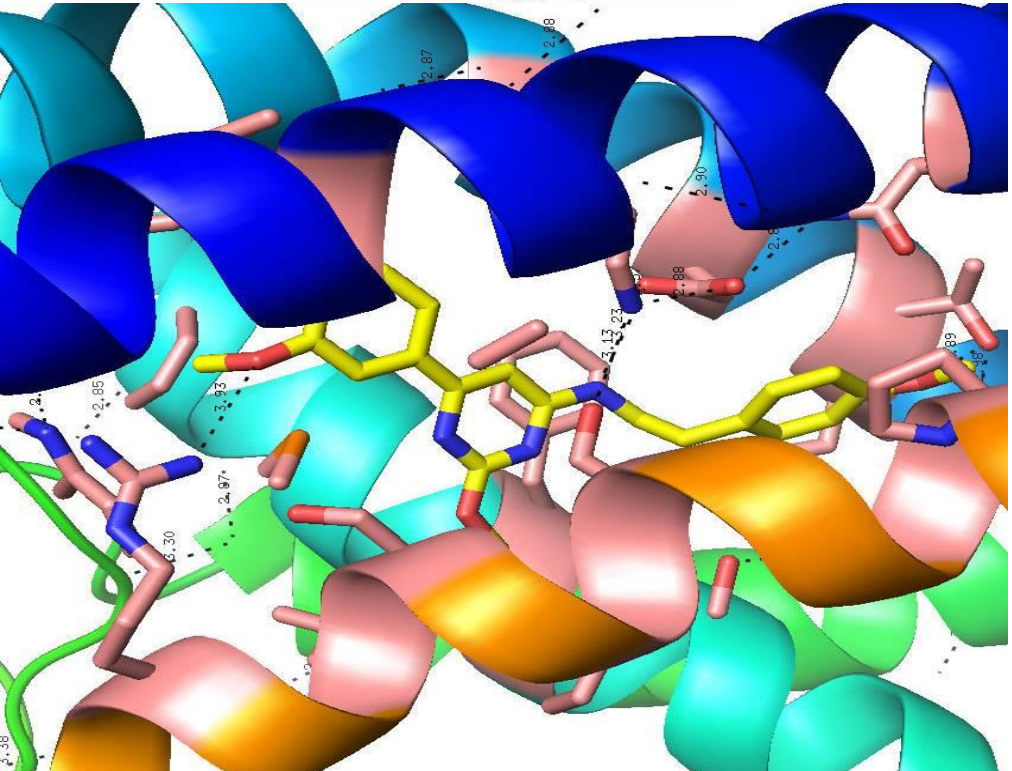

- Aventis discovered Pyrimidine **lead compound** using HTS with binding constant of **IC_{50}=800 nM** to DP receptor
- Caltech **predicted binding site** to DP lead. Similar to agonist, interacting with TM7-Arg and TM2-Lys, but does not interact with TM7-S316 or TM7-S313. MD does not lead to rotation of TM7 and TM3, thus is antagonist.
- Caltech identified 4 key residues and did computational SAR on 20 new compounds. **Found > 8 improved compounds**
- Aventis synthesized ligands and measured binding.
- **Best predicted compound, was best exper case with IC_{50}=0.8 nM, 1000 times better than lead.**
- This new drug now in human trials (allergy, inflammation)

Success!

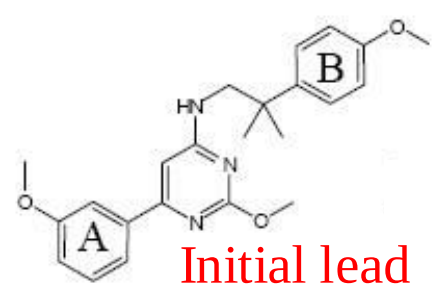

Initial lead

a) BE: -56.5 kcal/mol
IC50: 800 nM

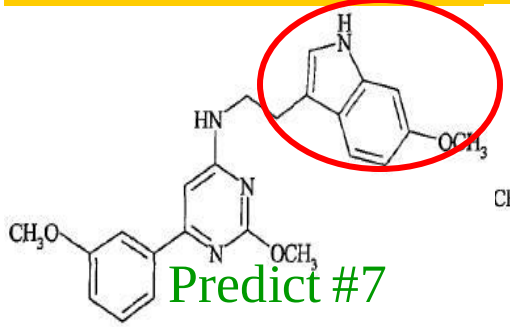

Predict #7

b) BE: -57.9 kcal/mol
IC50: 104nM

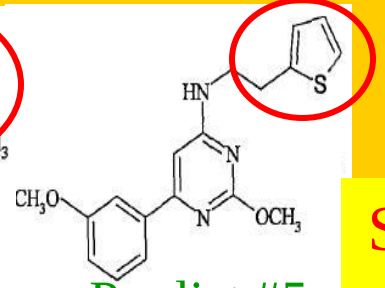

Predict #5

c) BE: -59.5 kcal/mol
IC50: 9.7nM

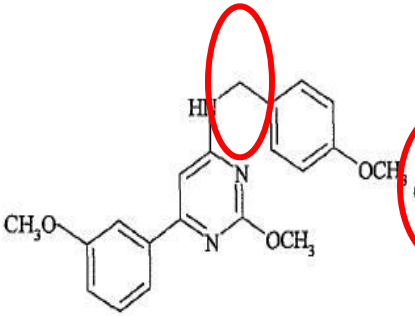

worse

d) BE: -54.8 kcal/mol
IC50: 1073nM

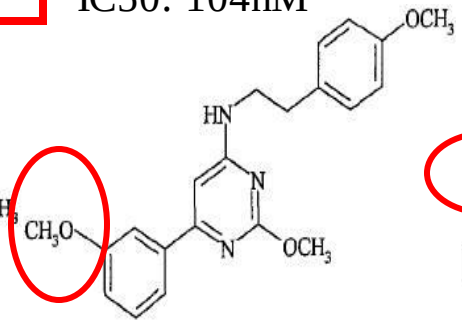

Predict #3

e) BE: -62.7 kcal/mol
IC50: N/A

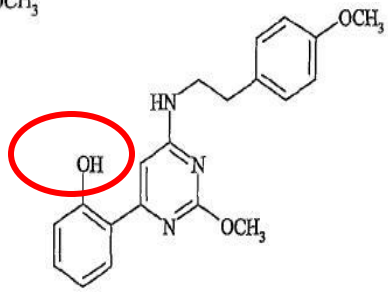

Predict #6

f) BE: -58.9 kcal/mol
IC50: 17nM

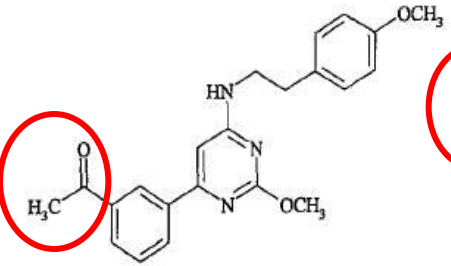

Predict #4

g) BE: -61.1 kcal/mol
IC50: 5nM

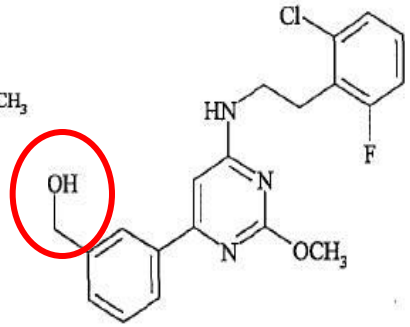

Predict #2

h) BE: -62.8 kcal/mol
IC50: 2.4nM

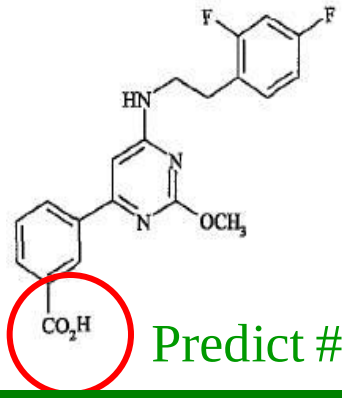

Predict #1

i) BE: -80.6 kcal/mol
IC50: 0.8nM

Start with lead compnd: IC_{50} = 800 nM

Theory predicted 20 compounds with >7 compounds having better binding.

Aventis synthesized and measured the binding for all 20

All compounds had binding energy in sequence predicted

Best: 0.8 nM, 1000 times improved

Same or similar compound in trials

Frustration

Based on our success in predicting 3D structures of GPCRs, we obtained funding from

- **Aventis (now Sanofi-Aventis),**
- **Berlex (part of Schering AG, now part of Bayer),**
- **Pfizer,**
- **Boehringer-Ingelheim**

But with the single exception of the Aventis-DP project (just one of 2 projects with Aventis), we were never allowed to work on the target ligands, which were consider proprietary

Instead we predicted structures for their target GPCR which we gave to them.

We validated our structure by comparing to literature data

Then our collaborators in the company struggled using both commercial and our software to make their own predictions of the binding sites and modifications to improve binding.

We could not help them.

Private funding

Recently (Oct. 2008) I convinced some US Venture Capitalists (who I knew because they had funded a successful spin-off from Caltech, Allozyne, of which I was a co-founder) to invest in a project in which my group

- would predict the GPCR 3D structure,
- would validate against literature data on binding and mutations,
- Would design new mutation experiments for precise validation of our structures
- Would use computational rapid through put to opbitmize a number of computational scaffolds to dramatically improve binding

They would fund commercial groups to synthesize the new compounds we predicted and to do the mutation validations

We chose AIDS as a disease target – which involves design of CCR5 and CXCR4 co-receptor inhibitors

Replicative cycle of HIV

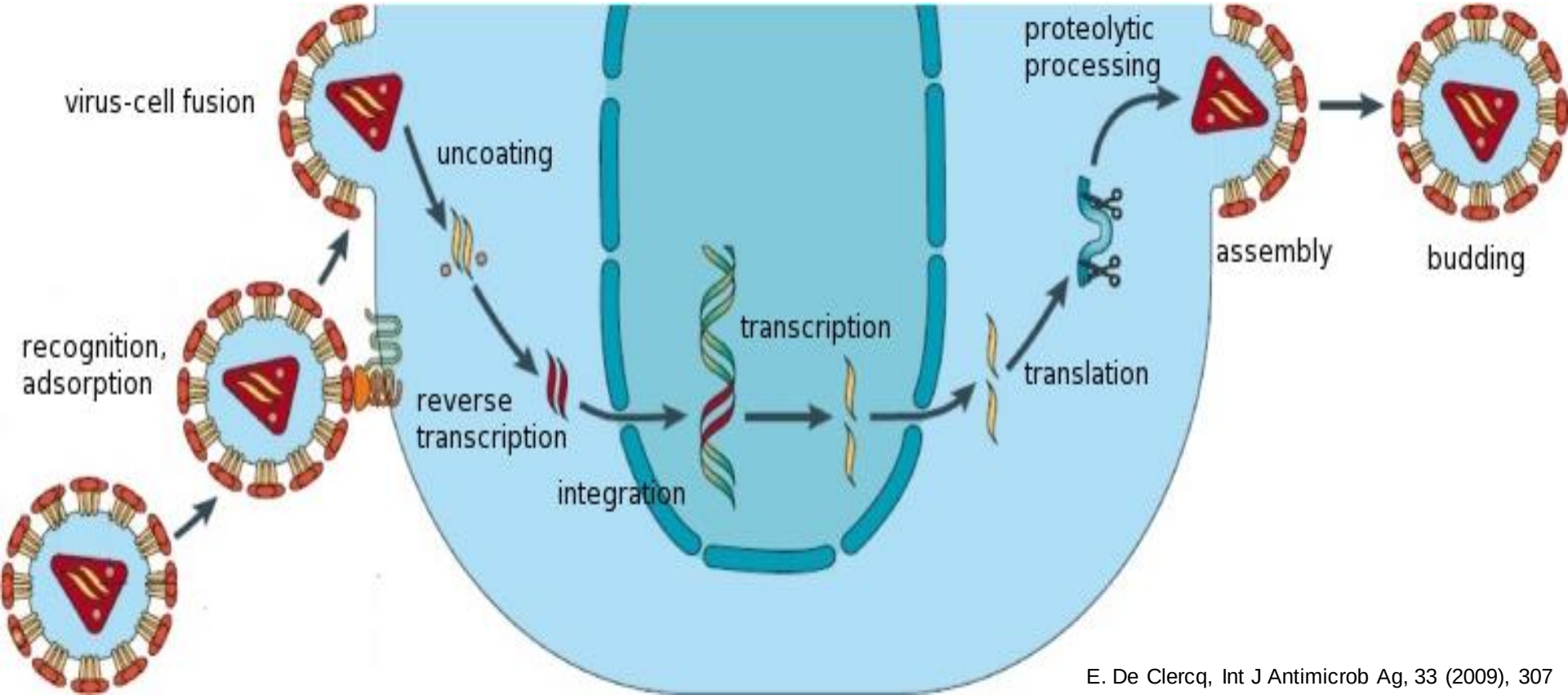

E. De Clercq, Int J Antimicrob Ag, 33 (2009), 307

CXCR4 and CCR5 Background

CXCR4 and CCR5 co-receptors involved in HIV-1 replication *in vivo.*

CCR5 principal co-receptor for HIV-1 strains most commonly transmitted between individuals. Predominates during early years of infection.

CXCR4 most relevant co-receptor for T-cell-tropic isolates that emerge after several years of HIV-1 infection.

HIV Binds by attachment of gp120 virus envelope glycoprotein to CD4 (primary receptor for HIV entry into the cells of the immune system) on the target cell.

Binding to CD4 triggers conformational change in gp120 that exposes a binding site for a chemokine receptor that acts as a co-receptor (either CXCR4 or CCR5).

Interaction with the co-receptor leads to fusion between the virus cell and the membrane.

HIV entry inhibition can be inhibited by some ligands that bind to CXCR4 and CCR5 to block steps involved in virus-cell fusion.

Complete absence of CCR5 from some humans strongly protects against HIV-1.

CCR5 deficient People who acquire HIV-1 infection are infected by strains using CXCR4 (not other potential co-receptors).

drug candidates that target CCR5

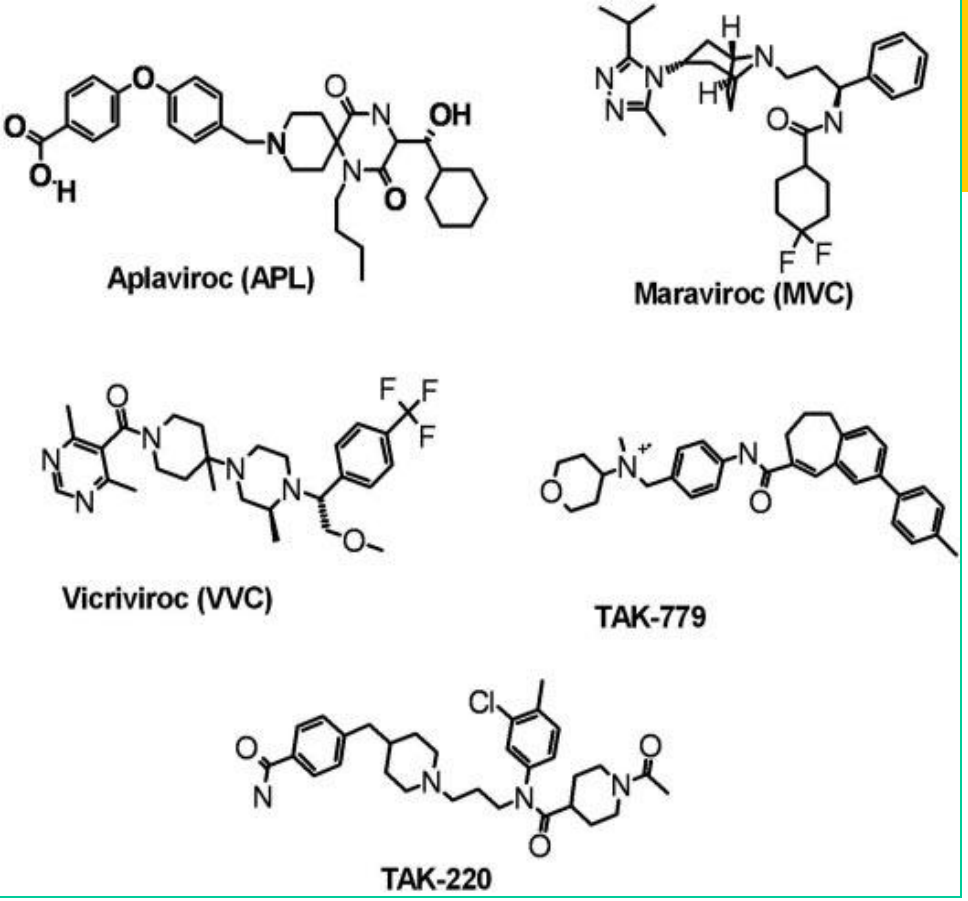

- Aplaviroc: Stopped during Phase 3 clinical trials because of liver side effects
- Maraviroc: Approved by the FDA in 2007 for the treatment of HIV
- Vicriviroc: In Phase 3 clinical trials
- TAK-779: Development halted because of side effects
- TAK-220: In Phase 1 clinical development

Factor changes of IC^{50} for CCR5 antagonists to inhibit RANTES binding to mutant CCR5, compared with binding to the wild-type (WT) CCR5

	WT	T195A	I198A	W86A	W94A	Y108A	F109A	W248A	Y251A	E283A	M287A
Vicriviroc	1	1.6	25	6.5	0.8	60	1.9	1.4	18.2	700	1.6
Maraviroc	1	1.6	89	10	2.0	70	0.9	1.4	12.2	2000	0.4
TAK-779	1	5.0	6.5	53	2.8	28	2.3	7.0	2.8	11	1.3
TAK-220	1	0.3	55	1.8	1.4	0.7	0.3	0.2	0.6	647	1.7
Aplaviroc	1	12.2	35	39	3.3	5.7	158	0.7	2.5	61	6.6

Overall Strategy of our CCR5/CXCR4 Program

- Predict 3D structures for CCR5 and CXCR4 models.
- Validate against literature data for binding of various ligands and mutations
- Predict novel scaffold space based on validated protein structures
- Test new mechanisms for interrupting gp120 binding to CCR5 and CXCR4.
- Move towards our ultimate goal of a dual CCR5-CXCR4 antagonist.

CCR5: Model b2-1 using β2 template

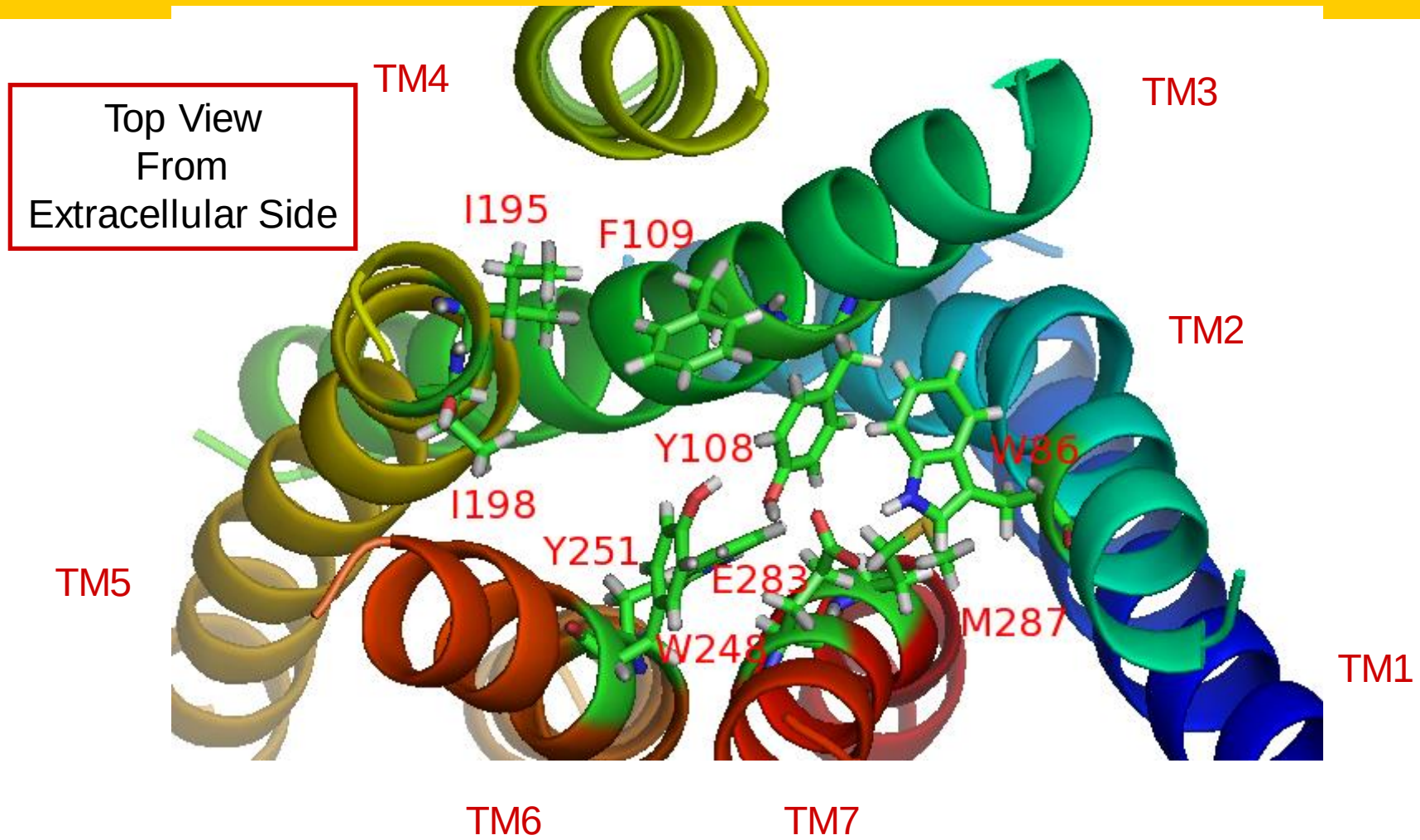

Predicted lowest energy structure:
TM rotations from β2 template: 345_0_0_45_15_0_0
All important binding residues face the putative binding pocket.

Maraviroc docked to CCR5

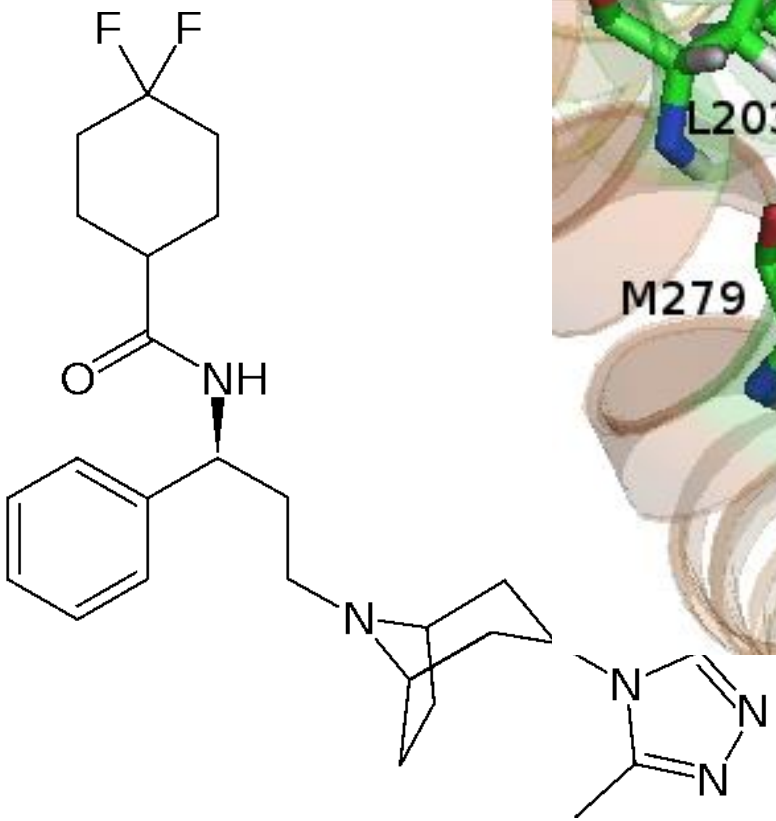

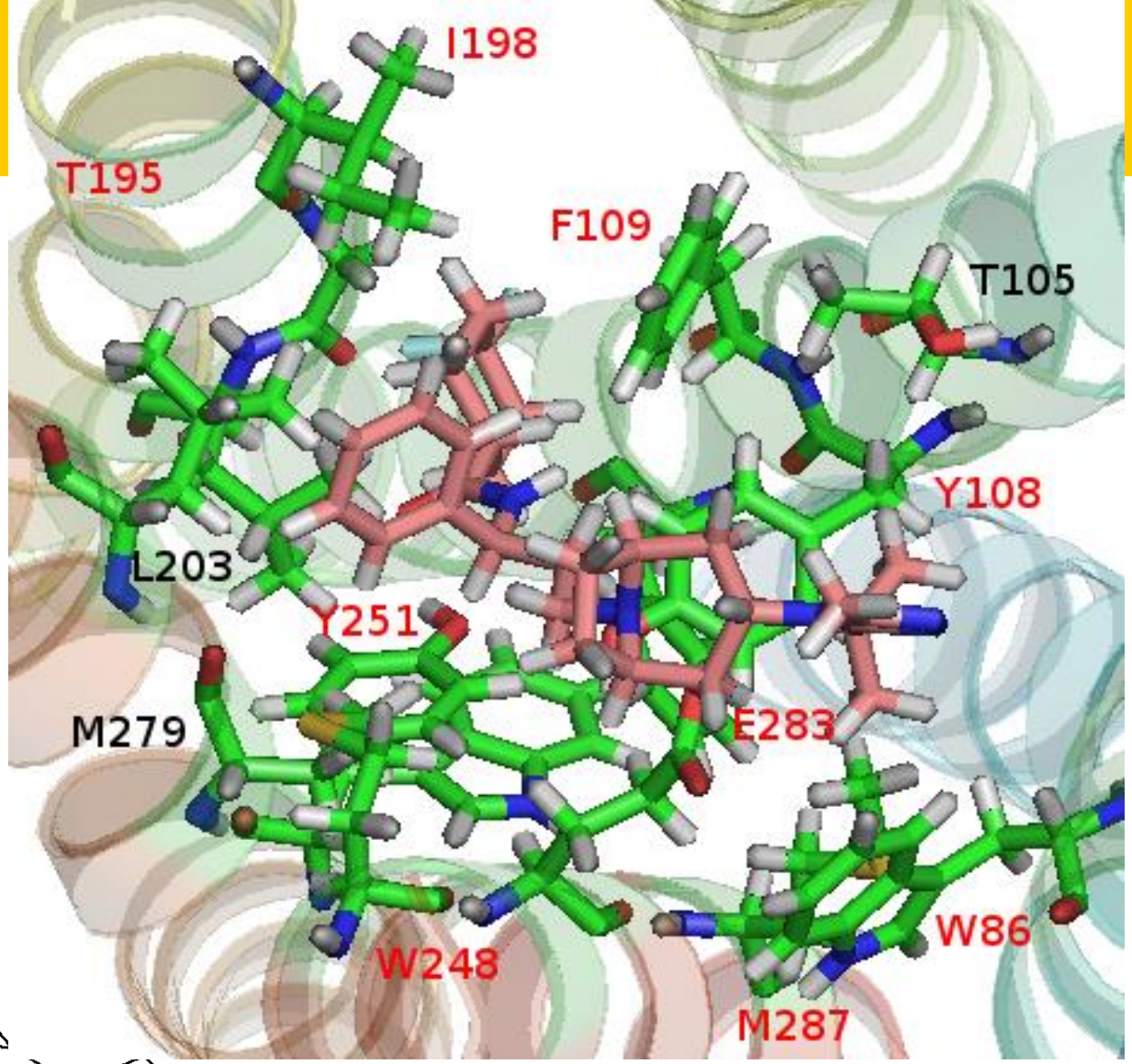

Best structure by energy: Ligand Pose 1 – Protein Model b2-1

Red – residues suggested in binding from mutation studies

Black – residues not yet studied experimentally that can be tested.

CCR5 Structure and Binding Sites: Maraviroc vs Tak-779 vs Aplaviroc Predicted Residue Contribution vs Experimental Fold Change

CCR5 Mutants	E283A	I198A	Y108A	Y251A	W86A	M287A	F109A	T195A	W248A
Experiment *	2000	89	70	12	10	~1	~1	~1	~1
Maraviroc	-4.1	-1.4	-3.6	-3.8	-3.2	-2.6	-2.2	-0.4	-0.4

CCR5 Mutants	W86A	Y108A	E283A	W248A	I198A	T195A	Y251A	F109A	M287A
Experiment *	53	28	11	7	7	5	3	2	~1
Tak-779	-8.1	-2.5	-2.0	-0.5	-2.5	-1.7	-2.3	-4.1	0.0

CCR5 Mutants	F109A	E283A	W86A	I198A	T195A	M287A	Y108A	Y251A	W248A
Experiment *	158	61	39	35	12	7	6	3	~1
Aplaviroc	-6.3	-4.0	-3.0	-1.9	-0.3	-0.1	-1.6	-5.2	-0.5

*** Kondru et al. *Molecular Pharmacology* 73, 789 (2008)**

- Experimentally,
  - E283 most critical for Maraviroc,
  - W86 for Tak-779,
  - F109 for Aplaviroc.
- Predictions reproduce this observation, providing a good validation of the predicted CCR5 protein structure.

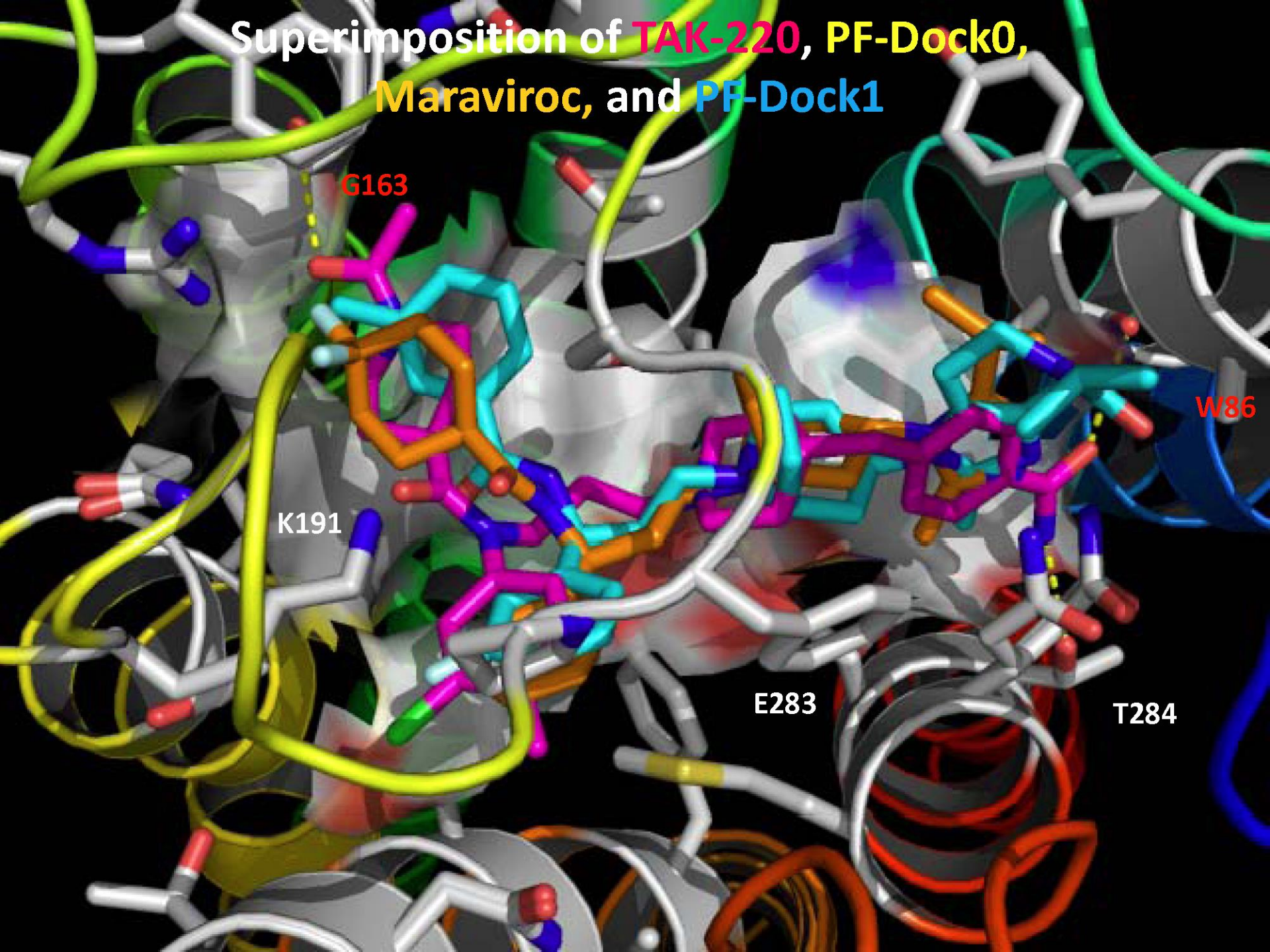
Superimposition of TAK-220, PF-Dock0, Maraviroc, and PF-Dock1
G163
W86
K191
E283
T284

Maraviroc binding site to CCR5

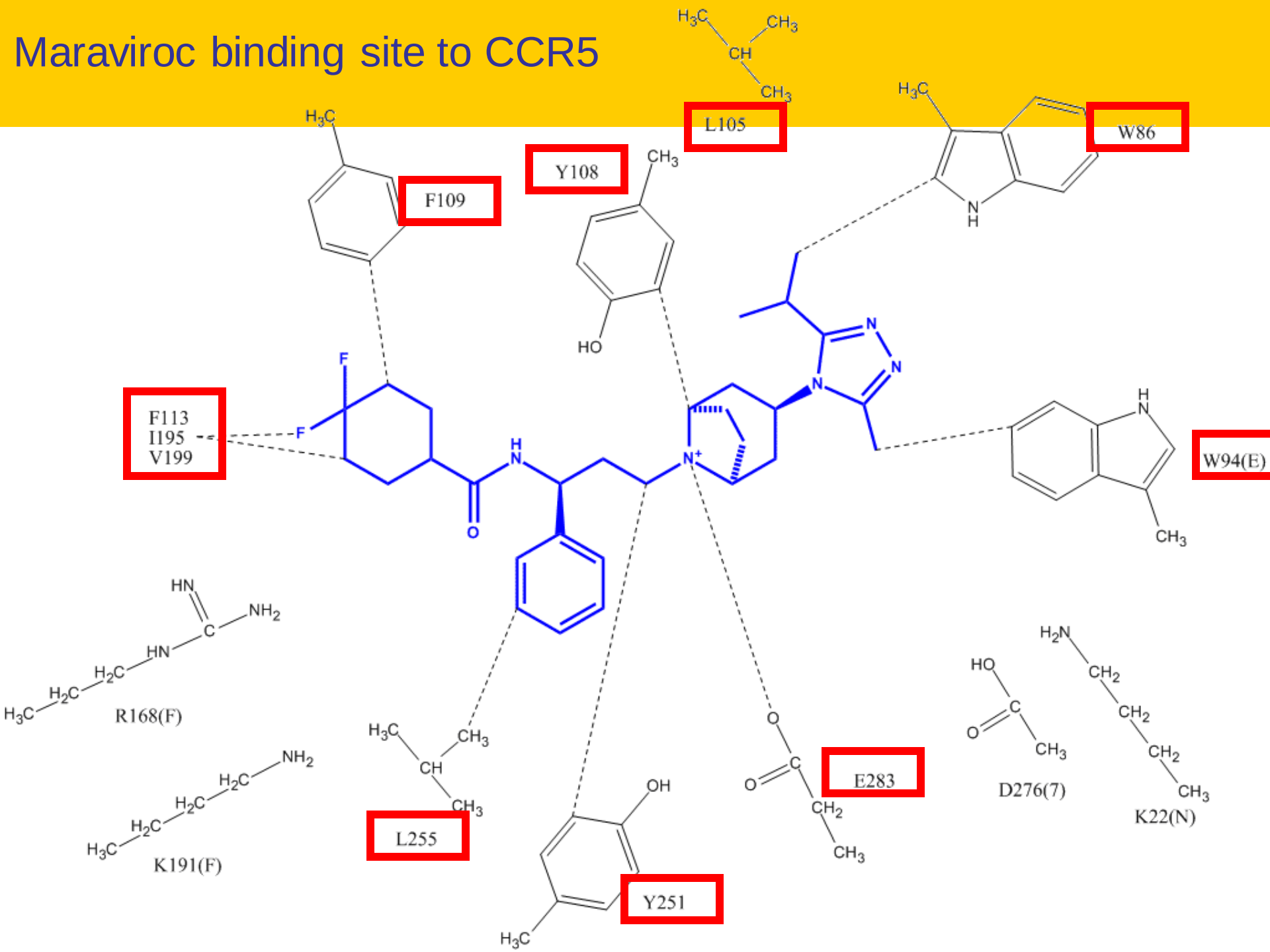

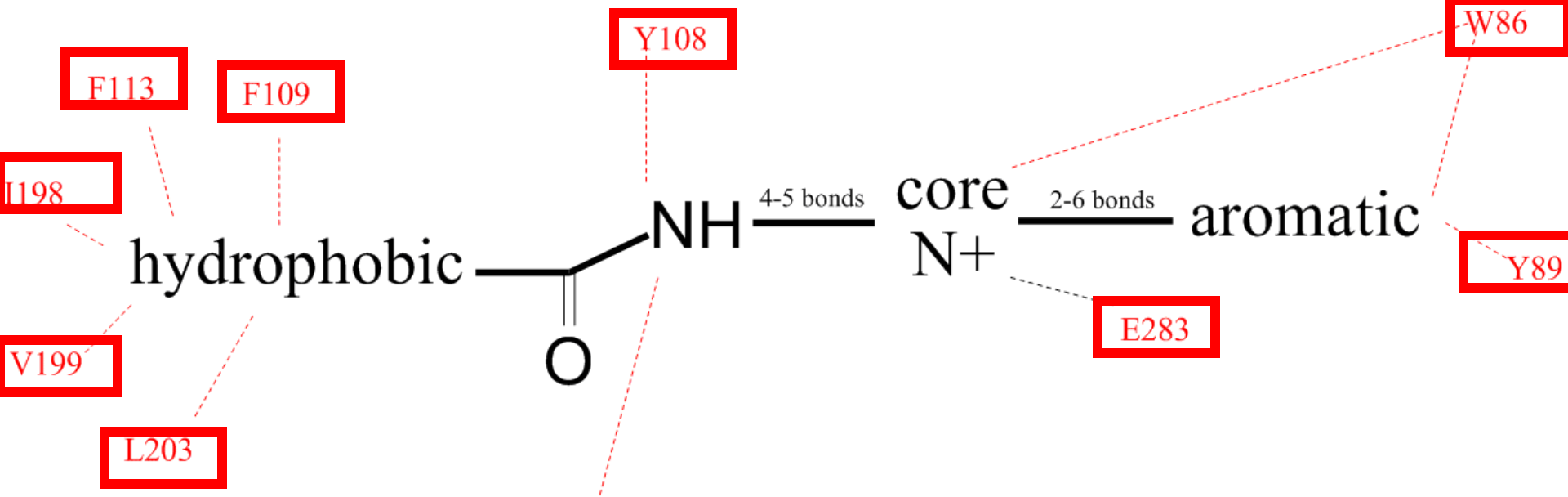

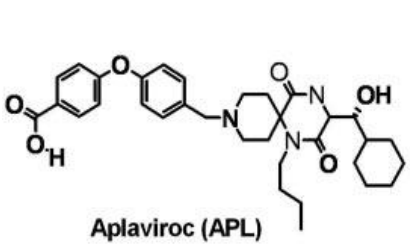
Aplaviroc (APL)

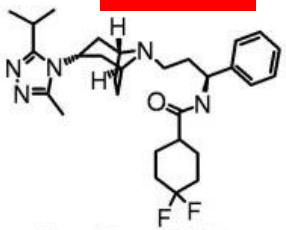
Maraviroc (MVC)

predicted binding sites consistently show same pharmacophore topology in the protein.

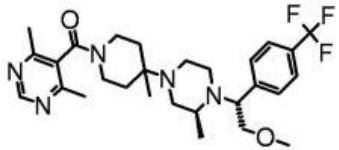
Vicriviroc (VVC)

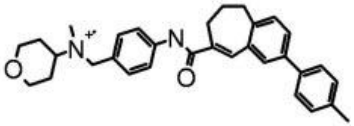
TAK-779

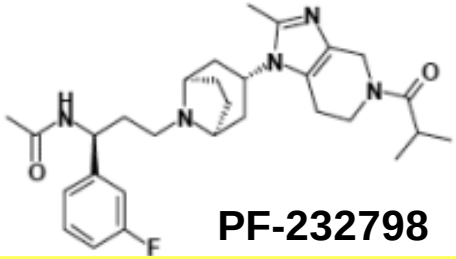
PF-232798

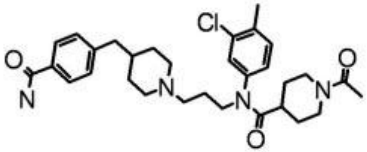
TAK-220

Pharmacophore for CCR5 Ligands

New scaffolds design - binding site

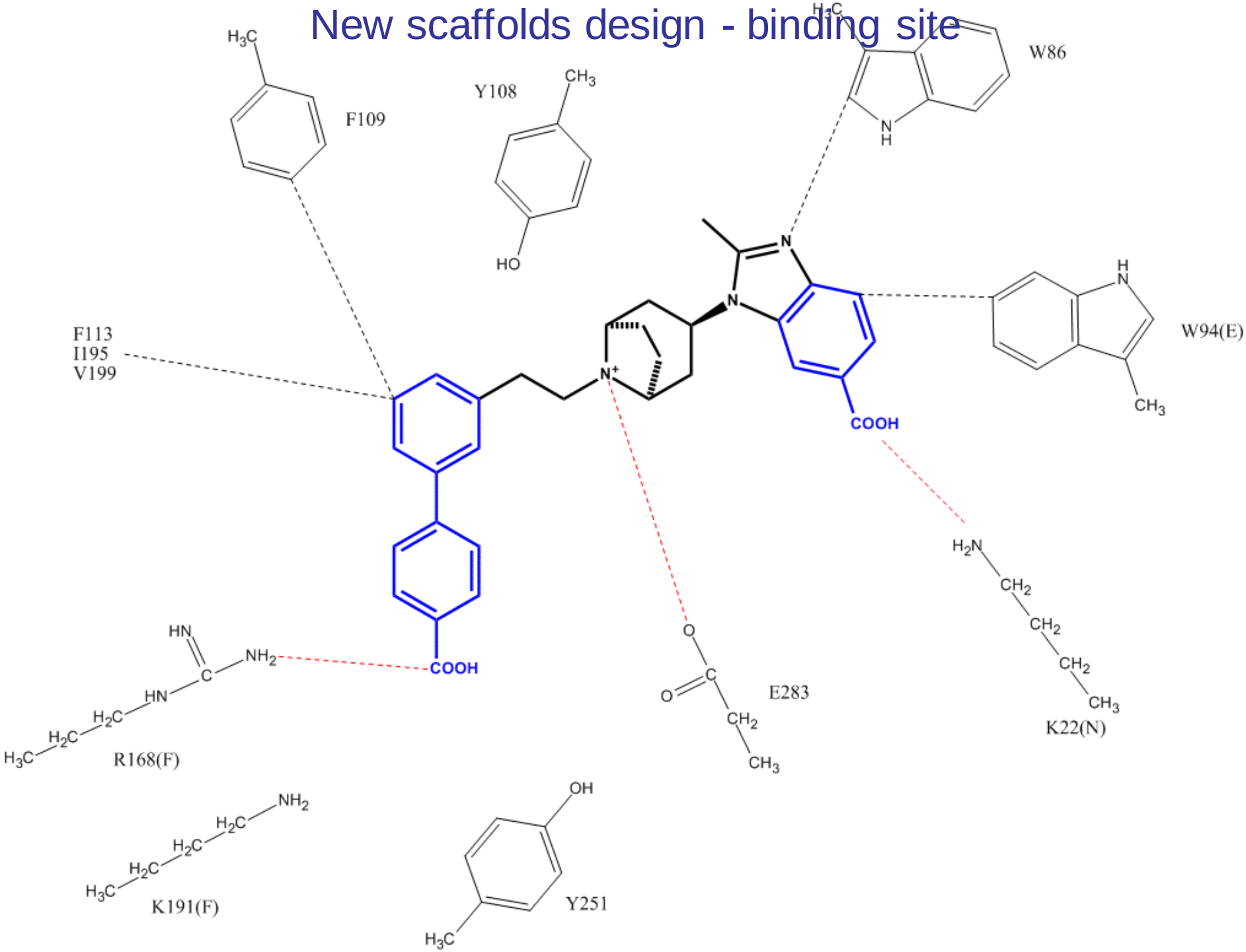

Combinatorial Computational screening to novel Scaffolds

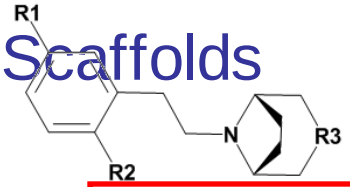

	0	13	14	15	16	17	18	19	20	21	22	23
R1:	H	H	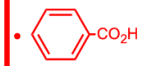	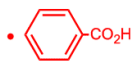		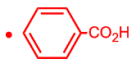	H	H	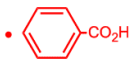	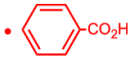	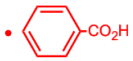	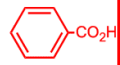
R2:	CH_3	H	H	H	H	H	H	H	H	H	H	H
R3:	H	H	H	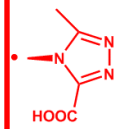	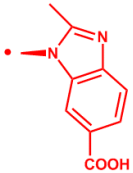	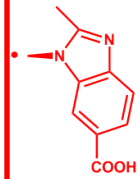	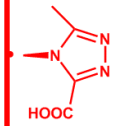	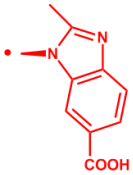	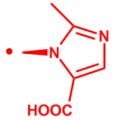	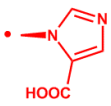	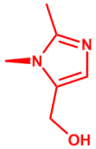	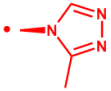
En =	0.0	+0.4	-10.5	-24.7	-27.9	-24.8	-11.0 no E283, K22	-17.2 no E283, K22	-26.8	-23.4	-29.8	-25.4
TM7	E283	E283	E283	E283	E283	E283	-	-	E283	E283	E283	E283
Nterm	-	-	-	K22	K22	K22	-	-	K22	K22	K22	-
EL2_1	-	-	R168	(R168, -22.6)	R168	R168	R168	-	R168	R168	R168	R168
EL2_2	F182	F182	F182	F182	F182	F182	F182	F182	F182	F182	F182	F182
TM5	-	-	-	K191	K191	-	-	K191	-	-	-	K191
TM5_2	-	-	-	Q194	-	-	-	-	-	-	Q194	-

Scaffold 15 – dock 17

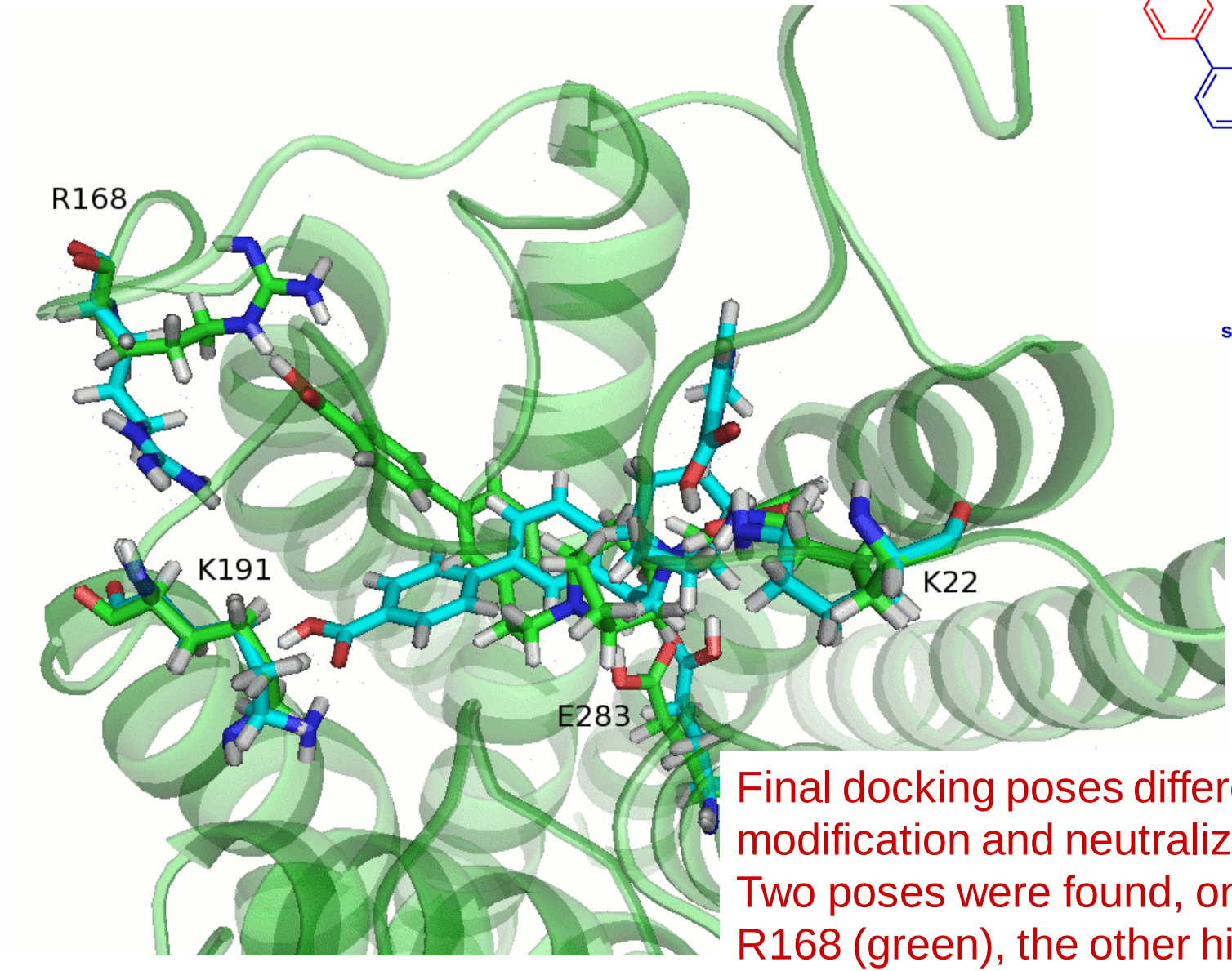

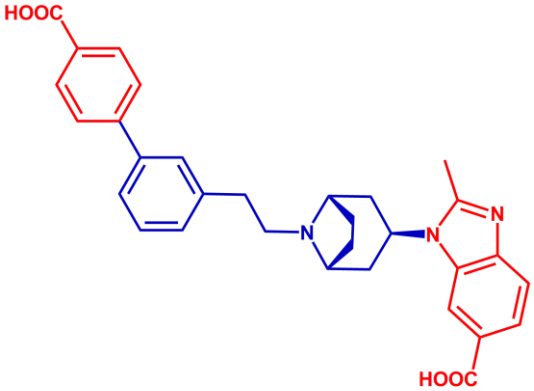

scaffold15 - dock17

Final docking poses different after modification and neutralization.
Two poses were found, one hits intended R168 (green), the other hits K191 (blue).
Both poses also hit intended E283 and K22

2nd best energy pose in Green
Best energy pose in Blue

First round design

Based on the above predictions we designed several new ligands which a commercial collaborator synthesized

Results ok, but not great, about ½ right and ½ wrong. Not successful in improving overall binding constant

We decided that our GPCR structure was not sufficiently accurate for drug design, it was not sufficient to optimize the $(12)^7$=35,000,000 combinations of eta,

Instead we need to optimize the tilts (θ, φ) for each of these eta.

We developed SuperBiHelix method to make it practical to optimize the tilts for each of the best eta's

Eliminate Bias from Template
Super BiHelix Sampling

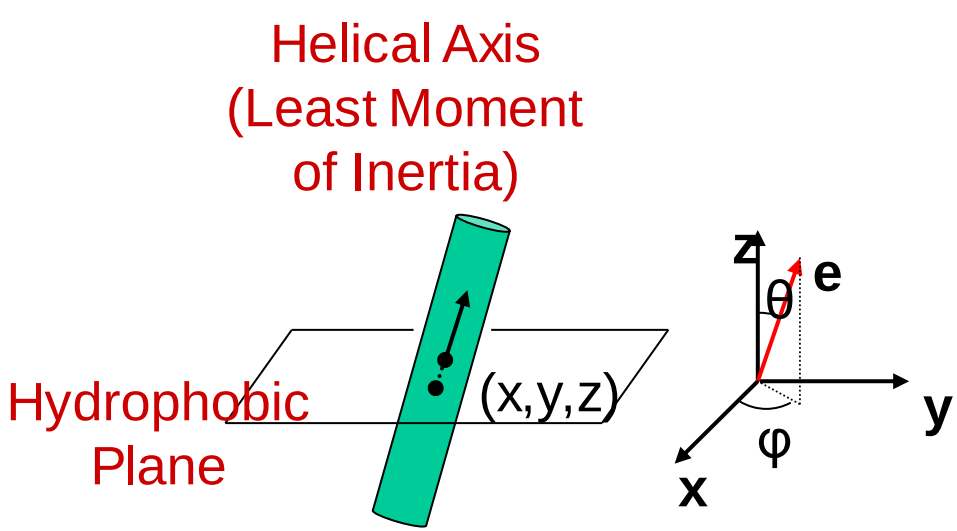

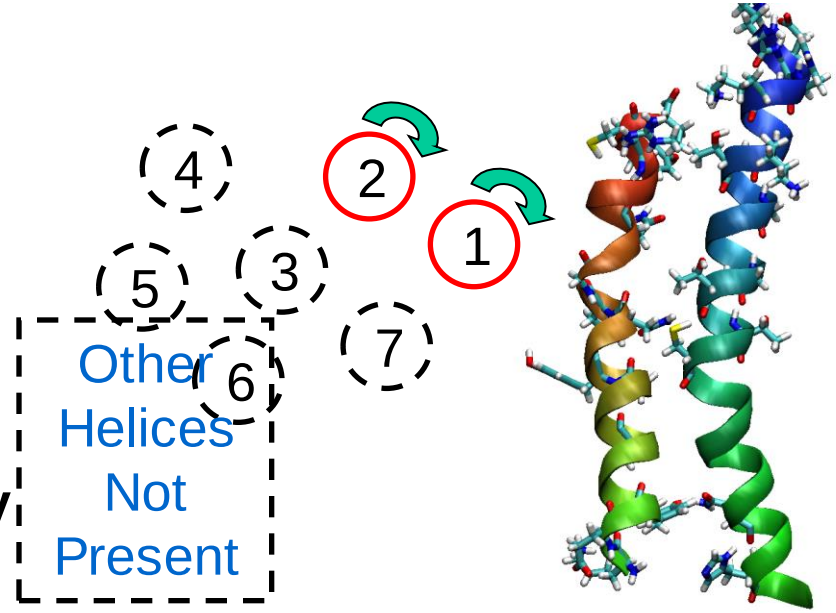

1. For a fixed x,y,z, sample variations on θ, φ, η
2. Typical sample 3 values of θ (+10 to -10º), 3 of Phi (+20 to -20º) and 7 of Eta (+45 to -45º)
3. Perform in BiHelix Mode
4. Generate all pairwise combinations for each interacting helix pair.
5. Sum pairwise energies to generate best bundle combinations.

SuperBiHelix Procedure

- Sample z, ϕ, θ and η values for each of 12 interacting pairs to get bihelical energies

H1_H2	H1_H3	H1_H7
H2_H3	H2_H7	H3_H4
H3_H5	H3_H6	H3_H7
H4_H5	H5_H6	H6_H7

- For each bihelical conformation, minimize sidechains for 10 steps, and use total energy of minimized structure
- Calculate bihelical energies of 3 quadhelix bundles:

  1-2-3-7, 2-3-4-5, 3-5-6-7
- Output top 2000 structure by energy for each quadhelix
- Do this for each templae
- Rank conformations for each helix, alternating conformations from each applicable quadhelix
- Take top 36 conformations for each helix and calculate the total bihelical energies for all $36^7 = 8 \times 10^{11}$ seven helix bundles.
- Output the top 1000 structures from this analysis by total energy for further analysis in SuperCombiHelix

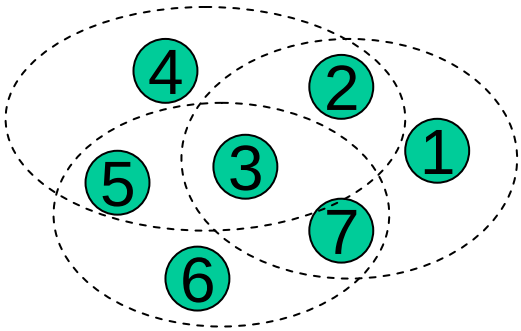

Test of SuperBiHelix for Bovine Rhodopsin

Theta = -10, 0, 10 Phi = -30, -15, 0, 15, 30 Eta = -30, -15, 0, 15, 30

SuperBiHelix select top 1000, xray is # 22

Thet	H1	H2	H3	H4	H5	H6	H7	Phi	H1	H2	H3	H4	H5	H6	H7	Eta	H1	H2	H3	H4	H5	H6	H7	TotalE
Thet	0	0	0	0	0	0	-10	Phi	-15	0	0	0	-15	-15	-30	Eta	0	-15	0	0	0	15	0	221.0
Thet	0	0	0	0	0	0	-10	Phi	-15	0	0	15	-15	-15	-30	Eta	0	-15	0	0	0	15	0	222.8
Thet	0	0	0	0	0	0	-10	Phi	-15	0	0	0	-15	-30	-30	Eta	0	-15	0	0	0	15	0	223.2
Thet	0	0	0	0	0	0	-10	Phi	-15	0	0	0	-15	0	-30	Eta	0	-15	0	0	0	0	0	224.0
Thet	0	0	0	0	0	0	-10	Phi	-15	0	0	15	-15	-30	-30	Eta	0	-15	0	0	0	15	0	225.0
Thet	0	0	0	0	0	0	-10	Phi	-15	0	0	15	-15	0	-30	Eta	0	-15	0	0	0	0	0	225.8
Thet	0	0	0	0	0	0	-10	Phi	0	0	0	0	-15	15	-15	Eta	0	0	0	0	0	0	15	227.0
Thet	0	0	0	0	0	0	-10	Phi	-15	0	0	0	0	0	-30	Eta	0	-15	0	0	0	0	0	227.5
Thet	0	0	0	0	0	0	0	Phi	0	0	0	0	-15	0	0	Eta	0	0	0	0	0	0	0	227.9
Thet	0	0	0	0	0	0	-10	Phi	0	0	0	-15	-15	15	-15	Eta	0	0	0	0	0	0	15	228.0
Thet	0	0	0	0	0	0	0	Phi	0	0	0	-15	0	0	0	Eta	0	0	0	0	0	0	0	228.3
Thet	0	0	0	0	0	0	0	Phi	0	0	0	-15	-15	0	0	Eta	0	0	0	0	0	0	0	228.8
Thet	0	0	0	0	0	0	0	Phi	-15	0	0	0	-15	0	0	Eta	0	-15	0	0	0	0	0	229.0
Thet	0	0	0	0	0	0	-10	Phi	-15	0	0	0	0	-15	-30	Eta	0	-15	0	0	0	15	0	229.4
Thet	0	0	0	0	0	0	-10	Phi	0	0	0	30	-15	15	-15	Eta	0	0	0	0	0	0	15	229.7
Thet	0	0	0	0	0	0	-10	Phi	-15	0	0	15	0	0	-30	Eta	0	-15	0	0	0	0	0	229.8
Thet	0	0	0	0	0	0	-10	Phi	0	0	0	15	-15	15	-15	Eta	0	0	0	0	0	0	15	229.9
Thet	0	0	0	0	0	0	0	Phi	0	0	0	30	-15	0	0	Eta	0	0	0	0	0	0	0	230.5
Thet	0	0	0	0	0	0	0	Phi	0	0	0	0	-15	0	0	Eta	0	-15	0	0	0	0	0	230.8
Thet	0	0	0	0	0	0	0	Phi	0	0	0	15	-15	0	0	Eta	0	0	0	0	0	0	0	230.9
Thet	0	0	0	0	0	0	0	Phi	-15	0	0	15	-15	0	0	Eta	0	-15	0	0	0	0	0	230.9
Thet	0	0	0	0	0	0	0	Phi	0	0	0	0	0	0	0	Eta	0	0	0	0	0	0	0	231.3

XTAL

SuperCombiHelix evaluate top 1000, xray is #1

Thet							Phi								Eta								ScreamE	PreMinE	PostMinE
Thet	0	0	0	0	0	0	Phi	0	0	0	0	0	0	0	Eta	0	0	0	0	0	0	0	-55.2	582.5	270.6
Thet	0	0	0	0	0	0	Phi	0	0	0	-15	0	0	0	Eta	0	0	0	0	0	0	0	-52.2	593.9	275.5
Thet	0	0	0	0	0	0	Phi	0	0	0	15	-15	0	0	Eta	0	0	0	0	0	0	0	-50.7	595.5	281.1
Thet	0	0	0	0	0	0	Phi	0	0	0	30	-15	0	0	Eta	0	0	0	0	0	0	0	-53.7	602.5	292.0
Thet	0	0	0	0	0	0	Phi	0	0	0	30	-15	0	0	Eta	0	0	0	-15	0	0	0	-48.4	656.4	299.6

CCR5-Optimize tilts and rotations simultaneously

Theta	H1	H2	H3	H4	H5	H6	H7	Phi	H1	H2	H3	H4	H5	H6	H7	Eta	H1	H2	H3	H4	H5	H6	H7	AvgRank	CCR5
Theta	-10	-10	-10	0	0	0	0	Phi	-15	0	0	-15	-15	-15	-15	Eta	0	240	0	0	15	0	0	12.8	wt1
Theta	0	-10	-10	0	0	0	0	Phi	-15	0	-15	0	0	0	0	Eta	345	225	0	0	345	0	0	14.5	wt2
Theta	0	-10	-10	0	0	0	0	Phi	-15	0	-15	-15	0	0	0	Eta	345	225	0	0	345	0	0	21.3	wt3
Theta	-10	-10	-10	0	0	0	0	Phi	-15	15	-15	-15	0	-15	-15	Eta	345	225	0	15	345	0	0	71.3	wt4
Theta	0	-10	-10	-10	0	0	0	Phi	-15	0	0	15	0	0	0	Eta	345	225	0	15	345	0	0	89.8	wt5
Theta	-10	-10	-10	10	0	0	0	Phi	-15	-15	15	-15	-15	0	0	Eta	15	0	0	15	30	0	0	98.5	wt6
Theta	-10	-10	0	0	10	0	0	Phi	-15	-15	15	-15	-15	-15	0	Eta	15	0	0	105	15	0	0	100.3	wt7
Theta	-10	-10	-10	0	0	0	0	Phi	-15	0	-15	-15	0	-15	-15	Eta	0	225	0	15	345	0	0	108.5	wt9
Theta	0	-10	-10	-10	0	0	0	Phi	-15	0	0	15	-15	0	0	Eta	345	225	0	15	15	0	0	109.8	wt10
Theta	-10	-10	-10	10	0	0	0	Phi	-15	-15	0	0	-15	15	0	Eta	15	15	0	15	15	0	0	111.0	wt11
Theta	0	-10	-10	0	0	0	0	Phi	-15	0	-15	-15	0	-15	0	Eta	330	225	0	15	345	0	0	122.0	wt13
Theta	-10	-10	-10	10	0	0	0	Phi	-15	-15	0	-15	0	0	0	Eta	15	0	0	105	345	0	0	126.3	wt14
Theta	0	-10	-10	0	0	0	0	Phi	-15	0	-15	-15	0	-15	-15	Eta	345	225	0	0	345	0	0	143.5	wt15
Theta	0	-10	-10	-10	0	0	0	Phi	-15	0	0	0	-15	0	0	Eta	345	225	0	15	0	0	0	145.5	wt16
Theta	0	0	-10	10	0	0	0	Phi	-15	-15	-15	-15	0	0	0	Eta	0	0	0	120	345	0	90	145.8	wt17
Theta	-10	0	-10	10	0	0	0	Phi	-15	-15	-15	-15	0	0	15	Eta	0	15	0	105	345	0	0	146.5	wt18
Theta	-10	-10	-10	10	0	0	0	Phi	-15	-15	0	-15	0	15	0	Eta	15	15	0	120	75	0	0	147.0	wt19

Selected 16 conformations from BiHelix sampling.
Performed complete local tilt (Thet, Phi, Eta) sampling (SuperBiHelix) for each.
Neutralized the bundles and ranked them.
Selected 9 low energy conformations for docking (highlighted rows)
Table shows the different tilt/rotation angles for these conformations.

Maraviroc Binding Site

From SuperBiHelix

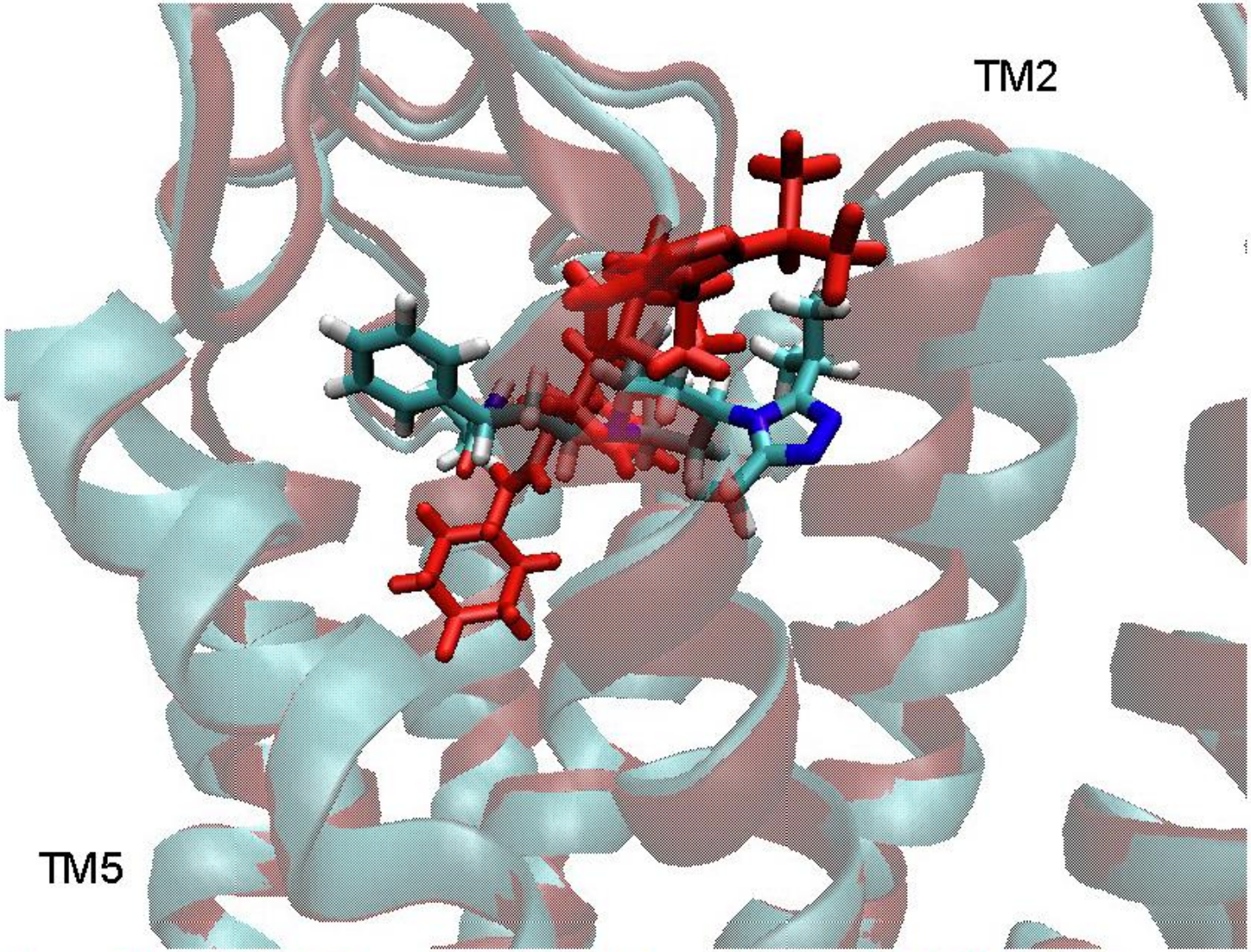

Same binding site but different pose.

Blue: Old CCR5 Structure; Red: New 4th Best CCR5 Structure

TMs 2 and 5 move closer that causes Maraviroc to bind differently.

Lesson must optimize the helix tilts for each set of rotations

Otherwise the binding site may distort too much for ligand optimization

Quantitative comparison with Ligand Binding Mutation experiments

Usual approach: look at contribution of each residue to the binding

Expect that mutation to Ala will have biggest effect on the strongest binders

More refined: mutate the residue and recalculate the binding

We found that this worked 2/3 the time but there were clear discrepancies

This raised the issue of whether the mutated protein might pack differently

Our approach. Use the best 100 packings from the SuperBiHelix of apo protein

Do the mutation on all 100, reoptimize side chains and re-rank

Reordering of CCR5 conformations for F109Y, F112A, and Q194A

F109Y	AvgRank
wt3	8.3
wt2	11.5
wt1	12.0
wt21	18.0
wt22	19.0
wt6	27.8
wt11	27.8
wt17	28.3
wt5	28.5
wt12	28.8
wt64	33.5
wt19	34.0
wt30	34.3
wt4	34.3
wt7	35.3
wt43	36.3
wt20	36.3
wt10	36.3
wt8	36.3
wt18	37.3

F112A	AvgRank
wt1	6.0
wt2	10.3
wt3	10.8
wt9	11.3
wt4	20.8
wt6	22.0
wt5	23.8
wt85	27.5
wt28	27.8
wt13	28.5
wt43	28.8
wt33	32.5
wt16	32.5
wt7	33.0
wt14	33.3
wt8	34.0
wt30	34.8
wt11	35.5
wt12	36.5
wt27	37.8

Q194A	AvgRank
wt1	6.5
wt2	6.8
wt3	7.0
wt4	25.0
wt9	28.0
wt5	29.0
wt27	30.5
wt13	30.8
wt11	31.0
wt12	32.0
wt7	32.5
wt6	32.8
wt8	33.5
wt64	34.3
wt15	34.5
wt18	35.5
wt10	35.5
wt20	36.5
wt30	38.3
wt32	38.5

Wildtype #21 and #22 become #4 and #5

wt85 becomes #8 !

4

Now use the best ~10 conformations of each mutant and redock the ligand

Usually can match from previous docking, reoptimize the sidechains and minimize

Effect of Mutations on Maraviroc

	CCR5 Confs				
Mutations	Apo	Mara	ΔE	Confidence	Comments
F109Y	wt3	wt5	-6.5	Neutral	Sign ok, but too high magnitude.
F112A	wt1	wt5	+1.9	Good	
Q194A	wt1	wt5	-0.9	Good	
Y251F	wt1	wt2	+0.6	Good	
D276A	wt1	wt2	+2.6	Poor	Mainly hydrophobic interaction.
Q277A	wt1	wt5	+3.6	Good	
W86A	wt1	wt3	+3.0	Good	
A90H	wt3	wt10	-4.2	Poor	Visually weakly interacting.
T105A	wt1	wt2	-1.4	Good	
Y108A	wt3	wt2	+3.3	Good	
F109A	wt1	wt5	-0.1	Good	
I198A	wt1	wt5	+0.8	Poor	
Y251A	wt2	wt3	+2.3	Good	
Q280A	wt3	wt5	-0.6	Good	
E283A	wt3	wt3	+6.2	Good	

Protein conformation that binds ligand depends on mutation

Effect of Mutations on Maraviroc Binding: Comparison between Expt and Theory

Mutant	Ki(Mut)/Ki(WT)	log[Ki(Mut)/Ki(WT)]	ΔEpred
E283A	2000	3.301	6.2
Y108A	88	1.944	3.3
W86A	23	1.362	3
Y251A	22.2	1.346	2.3
Y251F	3.19	0.504	0.6
F112A	1.69	0.228	1.9
Q277A	1.44	0.158	3.6
T105A	1.02	0.009	-1.4
F109A	0.99	-0.004	-0.1
Q194A	0.825	-0.084	-0.9
Q280A	0.77	-0.114	-0.6

correlation of theory with experiment good (0.71). One main outlier Q277A, ~~might require~~ treatment of explicit waters in the binding site.

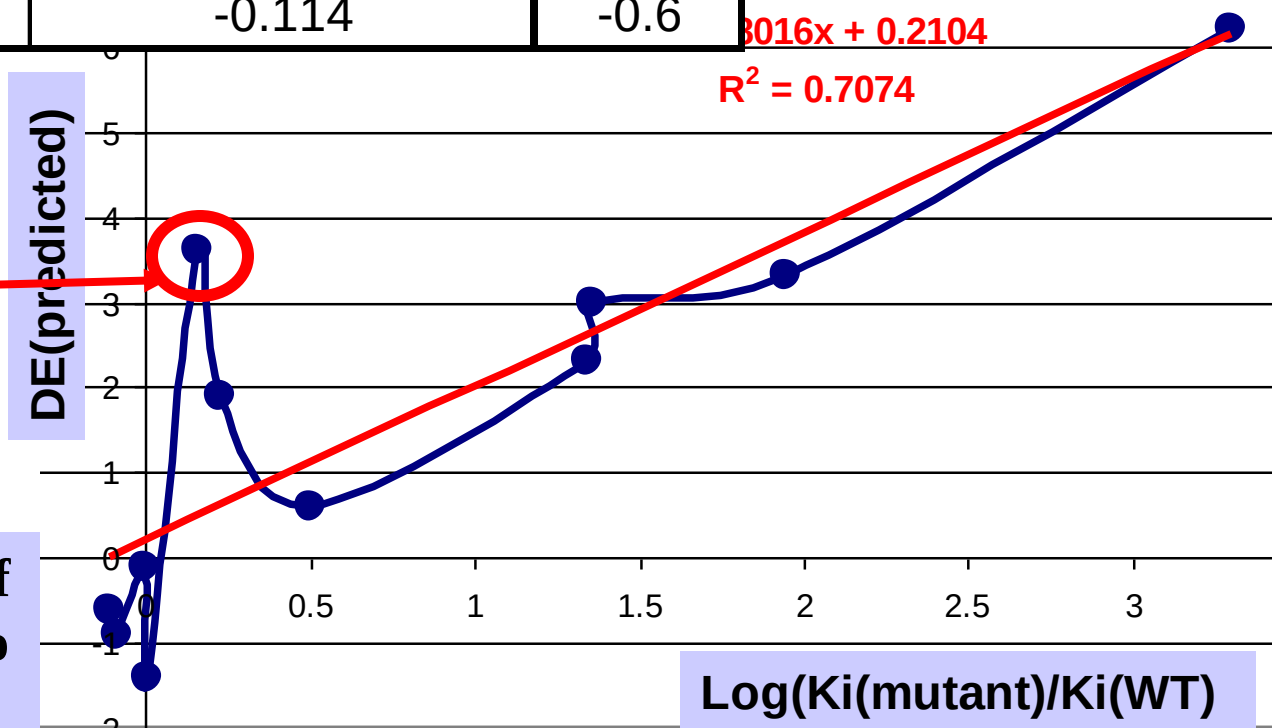

Unfortunately we ran out of $$ and must find new VC to continue

Summary of Results

First principles methods (no use of atomic experimental data), are now capable of predicting the 3D structure of GPCRs and the binding site for agonists and antagonists to GPCRs that they can be used for drug design

In addition, the theory is providing hints about the nature of activation.

This provides the basis to consider using theory and computation to design selective subtype selective agonists and antagonists

Grand Vision for GPCRs

Use theory and computation to Determine Structure and Function for **ALL** Human GPCR's (including orphans)

Use this "complete set" of targets and antitargets to design a subtype selective agonist and antagonist for every GPCR

Also do Rat, Mouse, Guinea Pig, Goat in order to select optimum animal model to mimic behavior with Human targets

Could be done in 5 years with sufficient funding

For 450 human GPCRs excluding olfactory and taste but including 150 Orphan: $80 million

For all 350 human Olfactory and taste: $60 million

No interest from NIH or big pharma, hope to continue working with VC's

Bio Collaborators

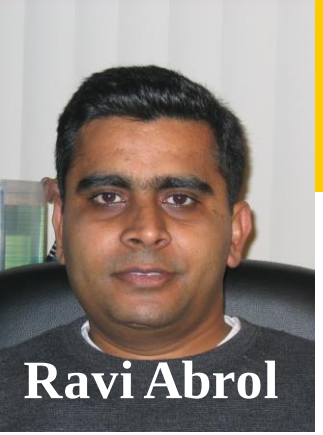

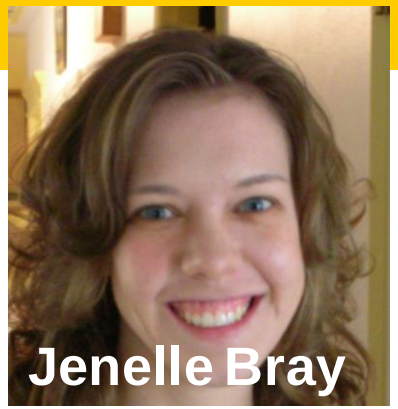

Griffith
Adam Reid

Support: DARPA, Pfizer, Boehringer, Aventis, Berlex, Allozyne, PharmSelex, NIH

Theory and simulation is now at the point where it can help substantially in developing improved materials for fuel cells and many other applications

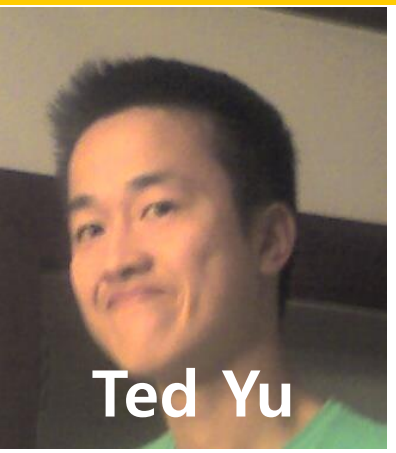

Experimental Collaborators
Omar Yaghi (UCLA)

Contributors to Fuel Cell applications including H_2 Storage

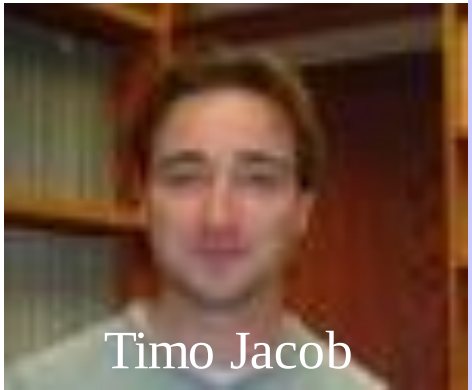

Support Initial GAPC/GM
Non Pt catalysts DOE-EERE H2 economy (with Debbie Myers)
Mesoporous-sulfonate membranes-DOE BES
Ceramic PEM [Ba(YZr)O3]-DOE-FETL
Dupont (membranes)
Ford

First principles theory and simulation are now at the point where it can drive the design and development of new materials

Hydrogen,
Energy,
Fuel Cell,
Battery,
Water Purification, and
CO2 Sequestration
Technologies

Ever Been to a Research Grant Review?

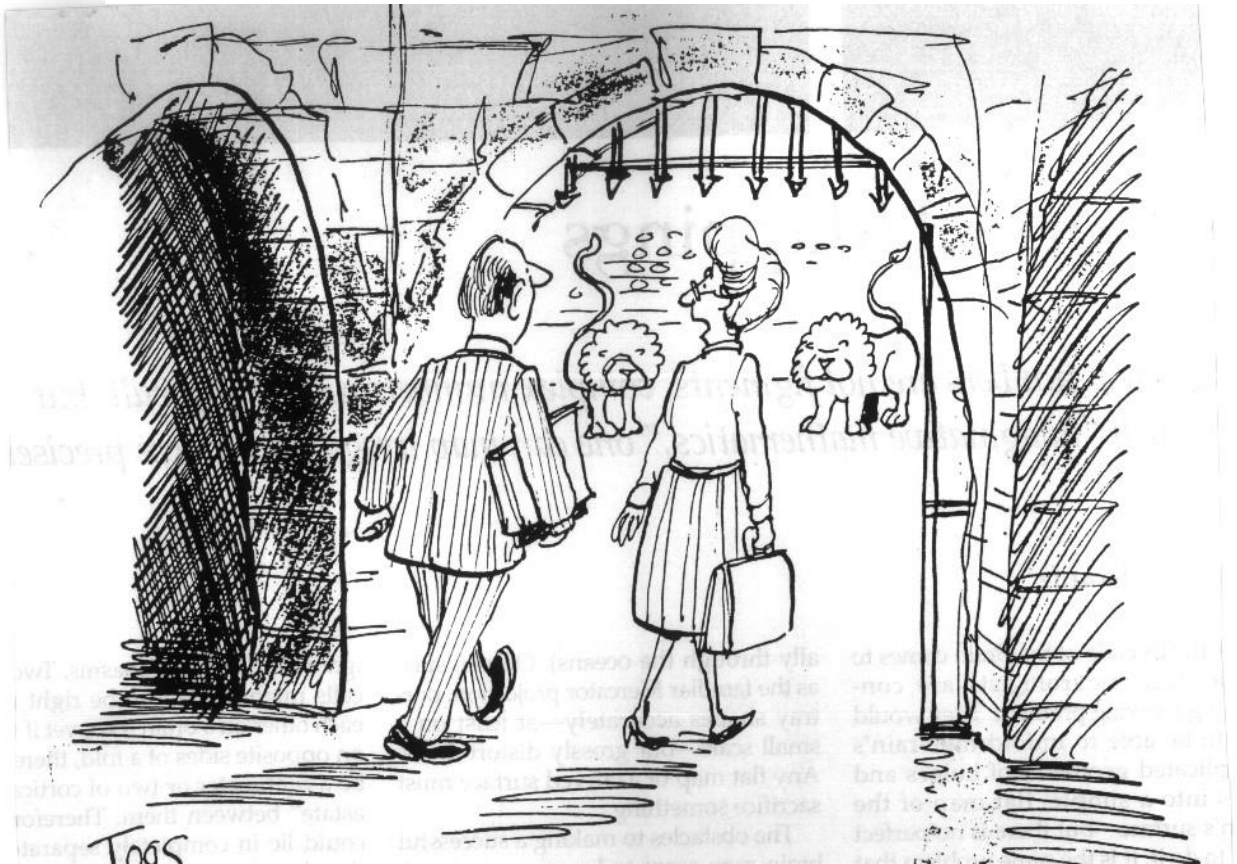

Support:

DARPA, DOE, ONR, ARO, NIH, NSF, EPA,

Intel, Ford, Dow-Corning, Nissan, GM,

Pfizer, Boehringer, Aventis, Allozyne

Stop already

Contacts between Metals with Carbon Nanotubes and Graphene

- Many studies of the electronic devices using carbon nanotubes (NTs)

  Dai, *Nature* **424**, 654 (2003). Dekker, *Nature* **393**, 49 (1998) etc.

- Contact resistance strongly affects electrical conductivity

… However, little is known about contact resistance.

How to make good contacts between the electrodes and nanotubes?

Experimental Procedure

(1) Deposition of metal electrodes on NT

(2) NT on top of two electrodes

Both processes usually followed by annealing

Objectives

Understand how metals bond to carbon surface.

Determine mechanical strength and contact resistance.

Considered Ti, Pd, Pt, Au, and Cu

(1)

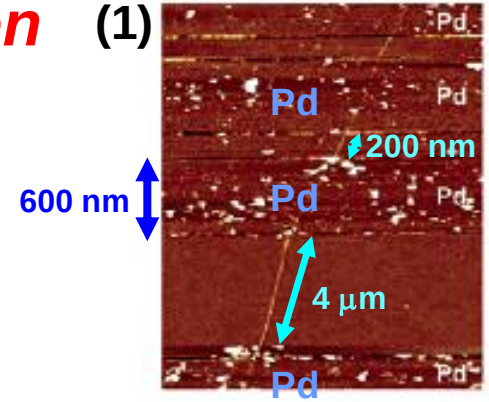

Metallic-SWNT (d=3 nm, L=1 μm) Pd electrodes (~30 nm thick) Dai HJ, *NanoLett.* 3, (2003)

(2)

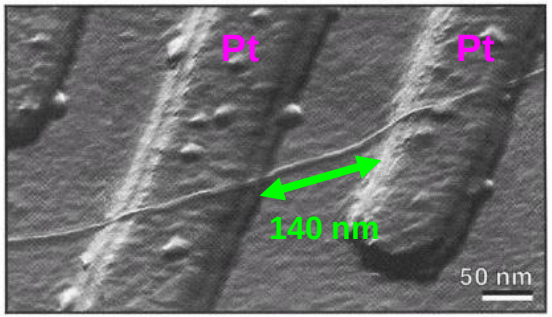

Metallic-SWNT (d=1 nm, L=4 μm) Pt electrodes (15 nm thick) Dekker C, *Nature* 386, (1997)

Carbon Nanotube Interconnects

Caltech: Yuki Matsuda, WeiQiao Deng and William A. Goddard III
Intel Components Research: Florian Gstrein, James Blackwell

Strategies

(1) Deposition metal electrodes on assembled CNTs

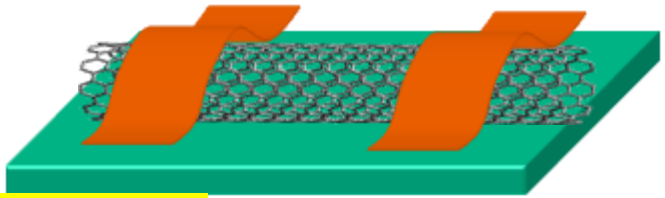

(2) Assemble surface modified CNTs on top of two electrodes

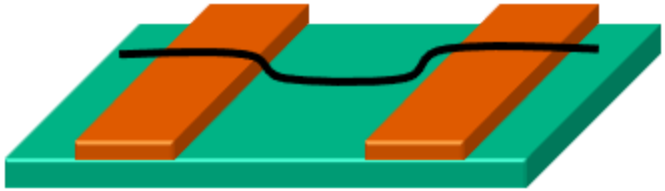

Objectives

a. Find the best metal to deposit on graphene or carbon nanotubes
b. Develop molecular Anchor to enhance conductivity and stabilize the geometry at interface

Deposition of Metals on Graphene – Ti, Pd, Pt, Au, Cu

Metal deposition on graphite: DFT optimization (PBE, periodic)

(1) Deposit metal on top of graphene one atom at a time and optimize the structures. Keep graphene sheet fixed.
(2) Find optimum first layer

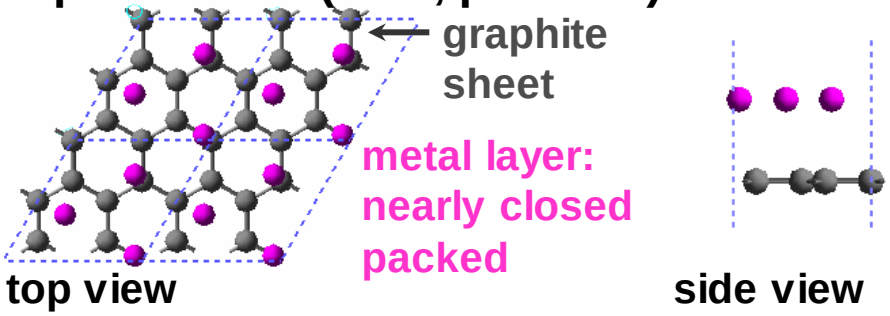

3 atoms / unit cell (unit cell: 2 x 2 graphite sheet, 4.89 x 4.89 Å)

Use QM to calculate current as a function of *applied voltage*

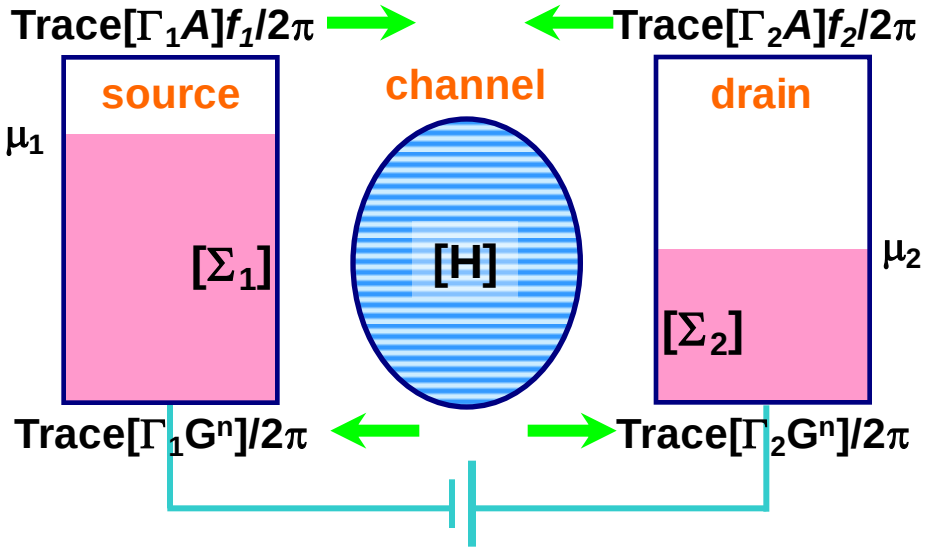

One-level	Multi-level	
ε	$[H]$	*Hamiltonian matrix*
γ	$[\Gamma(E)]$	*Broadening matrix*
$2\pi D(E)$	$[A(E)]$	*Spectral function*
$2\pi n(E)$	$[G^n(E)]$	*Correlation function*
U	$[U]$	*Self-consistent potential matrix*
N	$[\rho] = \int (dE/2p)[G^n(E)]$	*Density matrix*

Matrix Green's function method

$$G = (EI - H - \Sigma_1 - \Sigma_2)^{-1}$$

Channel Green's function

$$\Gamma_{1,2} = i\left(\Sigma_{1,2} - \Sigma_{1,2}^{+}\right)$$

Broadening matrix (anti-Hamiltonian part of self-energy matrix)

$$\Sigma_{1,2} = \tau_{1,2} g_R \tau_{1,2}^{+}$$

Self-energy matrix (the effect of contacts) g_R surface Green's function, $1/\tau$ escape rate ($\gamma\tau = h/2\pi$)

$$T(E,V) = \mathrm{Trace}\left(\Gamma_1 G \Gamma_2 G^{+}\right)$$

Transmission from Green's function

Landauer-Buttiker formula

$$I = \frac{2e}{h}\int_{-\infty}^{\infty} T(E,V)\left[f_1(E-\mu_2) - f_2(E-\mu_1)\right]dE$$

Datta S. (2005) *Quantum Transport*, Oxford University Press.

1. Side-contacted Metals on Graphene – Contact resistance

I-V model
(side view)

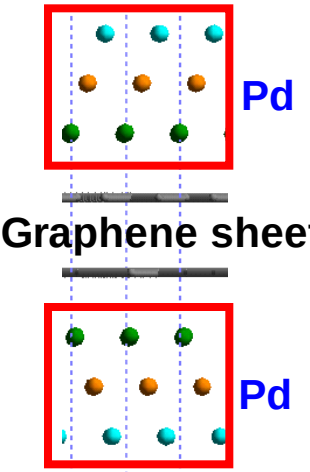

Density States C p-orbitals

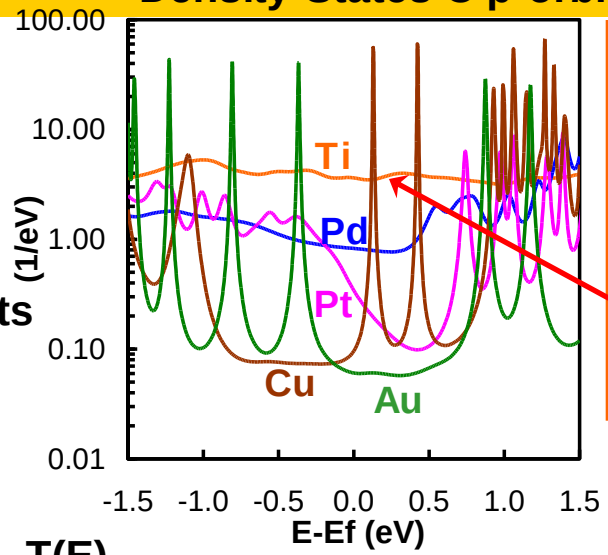

Ti has good Overlap (bonding) of C p-orbital with Ti d-orbital near the Ef
Pd next best

Density States Metal d

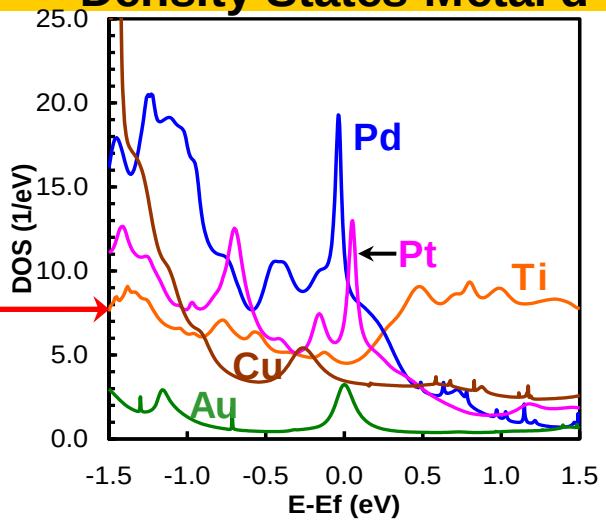

T(E)

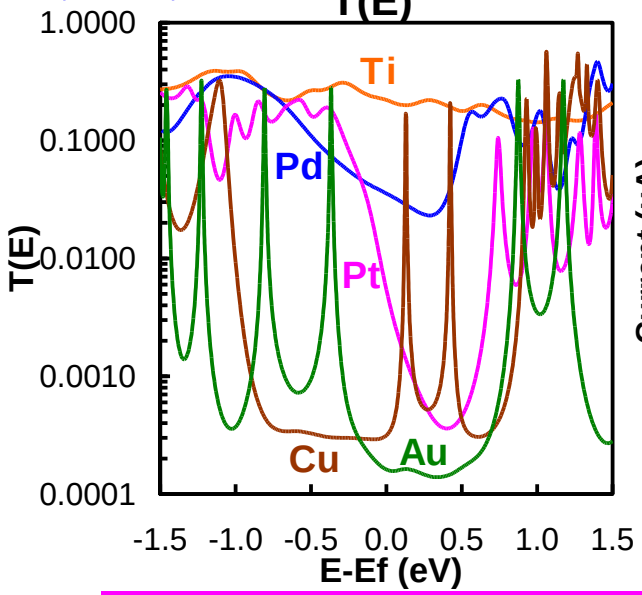

I-V

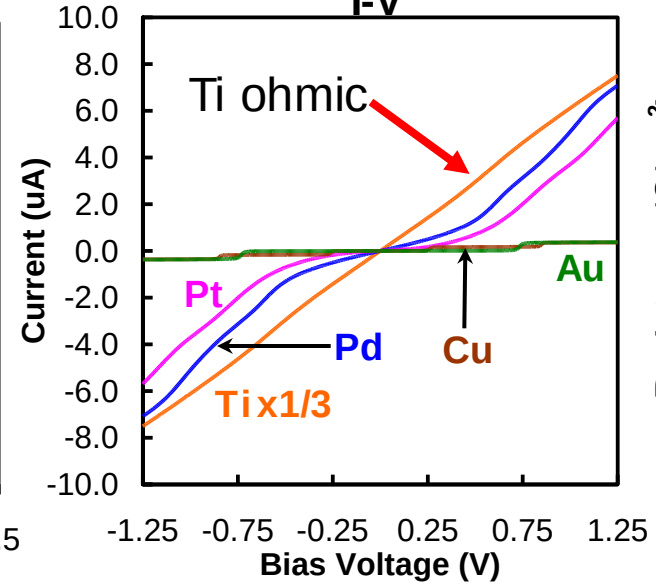

Contact Resistance

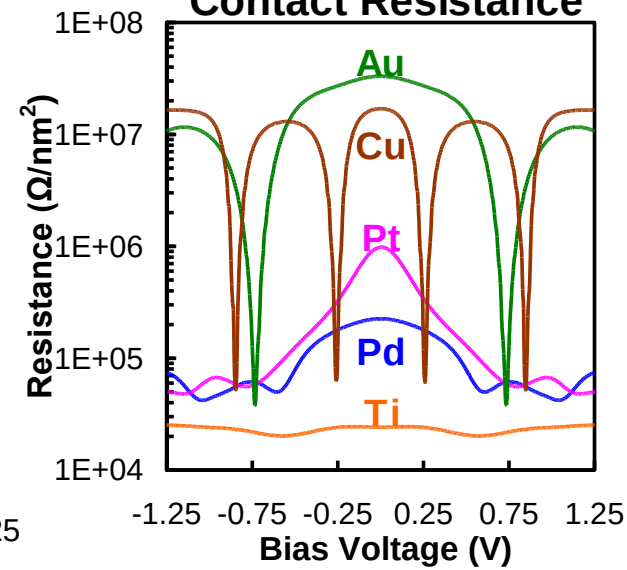

Contact Resistance Ti 24.2 KΩ << Pd 221 KΩ < Pt 896 KΩ < Cu 16 MΩ < Au 33 MΩ
(V< |0.1| V average, per nm²) Ti is the best metal for electrodes.

Ti-SWNT (7,7), Pd-SWNT (7,7) same results as for graphene

I-V model (side views)

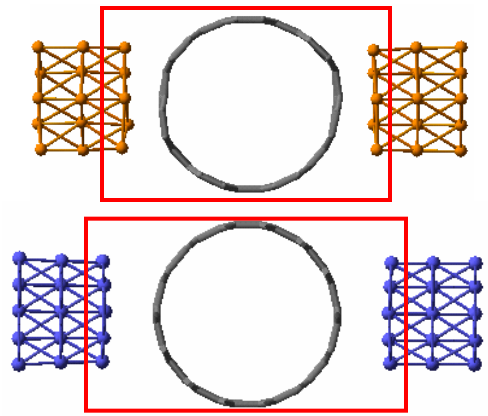

Ti-SWNT(7,7)
Unit cell:
C 56 atoms, Ti 30 atoms
SWNT (7,7) diameter: 9.5 A

Pd-SWNT(7,7)
Unit cell:
C 56 atoms, Pd 35 atoms

DOS, T(E)

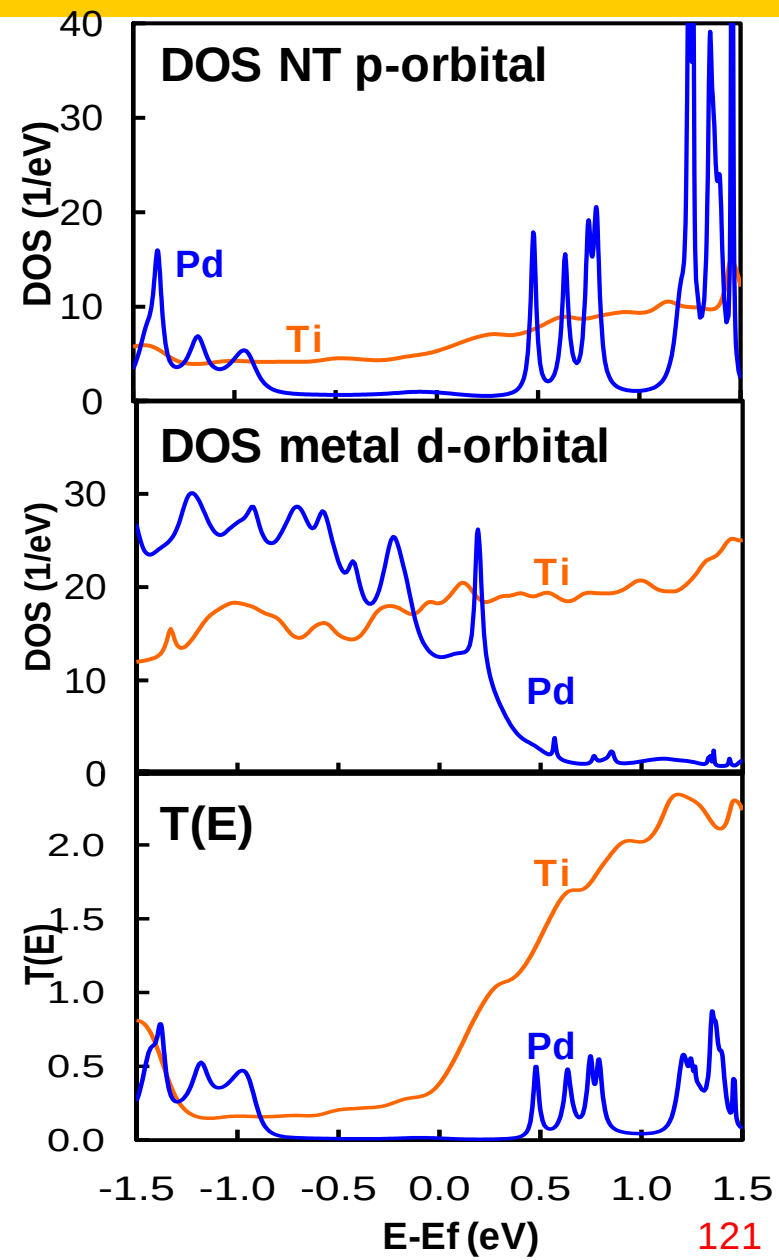

Ti-SWNT

Estrain 27.5 kcal/mol, *Ebond* 194.8 kcal/mol

DOS: good overlap between p-orbital of C on NT and d-orbital of Ti

T(E) >1.0 indicates multiple channels exist

Pd-SWNT

Estrain 0.61 kcal/mol, *Ebond* 17.5 kcal/mol

DOS: p-orbital of C on NT are discretized.

T(E): poor coupling due to the large distance at interface.

Comparisons of theory and experiment for contact resistance

Kanbara, T.; Takenobu, T; Takahashi, T.; Iwasa, Y.; Tsukagori, K.; Aoyagi, Y.; Kataura, H. *Appl. Phys. Lett.* **2006**, *88*, 053118

Pt electrodes (5 nm thickness and 200 nm width protected with 60 nm Au) deposited on top of SWNT (1.0 – 1.5 nm). Metal-SWNT side-contact

Four-terminal experiments ➔ contact resistance of *R*side-cont ≈ 5 kΩ with a CNT length between contacts of ~ 1 micron.

Assuming their SWNT to be (10,10) (diameter = 1.37 nm) with the electrode contacting about half of the CNT circumference this 200 nm electrode would be in contact with *N*side-cont = 8,096 carbon atoms. Thus we can estimate the **experimental contact resistance per carbon atom:**

*Rc*side-cont = *R*side-cont × *N*side-cont = 5,000 × 8,096 = **40.5 MΩ/Carbon**

Theory Pt- graphene (side contacted) ➔ *Rc*side-cont = **35.7 MΩ/Carbon**

Given all uncertainties, this is excellnt agreement.

Matsuda; Deng; Goddard. *J. Phys. Chem. C.* **2007**, *111*, 11113.
Matsuda; Deng; Goddard. *J. Phys. Chem. C.* **2008**, ASAP Article (in press).

Interconnects of Current LSI Technology

Cross section of Microprocessors

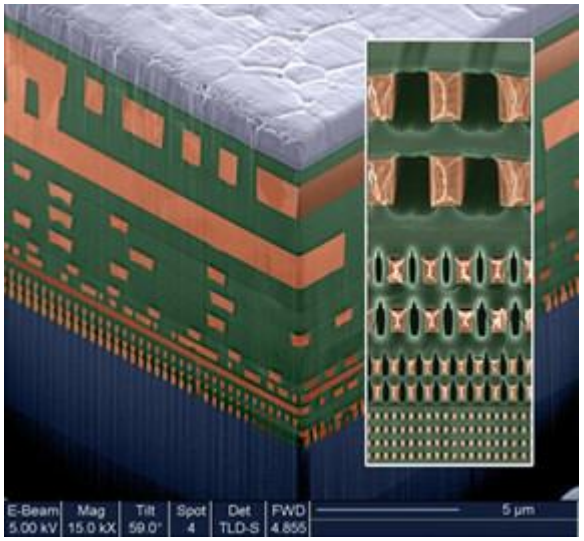

inter -connects

Multi-layer interconnect structures (45 nm)

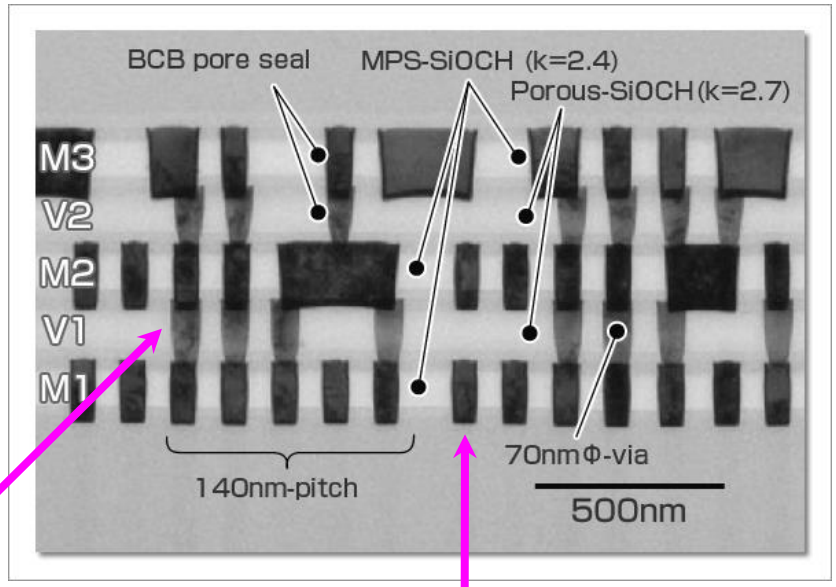

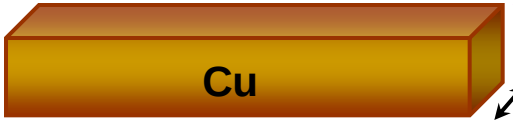

70 nm

Nanotube (NT)

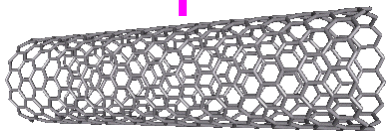

1~2 nm

Use CNT for lower level interconnects to realize the high integration density.

as deposited" electrodes: Ti << Pd < Pt < Cu < Au
Cu is terrible candidate as contact material.
Is there some way to modify contact to CNT to improve Cu

How to make good contacts between Cu and nanotubes?

www.dailytech.com, www.necel.com. *Matsuda, Y., Goddard, W. A., III. et al. *J. Phys. Chem. C.* **2007**, *111*, 11113.

4. Concept – functionalize the CNT or graphene surface with modest concentration of molecules that can react associatively with metal electrode to reduce the contact resistance and enhance structural stability at the interface

Proposed system

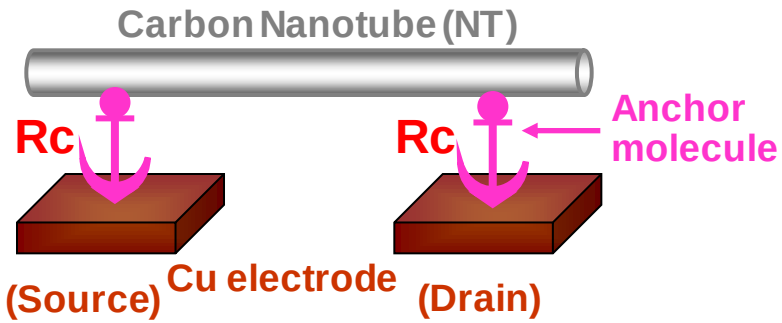

Model for calculation

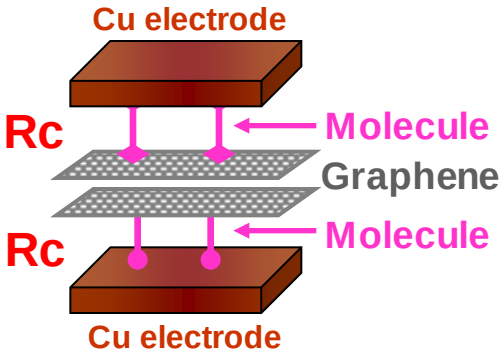

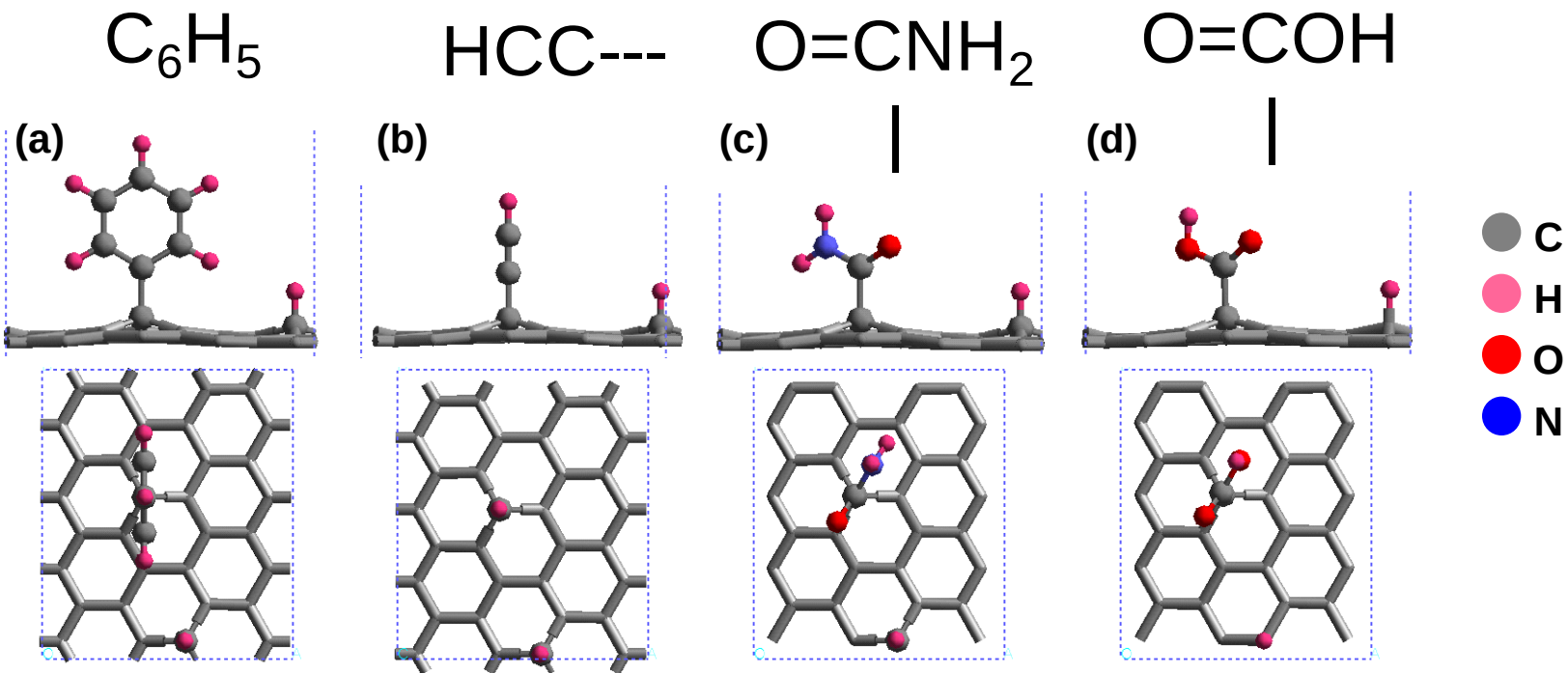

Which anchor leads to the lowest contact resistance?

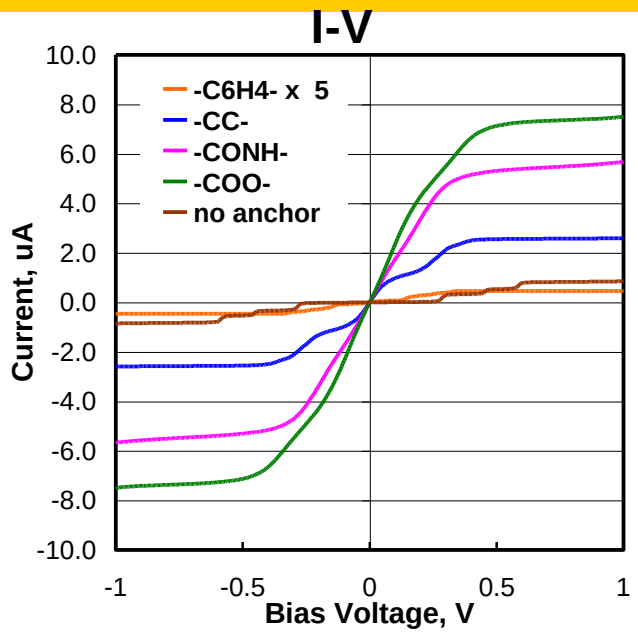

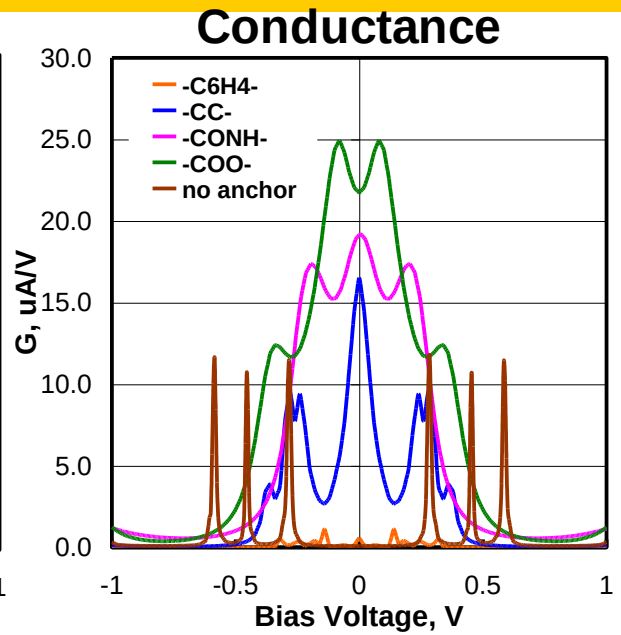

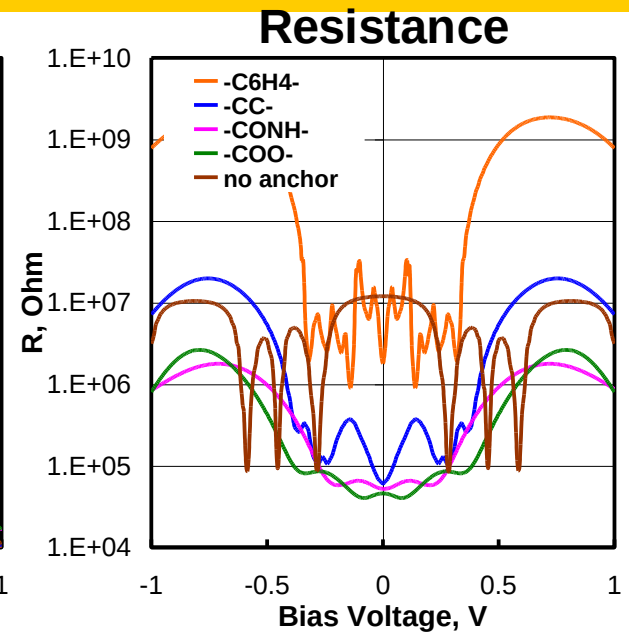

Interaction strength:

-CC- > -COO- > -CONH- > -C_6H_4- >> no anchor

All anchors can mechanically stabilize the interface at Cu and nanotube.
(bond energy > 100 kcal / mol anchor)

Contact Resistance (V< |0.1| V average, per unit area 0.83 nm^2):

-COO- 43 kΩ < -CONH- 58 kΩ < -CC- 128 kΩ < -C_6H_4- 10.3 MΩ < no anchor 11.7 MΩ

Pd-graphene (no anchor, best of non-Ohmic contacts) : 159 kΩ

Best Case: -COO- functionalized NT reduces the contact resistance to the Cu by a factor of 275 and increases the mechanical stability by 26 times.

Preparation methods for functionalized SWNTs

	Functionalization	Procedure	Feature
5	Aryl groups	Make reactive radical by electrochemical reduction of aryldiazonium salts. (5a) Reaction of aryldiazonium salts with SDS-coated SWNTs in water. (5b)	One out of ~20 carbons can get up to 9 carbons. Soluble in organic solvents.
6	Alkyl groups	Lithium and alkyl halides in liquid ammonia	Soluble in common organic solvents.
7	Carboxl groups	Sonicate in 3:1 sulfuric/nitric acid solvents for three hours at 40C	
8	Amido groups	Do case 7 and further treat with ethylenediamine (NH2-CH=CH-NH2) using the HATU coupling agent	

5a. Bahr, J. L.; Yang, J.; Kosynkn, D. V.; Bronikowski, M. J.; Smalley, R. E.; Tour, J. M. *J. Am. Chem. Soc.* **2001**, *123*, 6536.

5b. Dyke C. A.; Tour, J. M. *Nano Lett.* **2003**, *3*, 1215.

6. Liang, F.; Sadama, A. K.; Peera, A.; Chattopadnyay, J.; Gu, Z.; Hauge, R. H.; Billups, W. E. *Nano Lett.* **2004**, *4*, 1257.

7. 8. Ramanathan, T.; Fisher, F. T.; Ruoff, R. S.; Brinson, L. C. *Chem. Mater.* **2005**, *17*, 1290.

Proposed Processes for forming Cu-Anchor-NT interconnects

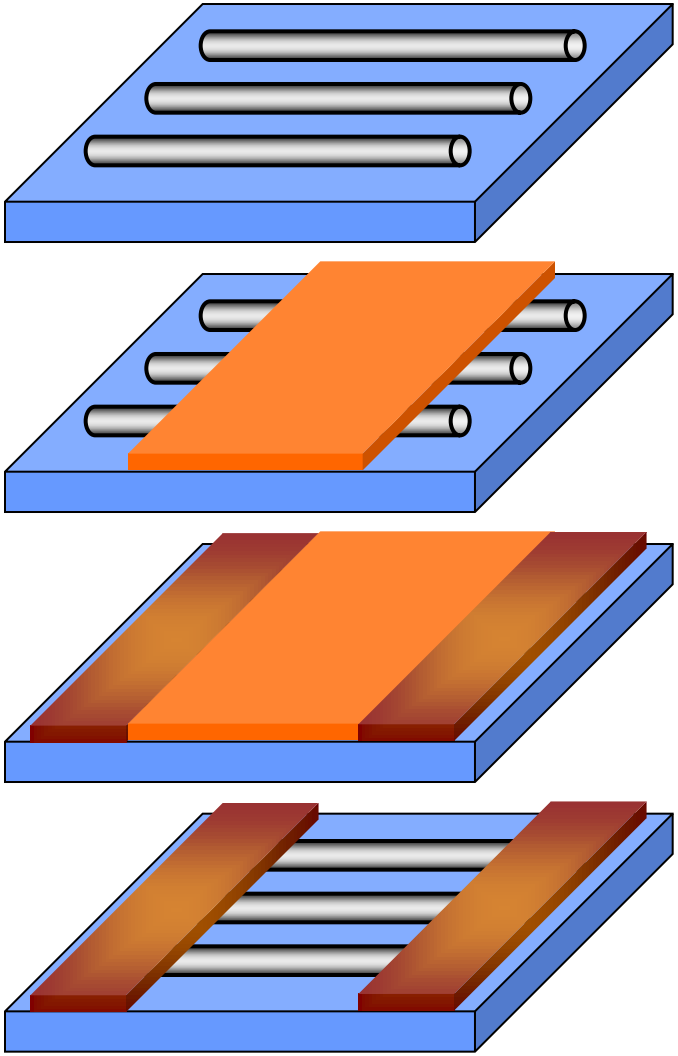

Position NTs at specific places on the wafer by depositing appropriate film on substrate

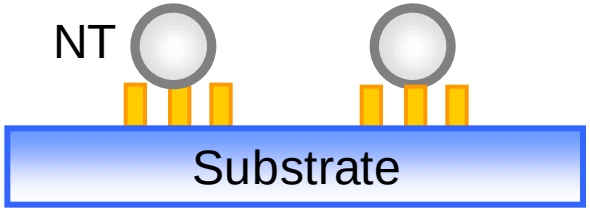

Mask NTs for implementing electrodes.

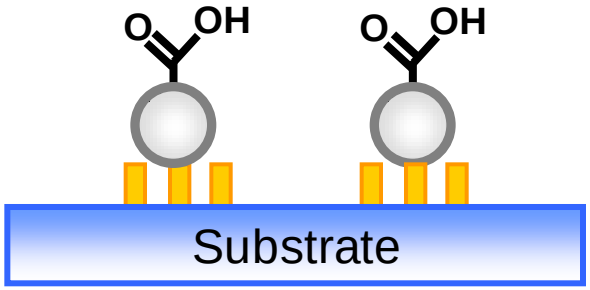

Treat with anchor precursors. then deposit Cu electrodes.

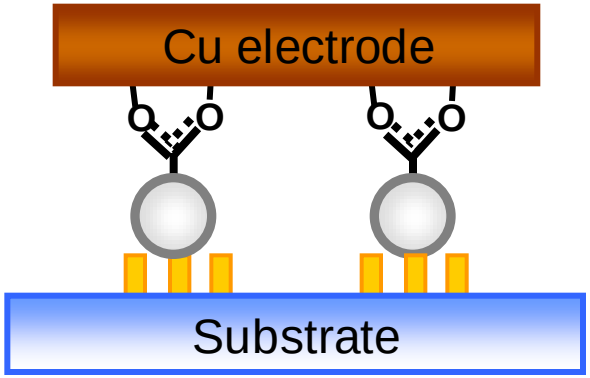

Remove of masks.

Similar strategies using bifunctional anchors might be useful for making stable catalyst-carbon interfaces for fuel cells